Investigation of velocity and turbulence measurement techniques for riverine hydrokinetic turbine sites

by

Samuel d'Auteuil

A thesis submitted to the Faculty of Graduate Studies of
the University of Manitoba
in partial fulfillment of the requirements of the degree of

MASTER OF SCIENCE

Department of Mechanical Engineering
The University of Manitoba
Winnipeg

Abstract

Multiple flow devices, techniques, procedures, and approaches are tested and validated to characterize the velocity, turbulence, and length-scales of high-velocity riverine sites for distributed hydrokinetic turbine applications. Measurements are performed at the Canadian Hydrokinetic Turbine Testing Center located on the Winnipeg River. Devices tested include the acoustic Doppler velocimeter (ADV), acoustic Doppler current profiler (ADCP) and the shear probe. ADV and ADCP streamwise mean time-averaged velocity measurements agree within an average of 4.38% difference. These velocity profiles are affected by upstream turbine wakes. In contrast, turbulence intensities differ to a larger degree between the ADCP, ADV, and shear probe. The average percent difference in turbulence intensity between ADV and ADCP is observed to be 30%. In the ADV results, vortex shedding suppression is suspected when the ADV is in the wake of an underwater turbine. Finally, the shear probe measured micro-turbulence scale and cannot capture macro-turbulence.

Acknowledgements

First and foremost, I would like to acknowledge Dr. Eric Bibeau for providing the opportunity through which I was able to complete this thesis and for imparting his wisdom and experience to me. I would like to thank Dr. Amir Birjandi for his guidance, advice and assistance. I would like to acknowledge the support of Zeev Kapitanker for his assistance in the design, maintenance and operation of research equipment in the lab and at our research site, as well as Kirk Dyson who assisted in collecting data and operations at the CHTTC. I would like to thank NSERC, GETS, and NRCAN for their financial support of the project, allowing the purchase and construction of the apparatus required to perform the experiments. I would also like to thank all of my peers who challenged me throughout the project. My research group was supportive and challenged me to make my research the best that it could be. Also, I am thankful for all of the undergraduate student research assistants who helped us throughout each summer. This allowed us to perform many tasks which would not have been possible otherwise. Lastly, I would also like to thank RG Enterprises for their support of our research, equipment development and in the development of our research site.

Contents

List of Figures

List of Tables

Nomenclature

U, V, W	Instantaneous streamwise, spanwise and vertical velocities respectively
X, Y, Z	Streamwise, spanwise and vertical directions respectively
R_h	Hydraulic radius
L_Y	Spanwise length
P	Wetted perimeter
A	Cross-sectional area
D	Depth
Ar	Aspect ratio, $Ar = L_Y/D$
U_∞	Free-stream velocity
Y_∞	Vertical location of free-stream velocity
U_N	Nominal turbine design velocity
δ	Boundary layer thickness
u', v', w'	Streamwise, spanwise and vertical root mean square velocities respectively
L_x	Integral length scale
μ	Dynamic viscosity
ν	Kinematic viscosity
ρ	Density
Re	Reynolds number
Fr	Froude number

$\overline{U}, \overline{V}, \overline{W}$	Mean streamwise, spanwise and vertical velocities respectively
u, v, w	Fluctuating components of the streamwise, spanwise and vertical velocities respectively
$\theta_x, \theta_y, \theta_z$	Angle of rotation about the X, Y and Z axes respectively
$\overline{u^2}, \overline{v^2}, \overline{w^2}$	Reynolds normal stresses
$\overline{uv}, \overline{uw}, \overline{vw}$	Reynolds shear stresses
$[R]$	Reynolds stress tensor
ϵ	Dissipation rate
TKE	Turbulent Kinetic Energy
TI	Turbulence intensity
CHTTC	Candian Hydrokinetic Turbine Testing Centre
HKT	Hydrokinetic Turbine
ADV	Acoustic Doppler Velocimeter
IMU	Inertial Motion Unit
ADCP	Acoustic Doppler Current Profiler
GHG	Green House Gas

List of copyrighted material for which permission was obtained

Chapter 1

Background

As the global population increases, so too does the demand for energy. Opportunities for new forms of energy production are emerging to address new market opportunities. With dwindling resources of fossil fuels remaining [3] and more evidence of anthropogenic global warming [4], societies require to increase their share of renewable energy in their energy portfolio. Many different types of renewable energy resources exist and many sources remain untapped. Power generation from hydrokinetic energies of rivers is a promising application to contribute to a plurality of approaches to generate distributed renewable energy in support of micro-grids.

1.1 Energy demand and consumption

According to the Enerdata [5], approximately 151,190 TWh of energy of all forms was consumed in 2016. Approximately 76% or 114,904 TWh of energy was consumed from non-renewable resources, in 2016 [5]. This means that, to meet the demands of the world, three quarters of the total energy consumption has to come from non-renewable, Green-House Gas (GHG) emitting energy sources. This poses a problem,

because the burning of coal, oil and natural gas are harmful to the environment and increase CO_2 concentration in the atmosphere. It has been shown that the burning of fossil fuels can have a lasting effect on the environment and climate [6]. In addition to this, the fact that they come from non-renewable sources means that renewable alternatives are eventually required. It is imperative to reduce the amount of fossil fuels consumed. To do this, clean and renewable energy sources must be found and used to replace unsustainable approaches to support generation at the utility and micro-grid scale.

In the age of climate science and change prediction, renewable energy has become of interest to not only governments, researchers and energy companies, but also to the general public. Many different fields of renewable energy are being researched and brought to mainstream energy markets. In 2016, approximately 5,040 TWh of electricity was generated from renewable resources [5]. This includes solar, wind, geothermal and hydro energy, and makes up approximately 24% of the total world electricity supply. These technologies are increasing in market share and have low costs compared to fossil fuels [7] [8]. This shows that, it is environmentally sound and economically favourable to develop renewable energy resources.

Hydrokinetic energy is an emerging technology. The energy of water is normally converted to electrical energy by using the potential energy from the height of a dam. This method uses the kinetic energy of flowing water to operate a turbine and generate electricity, albeit at much reduced power densities. Such turbines are referred to as hydrokinetic turbines, or HKTs. This technology is being researched in many locations around the globe. HKTs offer a larger energy density per unit area than wind or solar energies [7], as well as having the potential to be more cost effective than diesel generators [9]. This is particularly beneficial in remote communities, such as in northern Canada, that use diesel generators for electricity. Not only do HKTs offer

a lower cost option, it also comes with the added benefit of being environmentally friendly. HKTs can be operated in oceans and in rivers.

1.2 Flow characterization for highly energetic hydrokinetic turbine sites

A study was performed for riverine hydrokinetic resource in Canada. Jenkinson [10] found that there is an available 300 to 700 GW of hydrokinetic power throughout all rivers of Canada. This exceeds the nameplate capacity of electrical generation in Canada. These results were obtained from a hydrological assessment of rivers and watersheds in Canada. One aspect that most HKT studies lack is a comprehensive flow assessment of a site, providing details regarding components of the flow, such as mean flow and power statistics, combined with turbulence data. However, there are many considerations for the location of a HKT. Figure 1.1 shows how river hydrokinetic turbines are affected by flow with Table 1.1 detailing each of the component labeled in the figure and how they can measured in field. The table also includes the components addressed in this study for HKT river applications.

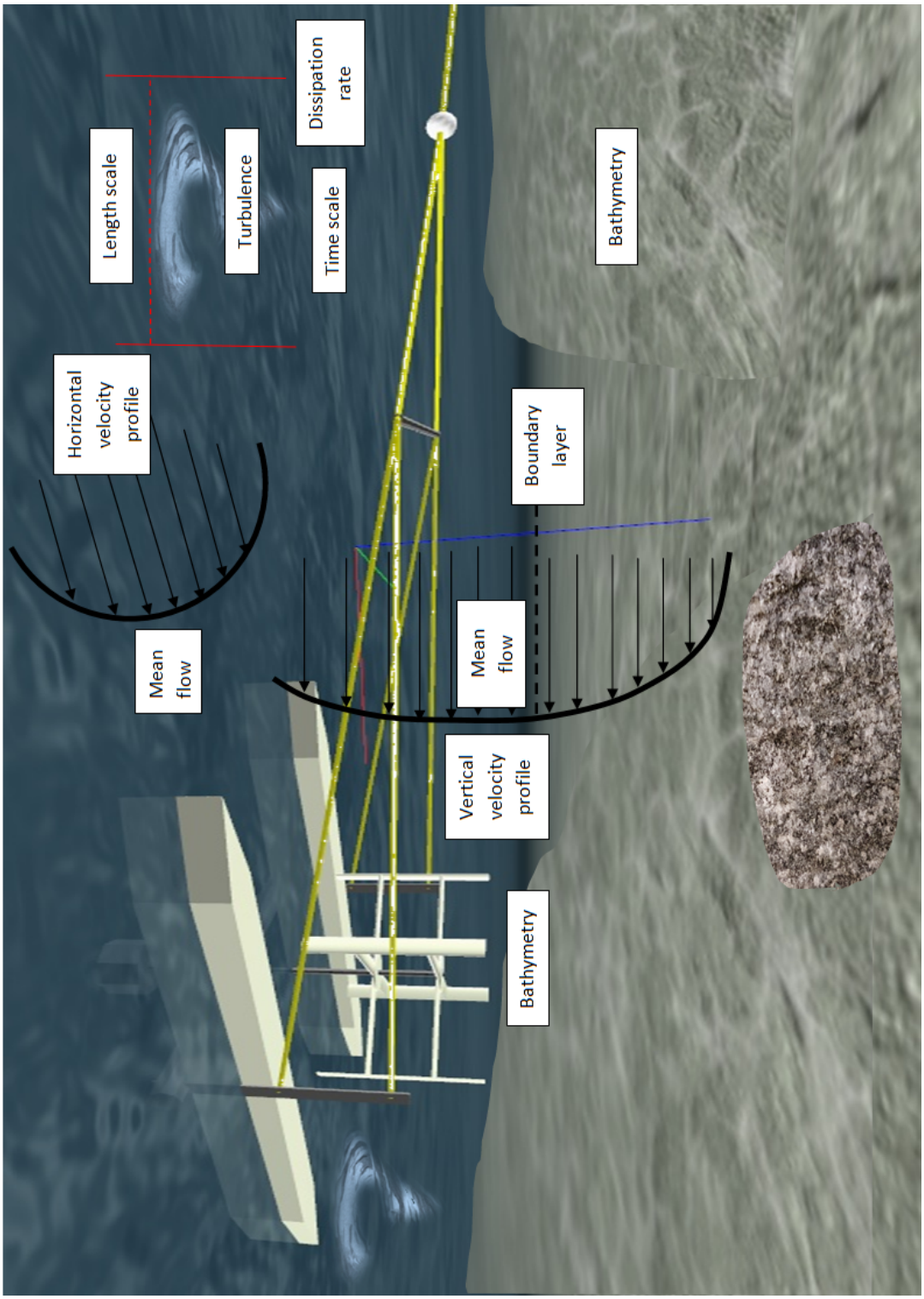

Figure 1.1: Hydrokinetic flow characterization requirements [1] [2]. (See Table 1.1 for details)

Table 1.1: Important flow characterization requirements of a hydrokinetic turbine site (see Figure 1.1)

Flow feature	Measurement	Contribution	Focus of study
1. Mean velocity	• ADV • ADCP • Flowmeter	• Power • Drag • Mooring	✓
2. Turbulence	• ADV • ADCP • Shear probe	• Wear • Vibration • Mooring • Safety	✓
3. Time scale	• ADV • Shear probe	• Wear • Cyclic loading • Vibration • Turbine design	✓
4. Length scale	• ADV • Shear probe	• Wear • Cyclic loading • Vibration • Turbine design	✓
5. Dissipation rate	• ADV • Shear probe	• Wear • Cyclic loading • Vibration • Turbine design	✓
6. Temporal flow variation	• ADV • ADCP • Flowmeter • Discharge	• Yearly power • Prediction	
7. Velocity profile	• ADV • ADCP • HADCP • Shear probe	• Max power • Prediction • Turbine design	✓
8. Boundary layer	• ADV • ADCP	• Turbine design • Max power	✓
9. Water level	• Sonar • ADCP	• Turbine design • Safety • Mooring	
10. Bathymetry	• Sonar • ADCP	• Safety • Mooring • Power cable	✓
11. Sediment	• ADV • Samplers	• Wear • Instrument use	
12. Wildlife	• Sonar • Trackers	• Safety • Environment	
13. Ice cover for resource assessment	• Satellite imaging • Aerial imaging	• Safety • Placement • Year round use	
ADV = Acoustic Doppler Velocimeter; ADCP = Acoustic Doppler Current Profiler; HADCP = Horizontal Acoustic Doppler Current Profiler			

A summary of terminology relevant to river environments, fluid flow and velocity measurement is presented in Appendix A.

1.3 Flow impact on HKT site selection

An important aspect to site a HKT is the available power that can be extracted. This is dependent on the mean velocity and velocity profile of the river. The free-stream velocity of the river limits the maximum power and design of a turbine. The velocity profile affects the depth at which a turbine can be located in the water column to maximize power.

Turbine mooring is also an important factor to consider. The mooring system for a turbine is dependent on a number of flow factors, such as the river velocity, river depth, bathymetry, river span, shore geography and geometry, turbulence and associated cyclic loading. The velocity of the river determines the drag on the turbine and mooring system, and therefore the tensile strength required for mooring lines. The shore geometry can allow the use of a shore anchoring system, or can indicate that a bottom-mounted anchoring system should be used. The shore topography determines if and how a shore anchor can be mounted into the shore. The river depth affects the design of the bottom-mounted mooring system, and the procedure for deploying the mooring system.

Flow prediction and year round use of turbines are also important factors for the location of a HKT. First, it must be known what times of year the turbine may be placed in the river. If, during cold months, the river is covered in ice, certain turbine designs cannot be left in the water during this time and must be removed prior to ice formation. This affects the yearly power production of the turbine and requires an alternative source of energy to be used. It is important to be able to predict temporal variations in flow velocity. This impacts the yearly power output of the turbine and is important for the power management of the communities that the turbine is supplying.

Wear and cyclic loading are important factors to consider for the long term placement of a turbine. The wear on a turbine is caused from the constant motion of the rotor, changes in water level of the river, turbulence causing vibration and cyclic loading, debris drifting into the turbine and thermal loading on the components of the turbine. This affects the lifespan of the turbine, the efficiency and therefore the power production of the turbine, and the amount of maintenance required.

Safety is an important concern for anyone working with operating turbines. Flow factors affecting the safety of working near the turbine include: splashing, rain and ice causing slippery conditions on the surface of the turbine, turbulence causing unpredictable flow and sudden movements of the turbine and bathymetry of underwater hazards impacting traveling to and from the turbine.

For the transmission of power from the turbine to the user, a power cable is required. Flow factors affecting the power cable include: bathymetry and the layout of the power cable underwater, high velocities causing difficulty in the deployment of the power cable and turbulence causing vibration and wear on the power cable. This affects the deployment of the cable.

Finally, monitoring of the turbine system and the flow around it is important for the power production and maintenance of the turbine, as well as for furthering studies of hydrokinetic turbines, leading to better designs in the future. Thus, the instruments used to monitor are important. Certain devices, such as the ADV, are better at measuring the turbulence of the flow than others. Flow conditions such as high levels of turbulence and poor water quality can cause errors in measurements using acoustic instruments. Additionally, visual monitoring of the turbine via sonar is important to understand the operation of the turbine and to help identify potential problems with the turbine before they cause the turbine to fail. The use of sonar and type of sonar are affected by the flow around the turbine and the mooring system of the

turbine.

These factors affect the performance of turbines in a river environment. It is important to consider each one individually and holistically to understand and to produce the best design for a hydrokinetic turbine. Some of these factors are addressed with the measurements in this study, however, more research is required to understand these factors.

Site characterization for a hydrokinetic turbine is an arduous process, as it requires energetic riverine locations. Site selection can involve the use of hydrologic equations and models, ice opening methods [11], mathematical and numerical approaches, among others. Once a specific river system has been selected, local measurements must be performed. Flow measurements and observations must be made to determine the best locations to place a turbine or an array of turbines. The determination is made based on the potential power or free stream velocity, turbulence level, geometry of the river and the type of turbine being considered. There are other considerations for turbine locations as well, from seasonal variations in flow to the sediment and makeup of the riverbed.

1.4 The Canadian hydrokinetic turbine testing centre (CHTTC)

The CHTTC was created to provide an opportunity for turbine developers to test their devices in a river at low cost, in collaboration with researchers at the University of Manitoba. The centre has since gathered interest from many HKT companies, and currently provides a facility to test prototype designs. As such, the CHTTC provides an opportunity for industry and researchers to collaborate and further the development of hydrokinetic turbines.

Among the different types of research being done for hydrokinetic turbines at the CHTTC, one is the characterization of potential sites for the placement of hydrokinetic turbines. This research is of interest to industry and academia, as this area is relatively new and has not been explored in detail. As this study is focused on the characterization hydrokinetic turbine sites, the CHTTC is where the majority of the experiments were performed.

The CHTTC is located on the Winnipeg River near Seven Sisters, Manitoba, downstream of the Seven Sisters Manitoba Hydro dam. The location is ideal for testing hydrokinetic turbines. Firstly, a portion of the reach is a man-made channel and approximately uniform depth. This removes difficulties in planning deployments and isolating specific locations for specific types of turbines. Additionally, the dam removes most of the debris coming from upstream in the river. This, as well as the fact that there are few trees along the sides of the channel, makes the channel reliable for operating turbines by preventing floating debris, such as trees or logs. Finally, river flow changes frequently due to differences in environmental conditions of the watershed feeding the Winnipeg River, as well as VAR control by operating a powered turbine as a motor and thus reducing the flow. Because the CHTTC is near a dam, information on the volumetric flow rate and water level are available on an hourly basis. Additionally, the changing flow rate allows companies to test their turbines in varying flow speeds. Figure 1.2 shows various aspects of the CHTTC: mooring infrastructure, new energy turbine testing and flow measurements using acoustic devices.

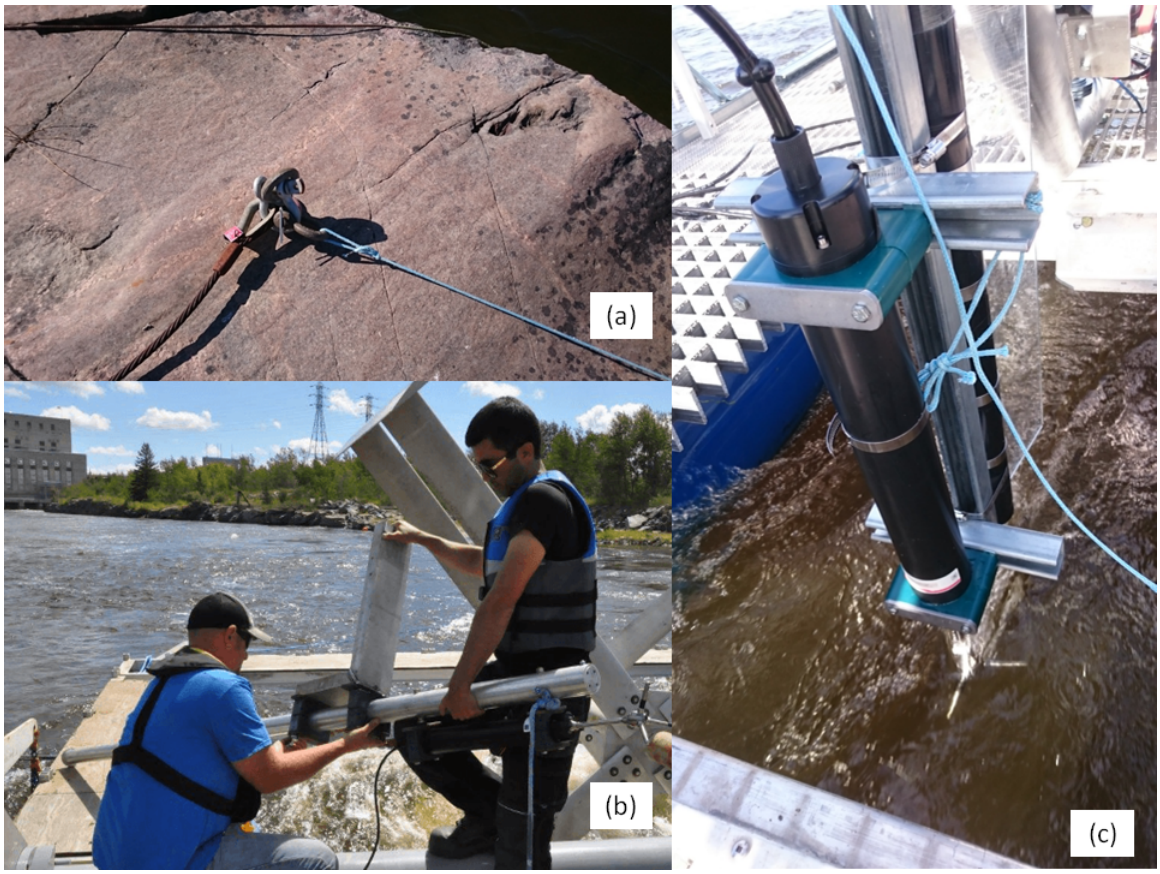

Figure 1.2: Example aspects of the CHTTC: (a) shore anchors where measurement platforms and turbines can be anchored, (b) acoustic measurements amid testing of the New Energy 25 kW hydrokinetic turbine, and (c) acoustic measurements occurring at the CHTTC on a measurement platform

1.5 Difficulty of flow measurements in energetic river sites

Although there exist suitable measurement instruments for laboratory environments or slow moving flows in rivers, these devices and procedures are not necessarily practical for high-energy river flows. For example, Particle Image Velocimetry (PIV) is a technique used to measure flow velocities in small scale settings, using a laser to illuminate seeding particles and using imagery to track the particles. This technique is not practical for HKT sites due to the requirement of a laser, the control required, seeding particles and a camera. Due to environmental concerns and cost, particles

cannot be seeded into natural flows. Additionally, using a laser that is large enough to illuminate an entire section of river is dangerous and impractical. Finally, placing a camera in such a way as to capture the vertical velocity of the flow is complicated by the fact that the camera must capture the side plane of the flow. This means that a method of installing a camera inside of a riverbank would have to be devised. A camera could be placed over the top of the flow, however, this would obtain a horizontal profile across the surface of the flow, and would not provide any information on the vertical profile.

Acoustic instruments, such as ADVs and ADCPs, have many advantages for flow measurements in river sites, such as their robustness and ability to measure velocities without adding particles to the water. However, they also have many disadvantages, from having data being affected by motion, to limitations on data recording frequencies. Moreover, holding devices in the flow is difficult. At the CHTTC, the flow velocity varies from 1.6 m/s and can exceed 3 m/s. The drag on a cylinder, such as an ADV or ADCP, can be calculated by [12]:

$$F_D = \frac{1}{2} C_D \rho U^2 A \tag{1.1}$$

where C_D is the drag coefficient of the body experiencing the drag and A is the cross-sectional area that is exposed to the flow. For example, using a C_D of 0.35 obtained from Fox and McDonald [12], 3 m/s for velocity and 0.062 m^2 for the cross-sectional area, an ADV alone in the flow experiences a drag force of 100 N, which is similar to holding 10 kg. This force is not trivial, when considering the stillness required of the instrument during measurement, the weight of the instrument itself, the length of time that a measurement must be taken for and vortex shedding causing vibration problems and the ADV support structure will significantly add to this force.

Considerations for flow measurements in high-energy river environments include:

1. Safety concerns of the personnel
    (a) Personnel falling into a fast flowing river
    (b) Risk of hypothermia
    (c) Large drag forces on ropes or cables located below the water line
    (d) Weight and lifting requirements for research equipment
    (e) Fatigue
    (f) Hidden underwater hazards, such as rocks
    (g) Movement of watercraft used to carry research personnel
    (h) Tripping hazards on watercraft or on shore
    (i) Slipping hazards on watercraft or on shore
    (j) Injury like fingers getting caught in ropes
    (k) Navigation through rapids when changing location in a river
    (l) Mooring lines becoming entangled in the boat motor propeller
2. Large forces on measurement instruments and support structures
3. Design of a rigid support system for measurement instruments
4. Transporting the measurement instrument and support system to the desired measurement location
5. Complexity and length of time required to assemble and secure the measurement instrument to support system
6. Vibration due to turbulence on objects that contact the water, especially if rigidly mounted

7. Velocity, significant turbulence, low temperatures and rapids
8. Lack of control of surrounding environment, including weather and civilians in private boats
9. Trained personnel required to carry out desired procedures
10. Availability and maintenance of watercraft
11. Equipment falling into water
12. Documented procedures and safety risks assessed before work is permitted to proceed

Experience performing flow measurement activities in energetic flows has been obtained by CHTTC members. The above considerations need to be addressed for measurements in energetic flows.

1.6 Objectives

The objective of this research is to develop methods and procedures for the measurements required to characterize a hydrokinetic turbine site using a fixed or mobile platform at the CHTTC. The secondary objective is to compare the instruments used in these methods and determine the level of agreement between them.

1.7 Methodology

The CHTTC is used as a large-scale water tunnel. This facility that is discussed in Section 1.4 has been adapted to test river hydrokinetic turbines. The facility maintains natural river characteristics but enables detailed measurement operations

to be performed, similar to a controlled laboratory. Included in the facility are anchors for mooring vessels, stationary platform and motorized vessels, instruments such as ADVs, ADCPs and shear probes, operating turbines to apply the research and to enable hydrokinetic standards development.

To achieve research objectives, the methodology adopted in the current study includes:

1. Select the CHTTC as the test site to measure flow features in an energetic hydrokinetic river
2. Identifying the flow features required for characterization of a hydrokinetic site
3. Selecting acoustic instruments which are appropriate for measuring the identified flow features selected in Table 1.1
4. Designing and manufacturing instrument support systems to allow measurements in highly energetic flow
5. Developing the selected channel to work with the designed support systems
6. Testing each instrument and support to identify improvements and re-design the support system accordingly
7. Performing characterization of the CHTTC with the finalized design
8. Performing post-processing of collected data to visualize flow characterization results and identify issues with the measured data. A separate study quantifies the measurement error.

1.8 Contributions

As a result of this research, a conference paper has been published using data collected with the surface measurement procedure, and a second conference paper has been published on the velocity profile measurement procedure, using a cable system to position the ADV. Technical reports were also published and are available on the CHTTC website using the measurement procedures developed in this study. The measurement procedures themselves have been documented and are available for download. An example is shown in Appendix B for the ADCP.

In addition, infrastructure and custom modifications to CHTTC equipment have been performed to allow flow measurement in highly energetic flow. Since the inception of the procedures, additional flow measurements have been performed at the CHTTC. These procedures have also since been performed outside of the CHTTC, in a less controlled environment, to demonstrate the flexibility of the procedures. Some improvements procedures have since been applied using a sonar camera to monitor the procedure underwater for characterizing the boundary layer near the river bed.

Measurement considerations which were previously untested in a highly energetic river environment were documented through this research. This includes the extent of motion of the ADV when performing measurements. Issues like cable entanglement and mooring line obstruction are examples of improvements that were required to perform measurements safely and properly. Additionally, a description of the forces, vibrations and difficulty of performing measurements in energetic river sites safely was documented, as this is not yet common knowledge or practice.

The adopted methodology and results realized the objective for the marine industry to be able to characterize a river test site. The data is now available for download on the CHTTC website [13], as well as being available publicly online. Having this

knowledge of the CHTTC allows the centre to provide comprehensive flow data, allowing turbine manufacturers to choose the desired testing conditions for their turbines, while maintaining a natural setting; other research groups can use the data to further the analysis of flows in highly energetic river locations.

1.9 Outline

In the next chapter, the literature on flow measurements applicable to river sites is explored. Literature pertaining to the measurement instruments used in the current study is also discussed. Previous research on hydrokinetic turbines and the characterization of hydrokinetic sites and resources is explored. A discussion on topics in turbulent flow and river environments, and how they are relevant to the current research, is presented. Finally, literature is reviewed that pertains to the effects that HKTs have on the surrounding environment.

In the following chapter, a detailed description of the procedure taken to acquire flow data in an energetic site is provided. In Section 3.1.1, the developed procedures to obtain measurements of the velocity profile is described. Section 3.1.2 details procedures to take measurements of the free-stream velocity. This is divided between the different sets of equipment used to take measurements, one being a fixed measurement platform and the other being a mobile platform. This includes a separate procedure employed for each of the measurement instruments used to collect data on the river. Section 3.3 contains a description of how the boundary layer of a river can be characterized, as well as the difficulties associated with those methods. Additionally, Section 3.4 discusses how the bathymetry of a site can be characterized and the equipment with which it can be performed. Finally, there is a discussion on large scale resource characterization in Section 3.7.

The flow results are discussed in Chapter 4 according to each type of measurement. Additionally, a discussion on the turbulence statistics is presented. Effects, such as errors and spikes in data, as well as device vibration are discussed.

Chapter 5 lists the conclusions and the recommendations to improve the act of flow measurement in energetic river flows.

Chapter 2

Literature review

Literature pertaining to flow measurement devices, HKT site characterization, hydrokinetic turbines, and velocity profiles are presented, that are the foundation of how to measure flow in highly energetic river flows.

2.1 Instruments at low and high velocities

In order to perform the required measurements to address flow measurement requirements in Figure 1.1, specialized instruments are required for the riverine environment. The instruments shown in Figure 2.1 and used in this study are reviewed. There is no literature to report on the equipment required to secure and apply such flow devices in highly energetic river environments.

2.1.1 Acoustic Doppler velocimeters

ADVs are a common measurement device to measure flow velocity. They operate upon the Doppler principle, as detailed in Appendix A. ADVs average the flow velocity in

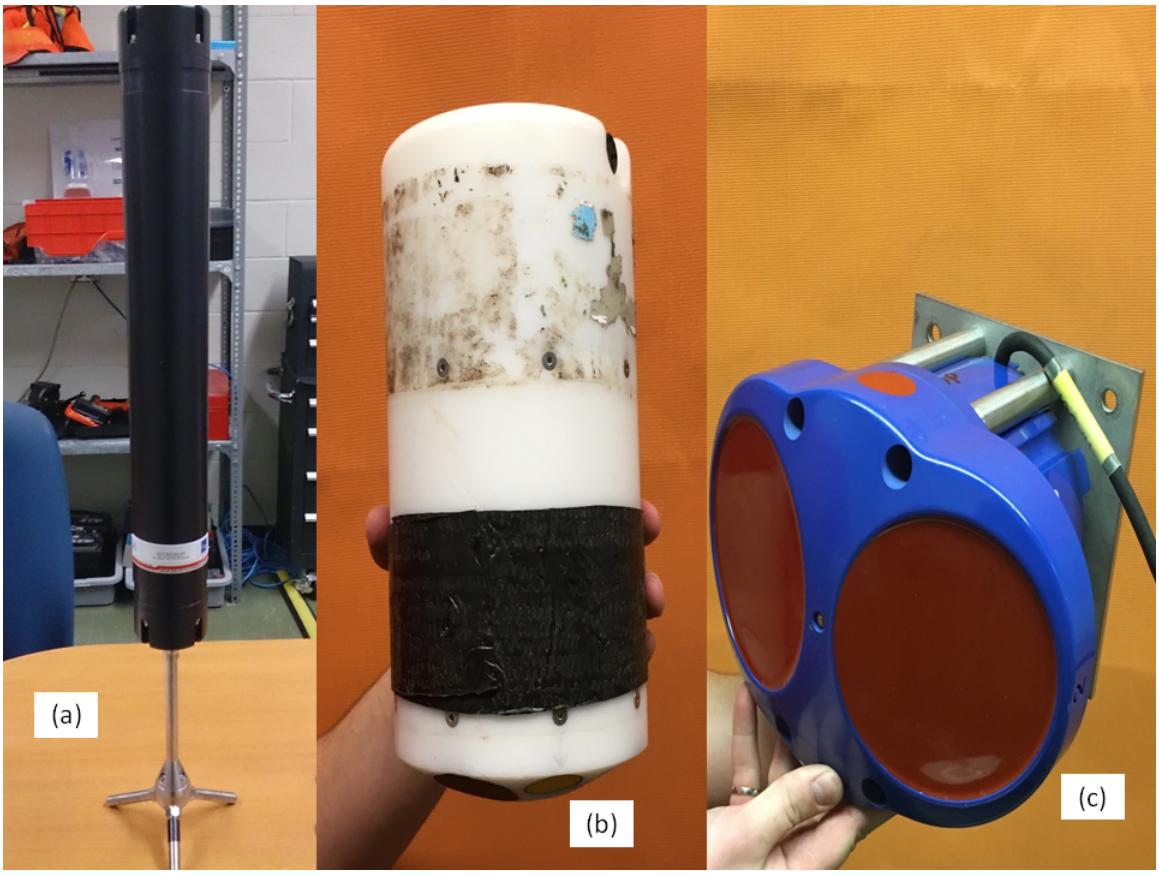

Figure 2.1: (a) ADV, (b) ADCP and (c) Horizontal ADCP instruments used in flow measurement. These acoustic devices are suitable for in-field river measurements.

a relatively small control volume. The measurement volume is assumed to be a point measurement, as it is small relative to the flow environment. For example, the measurement volume for the Nortek Vector ADV is a cylinder with a diameter of 14 mm and a height of 14 mm, located at a distance of 157 mm from the end of the probe [14]. Data is collected at a frequency set by the user and later output as a time-series. ADVs also collect other data as well, depending on the type of ADV. For example, the Nortek Vector ADV can provide information on the acceleration and rotation of the device, using the Inertial Motion Unit, or IMU, which includes devices such as an accelerometer and magnetometer. These additional measurements are stored with the velocity data. Table 2.1 summarizes relevant literature that details ADV in various environments for velocities, mostly below 1 m/s.

Table 2.1: Literature review for ADV devices at low and high velocities

Author	Device	Region	Max U [m/s]	Results
Nortek [14]	ADV	N/A	N/A	User manual for the Vector ADV, supplied by the device manufacturer
Nidzieko *et al.* [15]	ADV, ADCP	tidal	0.7 peak near bed	Comparison between ADV and ADCP. ADCP overestimates Reynolds stress by 20% when using ADV as benchmark
Horstman *et al.* [16]	ADV, ADCP	tidal	0.2-0.5	ADV and ADCP are comparable when assessing mean flow
Tritico *et al.* [17]	ADV	river	0.6	Profile measurement in shallow stream using ADV. Turbulence is heavily affected by flow obstruction.
Voulgaris and Trowbridge [18]	ADV	laboratory flume	0.3	Laboratory experiment to validate the validity of the ADV for turbulence measurements. Reynolds stresses are underestimated by 1%.
Gunawan *et al.* [19]	ADV	tidal strait	2	ADV used to collect long term data in tidal strait. Deployments should be planned such that the ADV does not corrode and cause failure. Corrosion is caused due to long term exposure to biological agents.
Clunie *et al.* [20]	ADV	laboratory flume	0.5	Testing of a technique to measure velocity with moving ADV. Near bed measurements affected by acoustic reflection but bad data can be removed by the beam correlation.
Vanzweiten *et al.* [21]	ADV	laboratory flume	0.4	Testing of the capability of the IMU in the ADV for compensating device motion. Error is too high in low flow for IMU to characterize motion, but in higher flow, it is possible.
Lovenbury [22]	ADV	laboratory flume	0.9 relative to moving carriage	Experiment testing the ability of a moving ADV to measure turbulence. Turbulence intensity has 9% error at high frequencies and 2% error at lower frequencies.

ADVs are considered to be relatively accurate, and are used as a benchmark for testing other devices, such as ADCPs. For instance, Nidzieko *et al.* [15] investigated the assessment of turbulence using an ADCP and found that it overestimated the Reynolds stresses by 20%, when compared to the ADV. Horstman *et al.* [16] performed a comparison between the ADV and ADCP as well, and found that the devices performed similarly when capturing the mean flow. They found that the ADV had a versatile design which allowed for many different types of setups, which could make it easier to use than the ADCP.

Studies at relatively low velocities have used ADVs to measure turbulence statistics in riverine environments. Tritico *et al.* [17] used an ADV to characterize turbulence in a shallow, gravel bed river, finding that flow obstruction can heavily affect turbulence characteristics. Voulgaris and Trowbridge [18] performed an assessment on the

validity of using an ADV for turbulence measurements. They compared the ADV with a laser-Doppler velocimeter and found that for mean flow, the variation between the two devices was less than 1%. In the analysis of Reynolds stresses, they found that the ADV under-predicted Reynolds stresses by 1%, without removal of noise from the data. They do caution use of ADV for turbulence assessment, citing high noise levels which result from the geometry of the ADV.

While ADVs are good for measuring turbulence, there exists a difficulty in using the measurement device in riverine environments. For example, Clunie *et al.* [20] developed a technique for ADV measurement called the "flying probes" technique. This technique was used to gather data in a flume setup in a laboratory. The technique was developed to remove ambiguity as to the motion of the probes, as the motion of the probe is controlled by a motorized device [20]. While this technique is applicable to laboratory experiments, it is difficult to apply this technique to a riverine environment, as the size of the motorized device and support structure would have to be too large to be practical. In the study done by Tritico *et al.* [17], a custom-built structure to stabilize the ADV and reduce vibrations was used. While this improves quality of data, it limits the scope of the design to shallow rivers, where the structure is accessible. Their results show that customization of support and design, as part of the methodology, is a critical component to characterize flow in an energetic site. Nortek [14] offers a number of options for performing measurements in deep locations, such as using a cable attached to a surface buoy. However, for high velocity environments, this makes data collection difficult, as the high velocity creates large drag forces and can push the device, forming an angle. While this angle is able to be corrected by using the IMU, the severity of the angle causes problems with cable entanglement and interference by the cable. The angle can also pose a threat to the device itself, as it is possible for the cable to tangle with, or even break the probe of the ADV.

In terms of applications to HKTs, Gunawan *et al.* [19] used an ADV to collect long term measurements in the tidal portion of the East River in New York City to assess the potential hydrokinetic resource from the tides. They found that measurements can often under-predict the hydrokinetic resource. They also mention that there are environmental concerns with taking long term measurements with an ADV. They found that damage can be caused to the device due to corrosion, and caution other users to protect their device [19].

Based on literature findings, the device that is most suitable to measure velocity is the Nortek Vector ADV. This ADV contains an IMU, which collects data pertaining to the motion of the ADV itself. In this way, motion compensation can be performed on the motion of the ADV. Vanzweiten *et al.* [21] showed that the error of the IMU is too large to be able to properly compensate the motion of the ADV in low current channels. However, they state that in channels with velocity higher than 2.5 m/s, the IMU error is overshadowed by the turbulence data, implying that it is possible to use the IMU to compensate the motion of the ADV. These measurements were performed in-stream. Other studies, such as the study done by Lovenbury [22] showed that the IMU can be used to accurately compensate for ADV motion in a controlled laboratory setting at low flow speeds. However, none of the studies address the problem in Figure 1.1 where an ADV can be used to measure the velocity profile. There is no literature on this at high velocities in rivers. Moreover the velocity profile is required by the marine industry for high energy flows.

2.1.2 Acoustic Doppler current profilers

ADCPs are another type of instrument that measures flow velocity in water using the Doppler effect. It is commonly used in hydrological surveying to measure the volumetric flow rate of a river. It is also used extensively to survey hydrokinetic

Table 2.2: Literature review for ADCP devices at low and high velocities

Author	Device	Region	Max U [m/s]	Results
Nidzieko *et al.* [15]	ADCP	Tidal	0.70 Near bed	Some ADCP modes can underpredict Reynolds sresses by up to 23%
Gooch *et al.* [23]	ADCP	Tidal	1.95 Mean 3.95 sustained	Able to obtain many useful flow characteristics such as maximum sustained velocity, velocity and power mapping
Colby and Corren [24]	ADCP	Tidal	2.50	Bin size of 20 cm or smaller for adequate shear results and reduction of spatial averaging. However, ADCP cannot capture small scale turbulence due to spatial averaging
Muste *et al.* [25]	ADCP	River	0.96 Mean	ADCP not sufficient to capture fine flow statistics although mean velocity and turbulence intensity can be accurately captured
Shives and Crawford [26]	ADCP	Tidal	2.00	ADCP can be used to predict TKE reasonably accurately but dissipation rate calculations are problematic
Garcia *et al.* [27]	ADCP	River	3.29	ADCP can be used observe salinity and bi-directional flow statistics
Mueller *et al.* [28]	ADCP	River	N/A	ADCP can be used to measure streamflow, but adequate techniques and analysis are required. Issues such as side-wall interference can occur.
Muste and Spasojevic [29] and Muste *et al.* [30]	ADCP	River	N/A	ADCP should not be used to gather data on velocity profiles from a moving boat because of scatter from the beams. Additionally, a fixed boat can provide good velocity profile data, however, due to the spatial and temporal averaging, the ADCP cannot be used to accurately analyze turbulence characteristics

potential in tidal applications. A summary of literature on the capabilities of the ADCP is shown in Table 2.2. Unlike ADV, which measures a single volume, they can be used to measure the velocity profile, as the beams allow for collection of multiple flow volumes through the water column.

Gooch *et al.* [23] performed a tidal hydrokinetic assessment with an ADCP. They found that the ADCP is useful for obtaining power maps and sustained velocities, which are of importance for the placement of hydrokinetic turbines. Additionally, Garcia *et al.* [27] found that the ADCP can reliably collect data on the salinity of the environment, as well as statistics related to flow bi-directionality.

However, Colby and Corren [24] performed a hydrokinetic assessment of a tidal site with an ADCP. They determined that for adequate shear results, a maximum bin size of 20 cm is required. This presents a problem, because for some ADCP devices,

the bin size is set automatically, without the control of the user. Additionally, even with this small bin size, the ADCP cannot capture smaller scales of turbulence due to the spatial averaging present in the method of the device. Nidzieko *et al.* [15] found that the ADCP can underpredict Reynolds stresses by up to 23%. This can cause problems for the assessment of turbulence in the region, which is an important factor for assessing the hydrokinetic potential of a site. However, studies such as the one performed by Shives and Crawford [26] state that turbulent kinetic energy and turbulence intensity were found with reasonable accuracy. They also state that the dissipation rate was difficult to assess due to low temporal resolution. Muste *et al.* [25] also suggest that some technical limitations of the ADCP be addressed by manufacturers before they can be used to capture detailed flow statistics. Finally, Mueller *et al.* [28] found that there are dangers with interference from channel walls on the data from an ADCP. The fact that ADCP have divergent beams make turbulence measurement challenging.

Of importance to note is that moving platforms are not desired for flow characterization studies. Muste and Spasojevic [29] performed a study on a mobile platform and then Muste *et al.* [30] performed a follow up study on a fixed platform. What they found was that a moving platform does not allow for accurate measurement of velocity profiles. In the follow up study, they found that a fixed boat was acceptable for such an application, but that turbulence characterization with the device was still not feasible.

The consensus is that, while ADCPs are useful devices because of their simplicity, robust design and ease of deployment, they are good at measuring mean flow statistics. They can be used to predict turbulence, however, they having difficulty with small scale turbulence and dissipation rate. ADCPs also have the shortfall of having wide, divergent beams that can cause errors in the data if there is reflection on the side walls.

Table 2.3: Literature review of shear probe devices

Author	Device	Region	Max U [m/s]	Results
Wolk *et al.* [31]	Shear probe	Tidal	2.00	Shear probe resolves turbulence scales between 0.01 and 1 m, low noise, turbulence parameters velocity shear and dissipation rate can be resolved
Ross [32]	Shear probe and VPR	Ocean	N/A	Obtained "good" measurements of dissipation rate in a wide range, even with other structures which could cause errors in measurement due to vibration.
Kocsis *et al.* [33]	Shear probe and temperature microstructure profiler	Lake	N/A	Compared dissipation rate calculations between temperature microstructure and shear microstructure. Generally good agreement, dissipation rate ranges over 6 orders of magnitude
Woods *et al.* [34]	ADV and shear probe	Lake	N/A	Dissipation rate and TKE compare well between shear probe and ADV, but moving vessel and difference in deployment techniques make for a difficult comparison
Tanaka *et al.* [35]	Shear probe and LADCP	Tidal	1.50	Observed dissipation rates from the VMP are significantly smaller than the numerical predictions, although the trends agree
McMillan *et al.* [36]	Shear probe and ADCP	Tidal	2.50 depth averaged	When used in conjuction with acoustic instruments such as ADV and ADCP, shear probe can be used to help assess flow at all turbulence scales
Fer and Paskyabi [37]	Shear probe, ADV	Ocean	N/A	Can obtain time series/depth series of TKE and dissipation rate

In order to meet the objectives outlined in Section 1.6 and address the requirements in Figure 1.1, the ADCP and HADCP are employed to characterize the flow, and the results are compared with the ADV to determine the utility of the device for characterization measurements in Chapter 4. More importantly, all ADCP data is averaged for the duration of the ADV measurements. Many studies use the ADCP while traversing the river with a boat in motion. No traversing ADCP measurements were taken in this study to improve accuracy of results.

2.1.3 Shear probe

The shear probe is a device that is used in oceans to collect turbulence data. It operates using the piezo-electric effect, which is detailed in Appendix A The device facilitates the collection of turbulence data throughout a water column in oceans. A summary of literature of studies that have used the shear probe is shown in Table 2.3.

Wolk *et al.* [31] performed a study using the shear probe in a tidal channel, with a velocity near 2 m/s. They found that the shear probe exhibited low noise, can resolve turbulence scales over a wide range and that it can resolve important parameters such as the dissipation rate. Ross [32] also found that the shear probe can adequately collect sufficient data to resolve the dissipation rate. Kocsis *et al.* [33] collected data with two separate shear probe devices 35 m apart and found that the results agreed between the two devices.

Woods *et al.* [34] performed ADV and shear probe measurements in a lake. What they found was that the dissipation rate and TKE are comparable between the two devices, although motion from the boat may have had an effect on the ADV, making comparison difficult. The dissipation rate varied between 10^{-9} to $10^{-5} m^2/s^3$.

Tanaka *et al.* [35] observed in their study, that dissipation rate obtained by the shear probe is smaller than what is predicted using numerical models, however, when the trends are compared, there is agreement between numerical and experimental results.

The shear probe cannot measure mean velocity. For hydrokinetic assessment, mean flow is required for power assessment. Additionally, the shear probe is limited to a turbulence scale range of 0.01 to 1 m, which is inadequate in the river where some scales of turbulence can be as large as the depth of the river. However, the shear probe is unique in its ability to gather micro-scale turbulence data in a water column. McMillan *et al.* [36] put forth the idea that, with the shear probe and the aid of acoustic devices, such as ADV or ADCP, it is possible to gather information about all scales of turbulence. Additionally, with these other devices, the mean flow data and power data can be obtained as well, based on the approach in Section 1.7. Fer and Paskyabi [37] set up a unit which contains multiple devices, including the ADV and shear probe. This device was deployed in a single location and left to collect a

time series of data.

The study by Fer and Paskyabi collected a wealth of data about a single point, however, there is still a need to use multiple instruments at varying points to obtain a comprehensive data set for flow characterization for hydrokinetic turbine sites. For the experiments performed in Chapter 4, all three devices are used, allowing for a detailed comparison between the instruments, as well as resolution of all relevant data required to perform a hydrokinetic assessment in a river. However, significant development is still required to achieve confidence in all measurements.

2.2 Measurement devices applied at high velocities

Although acoustic devices can be used at 2 to 4 m/s, the measurements discussed in Chapter 1 are difficult, as cited by Neary *et al.* [38]. Birjandi *et al.* [39] measured velocities at Pointe du Bois in front of a HKT. The instrument selected for velocity measurement is the Vectrino ADV because of its capability to measure in field settings, as well as the compactness of the instrument. In that study, many challenges invovled with high-velocity river measurements are highlighted. For example, they cite a reduction in naturally occuring particle count in cold seasons. This impacts the ability of acoustic devices to accurately measure the velocity. To address this, milk particles were injected into the flow upstream of the ADV. Next, a significant number of spikes were found in the dataset. These spikes were due to excessive bubbles present in the flow. Despiking algorithms are developed to replace these spikes in post-processing, with valid, interpolated data points. Finally, these measurements were taken around an operating turbine. It was discovered that the flow upstream of the turbine is influenced by whether the turbine is operating or not.

The measurements performed by Birjandi *et al.* [39] and Woods [40] formed the knowledge base for the experiments in the current study, as these were some of the first measurements performed around an operating hydrokinetic turbine in high velocity flows.

2.3 Turbulent flow

Hydrokinetic turbines are used in high-energy, turbulent flows. This means that turbulence measurement is required to perform hydrokinetic turbine site selection. In this section, literature pertaining to naturally occurring large scale turbulence in rivers and micro-scale turbulent flows in laboratories are discussed.

Turbulent flow has been studied extensively, however, the most relevant research to river flow characterization are the studies that are focused on open channel flow. Table 2.4 provides a summary of pertinent literature on turbulence in laboratory and rivers.

Due to the nature of open channels, it is difficult to assess the length scale with which to calculate dimensionless properties. Some studies use depth, such as the study by Nikora *et al.* [41], hydraulic diameter, such as Arango [48] and others use hydraulic radius. As discussed in Chapter 1, hydraulic radius is the length scale used in the present study. This is because the hydraulic radius takes both the width and depth of the channel into account. This decision is supported by Sukhodolov [42], who found that longitudinal geometry has more effect on the flow than features such as channel bends.

In terms of calculable quantities in rivers, the turbulence dissipation rate varies significantly [41] [43]. In many cases, the value falls in the range of 0.005 to 0.2 $\frac{m^2}{s^3}$ [41] [43]. Other commonly calculated quantities are the Froude number and

Table 2.4: Literature review of turbulent flow in open channels

Author	Device	Region	Max U [m/s]	Results
Nikora *et al.* [41]	Pressure devices	River, shallow and narrow	3.43	Studied turbulence in 3 rivers, calculated Reynolds number using depth ranging from 1.6×10^5 to 5.7×10^6. Froude numbers ranged from 0.44 to 1.01 based on depth. Dissipation rate ranges from 0.006 to 0.118 $\frac{m^2}{s^3}$ and the kolmogorov length scales ranged from 0.05 to 0.11 mm
Sukhodolov [42]	ADV	River, bend and shallow	0.2	Uses a rigid structure to lower ADV to measure turbulence, however river is only 3.75 m deep at maximum. Reynolds 2.3×10^5 to 2.4×10^5, Froude 0.03 to 0.07. Conclusion is that longitudinal non-uniformity has more of an effect than channel curvature. Turbulence intensity increases closer to the wall.
Nikora *et al.* [43]	Micropropeller	River, shallow	0.5 to 0.75	Turbulence distributions satisfy log and power equations. Largest turbulence intensity near the river bottom, 15 to 20%, longitudinal velocities satisfy $\frac{-5}{3}$ kolmogorov law, ϵ decreases as distance from discharge source increases and ranges from 0.005 to 0.2 $\frac{m^2}{s^3}$
Tachie *et al.* [44]	LDA	Lab	0.33 to 0.77	Boundary layer was 50% of channel height in high speed flows and 80% in low speed flows, flow profile in the open channel reaches a maximum at the boundary layer height and then decreases until the free surface
Nezu [45]	Review	Review	N/A	Literature review of open channel turbulence. Turbulence intensity is shown to increase close to the channel bottom. Shows that in some cases, trends observed in the laboratory are relatable to the field
Roy *et al.* [46]	EM current meter	River, gravel bed and shallow	0.66	Large scale turbulence occupies entire depth of river, similar values to laboratory experiments,
Shvidchenko and Pender [47]	ADV	Lab, gravel bed	0.99	Turbulent flow does not appear random. Vertical size of eddies is close to flow depth, longitudinal distance is 4-5 depths on average. Conclusion is that large scale turbulence is ordered and common in open channel flows

Reynolds number, where Reynolds number can be in the range of 1×10^5 to 3×10^7, while Froude number indicates how gravity impacts the flow. $Fr < 1$ indicates sub-critical flow, $Fr = 1$ indicates critical flow and $Fr > 1$ indicates super-critical flow. These values vary due to the variation in geometries and velocities. However, typical Reynolds numbers at the CHTTC range from 1.3×10^7 to 2.5×10^7, based on the hydraulic radius.

In terms of turbulence statistics, many studies agree on the shape of the vertical profile. Sukhodolov [42], Nikora *et al.* [43], Tachie *et al.* [44] and Nezu [45] all

found that turbulence intensity increases as depth increases, or rather, the turbulence intensity increases close to the wall. This is found not only in rivers, but in controlled laboratory settings as well.

When observing the scales of turbulence in open channel flows, there is a large variability. Most agree that the large scales of turbulence occupy the entire depth of the water column, as well as multiple depths across the span of the flow [46] [47]. In terms of the small scales, there are few studies report their values. However, if dissipation rate is known, it is possible to estimate the kolmogorov length scale. Nikora *et al.* [41] found that in a shallow, fast moving river, the kolmogorov length scales can range from 0.05 to 0.11 mm.

2.3.1 Velocity profile in open channel flows

In this section, literature on vertical velocity profiles in open channel flow are intestigated. Many laboratory experiments and numerical simulations have been performed on open channel flows. However, there is relatively little information on velocity profiles in rivers, and not at high velocities. The experiments in this study will be compared to the profiles found in literature to observe the difference between laboratory and numerical studies, and a riverine environment. A summary of relevant literature on velocity profiles in open channel flow is presented in Table 2.5.

Most studies agree that in open channels at low velocities there exists a velocity defect below the free surface. This is described as a dip, or a location of maximum velocity below the surface. Such a phenomenon is reported by Abbaspour and Kia [49]. For the purposes of this study, it will be referred to as the location of maximum velocity, Y_∞. In some channel studies, such as the one performed by Afzal *et al.* [50] or as seen in Balachandar and Tachie [51], a velocity defect near the surface is not observed. In this case, the location of maximum velocity is simply the boundary layer thickness.

Table 2.5: Summary of literature on vertical velocity profiles in open channel flow

Author	Device	Reynolds number	Results
Abbaspour and Kia [49]	Propeller velocity meter, Numerical	6.2×10^4 - 1.4×10^5 based on R_h	$D = 0.1$ m $\delta = 0.4D$, surface defect, on average $0.8D$
Afzal *et al.* [50]	Laser-Doppler anemometer (LDA)	$2.3 - 7.2 \times 10^4$ based on depth	$\delta = 0.4D$ on average. No surface velocity defect
Balachandar and Tachie [51]	LDA	$1.3 - 2.6 \times 10^4$ based on R_h	$\delta = 0.69D$ for 80 mm depth and $0.81D$ for 50 mm depth
Tachie *et al.* [52]	LDA	$1.5 - 2.8 \times 10^4$ based on R_h	δ ranges from $0.4D$-$0.7D$. Case had low Re and low turbulence
Tachie *et al.* [53]	LDA	$4.5 - 4.9 \times 10^4$ based on R_h	δ is approximately $0.32D$
Bonakdari *et al.* [54]	Theoretical	N/A	Based on $Ar = \frac{L_Y}{D}$, correlations are found for point of maximum velocity
Wang *et al.* [55]	Theoretical	N/A	Correlations are found for the point of maximum velocity

These studies were performed between 0.3 and 0.5 m/s

Bonakdari *et al.* [54] developed a correlation for Y_∞ based on other experimental and numerical studies. The profile is based on the aspect ratio of the channel with

$$\frac{Y_\infty}{D} = \frac{42.4 + Ar^{4.2}}{94.7 + Ar^{4.2}} \tag{2.1}$$

where Ar is the aspect ratio, defined by channel width divided by depth. It is stated in this study that the correlation becomes asymptotic when Ar exceeds 6. This may be a problem for rivers, as they can often be more than six times wider than they are deep. Conversely, Bonakdari *et al.* [54] suggest the correlation by Wang *et al.* [55], where

$$\frac{Y_\infty}{D} = 0.44 + 0.106 \times Ar + 0.05 \times \sin(\frac{2\pi}{5.2}Ar), \qquad Ar < 5.2 \tag{2.2}$$

Both Equation 2.1 and Equation 2.2 will be compared to the experimental results discussed in Chapter 4 of this study. Their relevance to river applications and

Reynolds numbers are assessed. Since both correlations are created using relatively low aspect ratios, when compared to rivers, it is likely that their ability to predict the location of maximum velocity will be incompatible with a riverine setting.

It is also commonly found that the boundary layer thickness ranges from 40% to 70% [52] of the water depth in the channel, although it can be as small as 32%, such as in the case of Tachie *et al.* [53]. This is for Reynolds numbers from 10^4 to 10^5. This range is much lower than for rivers. In the current study, Reynolds numbers are on the order of 10^7. Details on the boundary layer thickness and their relation to the depth of the river for highly energetic flow will be presented in Chapter 4.

2.4 Energetic marine hydrokinetic site characterization

Since it is known that fluid structures impact HKT performance, it becomes apparent that to understand how well a turbine will perform in a given river location, it is required to characterize the flow. This type of research is still relatively new and under development for highly energetic river sites. There is no accepted way to assess an energetic site for the placement for a hydrokinetic turbine. However, there are some best practices from the limited research performed in this area. Table 2.6 summarizes the work done in site assessment. For instance, researchers at Oakridge National Laboratory have documented their characterization experiences for tidal and riverine HKT sites [38] [56]. They outline the theoretically expected outcomes before discussing results of their own, obtained at Marrowstone Island. They discuss aspects of site characterization, such as bathymetry, velocity and turbulence profiles, river sediment and bed forms, temperature and fluid properties, as well as other criteria. For obtaining their flow measurements, the researchers at Oakridge National

Laboratory utilized an ADV and an ADCP. They also mention that using these devices in high velocity flows can be challenging and even infeasible. The current study proposes a procedure which may address this issue. For bathymetry, they used the techniques outlined by Muste *et al.* [57], which involves the use of a multi-beam echosounder. Alternative methods are explored in this study, and will be compared with methods summarized in Table 2.6.

In terms of studies with various instruments, the work performed by Lueck *et al* [58] is of note. A measurement system was developed that contained shear probe, ADV and ADCP devices moored underwater to measure flow. Matt *et al.* [59] developed a platform which used several ADVs and temperature probes to assess turbulence in ocean environments. Finally, Hay *et al.* [60] use a series of instruments, namely ADV, ADCP and a time-of-flight velocity sensor to assess hydrokinetic potential in a tidal stream. All devices in that study were bottom mounted.

Numerical modelling of rivers is also a common method of hydrokinetic resource assessment. Thyng and Riley [63] performed one such study of the tidal resource in Puget Sound. Using a numerical model, they were able to asses the area of maximum power over the study area. Numerical hydrokinetic potential has been assessed in Canada with hydrologic data. Jenkinson [10] performed such a study with Marine Renewables Canada. It was found that Canada has a potential of 300-700 GW, however it is noted that for some rivers, there was not adequate data to provide a good assessment. The Canadian Hydraulics Centre [64] performed a study into the hydrokinetic potential of Canada using hydrologic modelling and the Manning Equation. A similar study was done for Alaskan rivers by Previsic and Bedard [65] using available data from the United States Geographical Service. They used the volumetric flow rate from measurement stations and a logarithmic correlation to approximate the velocity at each measurement site. Using oceanic models, a study

Table 2.6: Literature review of hydrokinetic site assessments

Author	Device	Region	Max U [m/s]	Results
Neary *et al* [38]	ADV, ADCP	Tidal and river	1.50	Best practices are prescribed for rivers and tidal channel flow measurement using ADV and ADCP. Fixed and cable-deployed ADVs are investigated
Neary *et al* [56]	ADV, ADCP, numerical	Tidal	2.00	Hydrokinetic power density is obtained using ADCP and ADV for an inlet tidal channel
Muste *et al* [57]	Echosounder	1.00-2.00	N/A	"Nemo" measurement vessel used to measure all 3 devices
Lueck *et al* [58]	Shear probe, ADCP and ADV	Tidal	3.00	"Nemo" measurement vessel used to measure all 3 devices
Matt *et al.* [59]	Shear probe, ADV, underwater imaging	Ocean	N/A	Goal to be able to take undewater imaging as well as record turbulence data. Were able to assess impact of turbulence on image degradation. Challenges with obtaining turbulence data. Getting TKE dissipation with ADV is more successful in high energy environments
Hay *et al.* [60]	ADCP	Tidal	1.60 depth averaged	Assesses turbulence characteristics in a tidal channel using ADCP. Also calculates the friction velocities and drag coefficients.
Kalnach *et al.* [61]	Aquadopp Profiler	River	2.42	In the area studied, approximately energy available is 1 GWh/year/km of river
Arango [48]	Numerical	River	2.70	Studied hydrokinetic assessment downstream of dams. Reynolds from 1×10^7 to 3.3×10^7 based on hydraulic radius, not a lot of focus on turbulence levels. Focus on capacity factor and performance of turbines in the area
Toniolo *et al.* [62]	ADCP and multi-beam echosounder	River	1.50	Performed bathymetric survey, Fr = 0.3, collected data in ENU coordinates, plot Reynolds stresses in ENU coordinates.
Thyng and Riley [63]	Numerical	Tidal	N/A	Goal to eliminate field work to cut costs, but comparison with field data is important. Looks at tidal forces but does not include information about turbulence statistics
Jenkinson [10]	Hydrological	River and large scale	Varied, depending on location	300-700 GW for all rivers in Canada, BC, Ontario, Quebec and NWT offer high potential in particular
NRCan [64]	Hydrological	River and large scale	Varied, depending on location	Hydrologic models and equations are applied to government-supplied data. Only preliminary phase completed thus far
Previsic and Bedard [65]	Hydrological	River and Large Scale	1.84	Large scale resource assessment of hydrokinetic power in Alaskan rivers. Velocity profiles are obtained by calibrating relationships between volumetric flow rate and velocity. Flow rate data obtained from USGS
Georgia Tech Research Corp [66]	Numerical	Tidal and large scale	Varied, depending on location	Numerical analysis of coastal United States. Shows power density, which is relatable to flow velocity, but does not show turbulence statistics
Duerr [67]	Numerical	Tidal	1.80	Publicly available data as input, assesses the power potential of an area over the course of 2 years
Lalander *et al.* [68]	ADCP	River and tidal	Varied, data are normalized	Study focuses on utlization of river sections, using velocities that were close to the turbine rated velocity, utilization in rivers is above 50% and 45% for tidal applications

was done on the tidal resource in the United States by Georgia Technical Institute Research Corporation [66]. Using the results of the study, a database is published for

all sites with an average power density of 500 W/m^2 or higher.

Numerical assessments can be used to ascertain how much power is actually extractable from the hydrokinetic resource. This involves turbine efficiency and velocity ranges. Lalander *et al.* [68] performed a study for rivers, finding that regulated rivers have a utilization of 23%, with 19% and 17% utilization for unregulated rivers and tidal currents respectively.

A numerical assessment of where to place turbines in a specific channel is presented by Duerr [67]. Power data is the result of a numerical assessment from an oceanic model. This data is available for specific cross-sections of the tidal channel. In this way, the cross-section with maximum power can be selected for turbine placement.

In the study performed by Kalnach *et al.* [61], an Aquadopp Profiler was used to determine the available hydrokinetic power of the Daugava River. An average maximum velocity was found to be 2.42 m/s, which is near the numerical values generated by Arango's study [48]. The depth of the river in their study, however, ranges only from 2.1 to 3.2 m, which is fairly shallow for most practical rivers. Even considering the flow depth, they found that the river offered hydrokinetic energy of 1 GWh per kilometer of river per year, which works out to 114 kW of power per kilometer of river. It is unclear in the paper how much of this river is potentially available for of hydrokinetic turbines. Another in-field river study was performed by Toniolo *et al.* [62], who found that the Tanana River has an average available power of 4500 W/m^2. Their work included field data collected with ADCP and numerical modelling of the river.

One important numerical study from Table 2.6, Arango [48] presents a numerical assessment of hydrokinetic power downstream of dams. The study focuses on the performance of turbines in a river setting. With a mean velocity of approximately 2.70 m/s and Reynolds numbers from 1×10^7 to 3×10^7 downstream of the dam.

Arango suggests to observe flow about 500 to 800 m downstream of the dam, as this river section has a large amount of kinetic energy [48]. It is not stated whether this is due to the geometry of the region, or whether it is due to the effects of the dam. In addition, the results are generated from a numerical model, which means that how well the results reflect the physical system is unknown. The study has no discussion of the turbulence of the river, and how this affects potential turbines.

The present study adds to the literature to satisfy the need for using accurate measurement instruments in energetic rivers. New procedures are required to be developed to characterize the flow profile along the water column and addresses the challenges dissused in Section 1.5.

2.5 Impact of flow on hydrokinetic turbines

Water velocity impacts the performance of turbines. These effects differ between different types of HKTs. For example, it has been shown that Reynolds number, vortex shedding frequency and inlet flow condition affect the performance of vertical-axis hydrokinetic turbines [69]. At low Reynolds numbers, the power coefficient increases with Reynolds number, while at high Reynolds numbers, the coefficient becomes less sensitive to Reynolds number. Reynolds number also affects the tip-speed ratio and stall characteristics of the vertical axis turbine. Vortex shedding frequency was found by Birjandi and Bibeau [69] to affect the power output of the turbine. Prime frequencies were found to decrease the power of the turbine, while frequencies between the two prime frequencies actually increased the power.

Additionally, for vertical axis turbines, Cavagnaro [70] found that turbulence significantly affects control. Since the turbulence fluctuations cause changes in the power output, controls can be applied to the turbine to optimize power output.

Examples of controls include changing the pitch and angle of attack of a turbine blade and altering the characteristics of the generator to optimize grid operation. These turbulence fluctuations, however, operate on varying time scales, from hours to seconds, and this means creating control schemes for each time scale and frequency domain. Cavagnaro [70] identified that it is difficult to control for turbulence frequencies below 1 Hz, since the turbine cannot respond well at these frequencies. Cavagnaro also pointed out that controlling at these frequencies results in negligible gains in power production.

Alternatively, for cross-flow turbines, increased turbulence increases the stall angle for the turbine. Bachant and Wosnik [71] found that this allowed for a larger range of angles of attack, which is beneficial for cross-flow turbines, which have varying angles of attack. They also found that the drag coefficients increase more rapidly in turbulent environments than non-turbulent environments, for high tip-speed ratios.

Depending on the type of turbine and surrounding area, the effects of the boundary layer in the river may affect the power output of the turbine. This is especially true for axial flow turbines, which can operate near the bottom of a river [72], which can potentially still be in the boundary layer, depending on the flow. The effects will depend on the boundary layer height, as well as the velocity defect and turbulence in the boundary layer.

Additionally, vortices can play positive and a negative role in the power production from HKTs, as shown in Figure 1.1. For example, some turbines operate purely on the principle of vortex-induced-vibrations, as some researchers are working on at the University of Michigan [73]. In the case of these types of turbines, they can operate in relatively slow flows, as low as 0.25 m/s, which give them a wider operating range than most existing HKTs. In terms of negative effects, Gunawan *et al.* [74] found axial flow turbines to have a reduction in power production, when introduced to the

vortices behind a cylinder. This effect, however, is dependent on the streamwise distance between the cylinder and the turbine.

2.6 Other measurement techniques

Other researchers have used alternative measurement techniques for riverine characterization. One of these methods is using PIV, on a large scale, which is called large scale PIV or LSPIV. Hauet *et al.* used this technique on a relatively small river [75]. They found that the LSPIV was effective at measuring discharge rate, when compared to USGS data, finding that it is more accurate than an ADCP. However, they mention that there are numerous challenges to the technique, such as having a sufficient number of seeding particles and uncertainty in measurement [75]. Techniques using hot wire anemometers are not suitable for riverine applications due to the size and accessibility challenges of the river.

Others use a hydrologic approach to characterization, such as a study done by the EPRI [76]. Using the hydrologic equation and GIS software, they performed a study to assess the hydrokinetic potential of rivers in the United States. They used the Manning equation to perform their analysis and calculate their results. However, some have said that the Manning equation is accurate for some situations, though, not for all rivers, because of the estimation of the roughness coefficient [77].

2.7 Environmental effects of hydrokinetic turbines

One of the benefits of HKTs is that they do not produce GHG during the energy conversion process. There are, however, other potential effects on the environment that these turbines may have. Some studies have been done to determine how these

devices affect local aquatic life. Jacobson *et al.* [78] at the Electric Power Research Institute (EPRI), found that HKTs create less harsh physical conditions than the environment experienced by traditional hydro turbines. This is due to low rotational speeds and a relatively minor physical impact on the environment. In terms of danger to aquatic life, Jacobson *et al.* [78] found that fish have a 98% survival rate when traveling downstream past these turbines. In a full-scale test, it was found that, while the path of certain fish species was impeded, there were no significant injuries or deaths.

Hammar *et al.* [79] also investigated the effects of HKTs on fish swimming behaviour. Additionally, in a study done by Normandeau Associates [80], it was concluded that there is little, if any effect on fish populations near operating hydrokinetic turbines. They found that the effects of the turbine are non-hazardous. Hammar *et al.* [79] also found that large arrays of turbines would restrict mobility of the fish, especially for large and predatory species. For this reason, the size of each turbine array should be related to the size of the river, as well as the fish species in the area.

Currently, there is more research going on in the environmental impact of hydrokinetic turbines, including projects at the CHTTC involving students from Carleton University [81], that monitors the impact of turbines on fish passages. Flow characterization provides information for fish research, however, this aspect is not covered in the current study.

Chapter 3

Experimental procedures

In order to meet the requirements of characterization of hydorkinetic turbines outlined in Figure 1.1 and Table 1.1, flow measurements involving multiple devices and procedures are formulated. The first type of measurement occurs just below the surface and is designed for a general understanding of flow over a large experimental domain. Next, a procedure is developed to allow for the use of a Horizontal ADCP, or HADCP, to take measurements from a side profile. Then, a procedure for collecting bathymetric data is required and is designed to minimize acoustic beam reflection from the river bank. Finally, a comprehensive procedure is designed to accommodate simultaneous, stationary measurements with an ADV, ADCP and a shear probe. All of these procedures together characterize the hydrokinetic resource. Table 3.1 shows the details of each instrument. Note the instrument error shown is only one of the many errors when taking measurements in highly energetic flows. A detailed error analysis is performed in a separate study.

Table 3.1: Details

Instrument	Model name/number	Developer	Manufacturer quoted error
ADV	Vector	Nortek	±0.5% of measured value ±1 mm/s [82]
ADCP	M9	Sontek	±0.25% of measured velocity ±2 mm/s [83]
Shear Probe	VMP 250	RSI	±5% [84]

3.1 Methods to secure measurement instruments in riverine environments

In order to take measurements, the measurement instrument must be secured in the water, using a measurement platform. This platform can be fixed, or free to move. Measurement procedures are developed to allow interchangeably fixed and mobile platforms to secure measurement instruments in the flow during measurements.

3.1.1 Fixed measurement platform

In measurement situations where being stationary is possible, a pontoon mounted fixed platform vessel is utilized. The vessel used at the CHTTC is shown in Figure 3.2.

The advantage of a fixed platform is that both point and profile measurements can be performed, without significant platform motion. This system can be anchored using electric winches to shore or river bed anchors. A point measurement system is designed for the fixed platform. Specifically, a horizontal arm is used to rotate a depth arm, to which is clamped the measurement instrument. This is done by rotating a crank which rotates the horizontal arm and the depth arm, which facilitates the deployment and retrieval of the instrument. Additionally, a mechanical stopper is

Figure 3.1: Fixed measurement platform used at the CHTTC without measurement instruments on the mounts.

designed and placed such that the depth arm cannot rotate beyond 90°. This makes the depth arm more stable, removing vibration of the measurement arm due to the turbulent flow and vortex shedding. The depth arm is designed such that multiple different types of measurement instruments can be attached to it, for various types of measurements. Instruments attached to these designs include the sonar camera, vertical and horizontal ADCPs, and ADVs. These point measurements allow the measurement instrument to be placed just beneath the water, at depths between 0.5 and 1.75 m. Structural pipes are thick walled, with an outer diameter of 7.62 to 10.16 cm.

For most turbines, the most important flow characteristic is the mean flow velocity, as shown in Figure 1.1. Because there are many different turbine designs, including

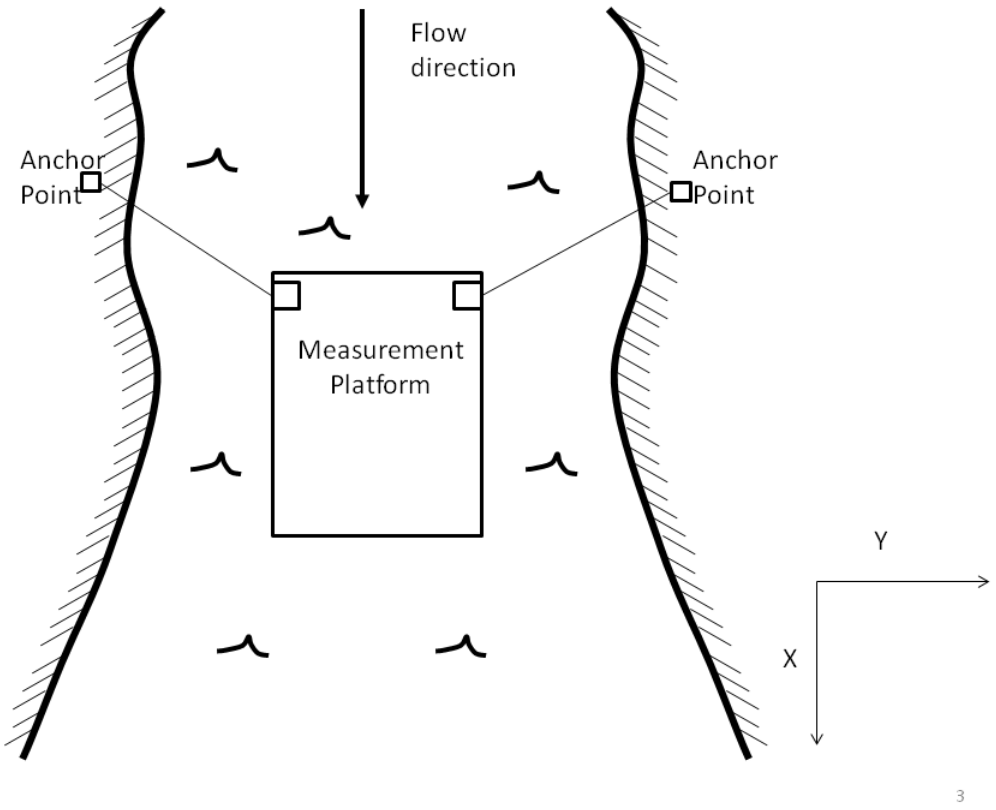

Figure 3.2: The method of fixing the platform. A secondary boat is used to carry winch cables from the measurement platform to the shore of the river. Then, the same is done on the opposite side of the platform. Winch controllers are used to tighten the anchor lines to fix the platform in the flow.

ones that are based on near-surface flow, and some that are well below the surface of the water, a flow profile is required to understand the power density contained in the river. This profile can be obtained in multiple ways. A design for obtaining flow profile data from the ADV and ADCP, as well as methods for obtaining turbulence profiles with the ADV, ADCP and shear probe, are facilitated with the fixed measurement platform. To fix the platform, battery operated winches are used to anchor to shore anchors, as shown in Figure 3.2. A detailed analysis of the measurement error is beyond the scope of this study.

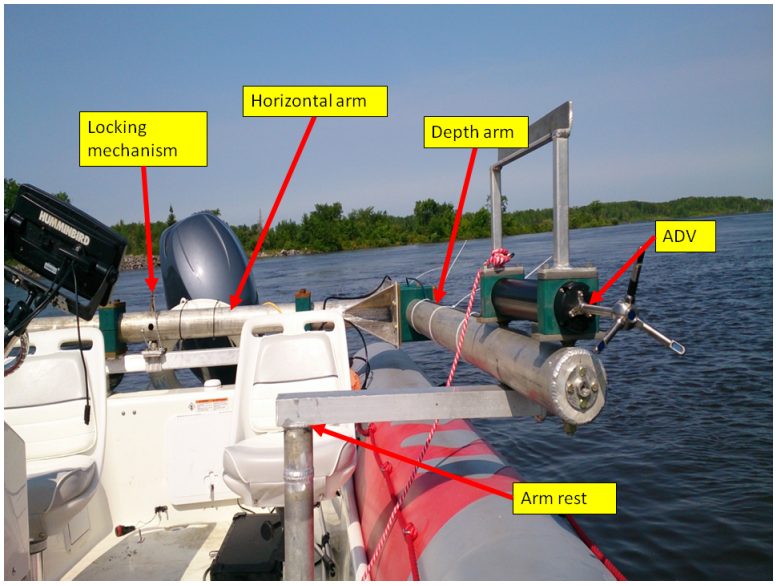

Figure 3.3: Measurement zodiac boat outfitted with equipment to perform surface measurements (mobile platform)

3.1.2 Mobile platform

When characterizing a large area, a light vessel is desired, to increase maneuverability through narrow channels or rocky areas. For the survey measurements performed at the CHTTC, a Zodiac is the boat of choice for mobile platform measurements. To outfit the boat for measurements, support structures can be designed to secure each instrument.

Instrument supports are made to be adjustable to facilitate multiple rapid measurements, in various environments and applications. The measurement equipment is to be attached to a depth arm which is held off of the side of the boat by a horizontal arm. These arms are secured using clamps, allowing them to rotate when the clamps are loosened. The design is shown in Figure 3.3.

The measurement procedure is performed with four people; a boat driver, an instrument operator and two operators of the support system. The boat driver is responsible for finding a landmark on the shore in the spanwise direction and

holding the boat steady while the short measurement, approximately two to five minutes, is taking place. The instrument operator is controlling the measurement instrument, operating the software, as well as recording relevant data and notes about the measurement. This person is responsible for selecting the measurement sites based on GPS coordinates and recording pertinent information about the measurement. The other two people operate the ADV mount. One person is at the stern of the boat and one person is near the bow, at the resting point for the depth arm. The person at the stern must loosen the bolts of the clamps holding the horizontal arm. While this is happening, the person at the bow of the boat ties a rope around the ADV mount, as shown in Figure 3.4. This rope is to retrieve the arm once the measurement is complete. Once these two tasks are complete, the person at the bow of the boat lifts up the depth arm such that it can clear the arm rest. Then, the person operating the instruments, the person at the stern of the boat and the person at the bow of the boat push the arm outwards. Once the depth arm is over the edge of the boat, the person at the bow of the boat allows the depth arm to rotate slowly into the water. While it is doing so, they hold on to the rope to prevent it from rotating past 90°. Once the depth arm has reached 90°, the person at the bow of the boat cleats the rope. At the same time, the person at the stern of the boat locks the horizontal arm with the locking key, securing the arms. This holds the depth arm at 90°. The person at the stern of the boat then tightens the bolts on the clamps of the horizontal arm.

Once the measurement is completed, the procedure is performed in reverse to bring the depth arm back onto the boat. If multiple measurements are to be made, the arm is brought to be parallel to the water surface and the rope is used to tie it in this position. The depth arm is suspended over the water surface. This makes for rapid re-deployment once the new location has been reached. Caution is to be exerted when this practice is used, because if the boat hits a large wave and the arm hits the water, it could cause instability in the boat or damage the probe. Additionally, the

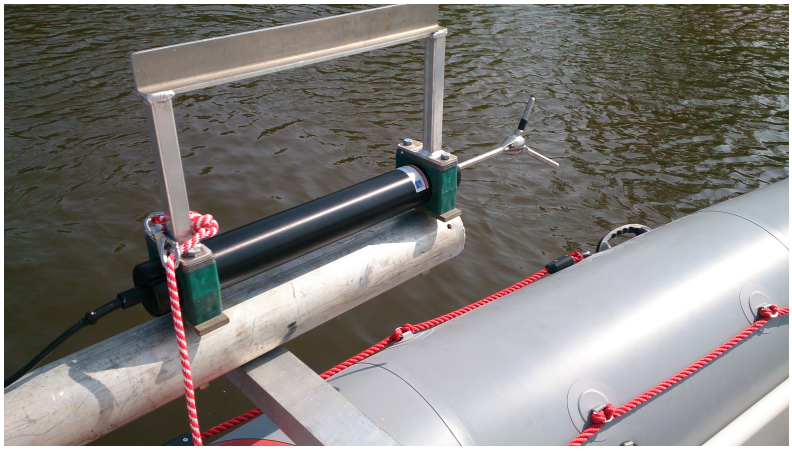

Figure 3.4: ADV attached to depth arm with safety rope for deployment and retrieval. Same arm can be used to attach other measurement devices such as ADCP, HADCP and sonar camera by changing the adapter

probe of the measurement device could contact protruding rocks.

Spatial awareness and operator safety during mobile measurements is a primary concern. Even though the boat driver is attempting to hold the boat stationary, there are still small motions that occur over the course of a measurement. Crew members have to be alert to potential dangers. For example, hitting underwater hazards with the probe in the water can cause damage to the instrument that is recording, which can result in repair costs exceeding $20,000 and 4-12 weeks of instrument repair time. Since motions during measurements are small and relatively controlled, safety to personnel is not significantly affected unless the flow at the measurement location is confined between narrow rocky river beds. If this is the case, performing measurements should be abandoned, or additional safety measures are enacted, as safety of the research personnel cannot be compromised.

3.2 Acoustic and flow measurement instruments

Involved in the development and characterization of hydrokinetic turbine sites is the use of acoustic and flow measurement instruments. Two of these instruments include the ADV and ADCP, the uses of which are discussed. In this section, use of the underwater sonar camera and HADCP are discussed and the shear probe instrument is presented.

3.2.1 ADV

In this section, the procedure and system designed for velocity profile measurements using the ADV is described. Since the ADV collects data over a small sample volume of approximately 8.5 mm^2, this is considered as a point measurement when compared to the overall size of the river. First, the needs and constraints of the measurements are identified.

1. Since the ADV collects point-wise data, a procedure is needed to move and hold the ADV underwater, at known, stationary depths, for the duration of a recording
2. This data may be recorded for a long period of time so as to understand flow variations over long cycles
3. The system must remain as stationary as possible during the recording
4. The system must be relatively easy to deploy and retrieve
5. The system must be able to be re-deployed, to perform measurements at different locations
6. The sensor head can hit mooring lines, the vessel or rocks, which may compromise the unit or instrument. Care must be taken in moving the

instrument

Next, a system must be designed to meet all of these needs and constraints. A cable based system was first designed and fabricated. The idea is to lower a cable to the bottom of the river using weights, somehow attach the ADV to the cable, then allow the ADV to slide up and down this cable at known depths. A fin is attached to the back of the ADV, to align the ADV with the flow such that the X direction of the ADV is aligned with the streamwise direction of the flow. Initially, a pulley design is tested, but it was found that having two cables caused tangling of the cables and made the ADV difficult to move, as the flow can exceed over 3 m/s and the resulting forces on the cable overpower an operator. Cable tangling also causes potential damage to the ADV, as the ADV can get tangled and consequently damage the sensor head. Additionally, the weight was difficult to retrieve, especially when deployed in high-energy flows. Moreover, the system required to be placed in the centre of the platform so as not to shift boat buoyancy to avoid increased drag on the pontoons. Figure 3.5 shows the cable-pulley system initially tested and proved inadequate.

To improve ADV profile measurement, a single steel cable holding the weight is deployed using a battery operated winch. The winch is secured to an arm mounted on the fixed platform deck. This improvement removes the possibility of cable entanglement, as well as making it easier for the operator to retrieve the weights.

Next, a method of attaching the ADV to the cable is devised. The ADV must be able to travel along the cable so as to measure different depths. For this purpose, a structure is fabricated using perforated steel channels and clamps. The steel channels are used to form the structure of the unit and to provide a place to locate clamps, as well as providing a method of ensuring the unit travels along the cable. The clamps, which hold the ADV to the unit, are fastened to the unit using bolts and nuts. The final assembly is shown in Figure 3.6. It is important to note that the ADV is to be

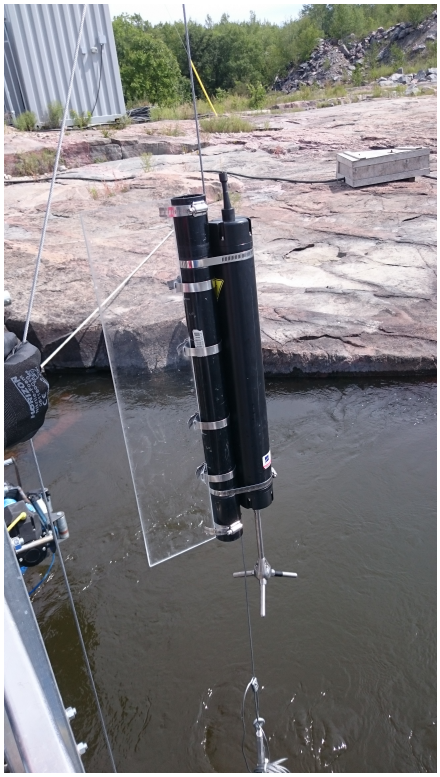

Figure 3.5: ADV first design using a cable pulley system about to be deployed in front of the fixed platform. Testing showed that instruments located in the front caused excess weight by operator and increased drag on the blue pontoon. A mid-section approach was then selected, along with a single guide wire to prevent cable entanglement.

oriented with the X direction probe pointing toward the flow direction. This is the standard orientation to be used with all other devices.

Finally, since a method is required to control the depth of the unit, a wire rope is tied to the unit, as shown in Figure 3.7, and kept on board the boat. The operator releases the ADV to let it fall to a lower depth, or pull up on the rope to bring it to a higher depth. Since there is a pressure sensor on the ADV, the depth is known when the ADV is connected to a computer.

The complete procedure is as follows: first, the measurement boat is taken upstream of the desired measurement point. Then, using a second mobile boat and the winches on the side of the boat, the measurement boat is tied to anchors on both sides of the

Figure 3.6: New ADV deployment unit fabricated from steel channel and clamps. To reduce operator requirements, a winch is installed to lower anchors (not shown). A rope is connected to the unit for operator-controlled placement of the unit in the water column.

river. This keeps the fixed platform as stationary as possible while the measurement is going on. At this point, the cable must be fed through the ADV unit and attached to the weights. Then, the cable and weights are lowered to the bottom of the river, while using the wire rope to keep the ADV unit above the surface of the water because the wire rope can be tied to the winch arm, as seen in Figure 3.8. Since the flow pushes the cable and weights downstream of the fixed platform, the fixed platform is slowly moved downstream using the winches. This should then place the platform over the desired measurement area. Once the platform is directly above the weights, the cable bends in the flow. To reduce this curvature, the cable is tightened using the electric winch. Care is taken in how much the cable is tightened, because reeling in the winch too much results in the weights being lifted off of the river bed and then being pushed

further back in the flow. This can be avoided by testing the tightness of the cable by pulling on it by hand. Once the cable is tighter, indicating that it will not come in anymore without lifting the weights off of the riverbed, the ADV can be attached to the unit and subsequently, the data cable to the ADV. At this point, the ADV can be lowered to any desired depth along the cable, with minimum bending of the cable, resulting in keeping the ADV vertical. The result is shown in Figure 3.8. In addition, the wire rope and the computer cable of the ADV are to be fastened together, so as to prevent cable entanglement, as shown in Figure 3.9.

Moreover, the more weight added to the bottom of the cable, the less downstream the weights drift. As much weight should be added as possible. However the capabilities of the electric winch and the ability of the operators to lift the weights into the water for set up need consideration.

Figure 3.7: Amsteel blue rope fastened to ADV unit so as to allow the user to control the depth of the unit

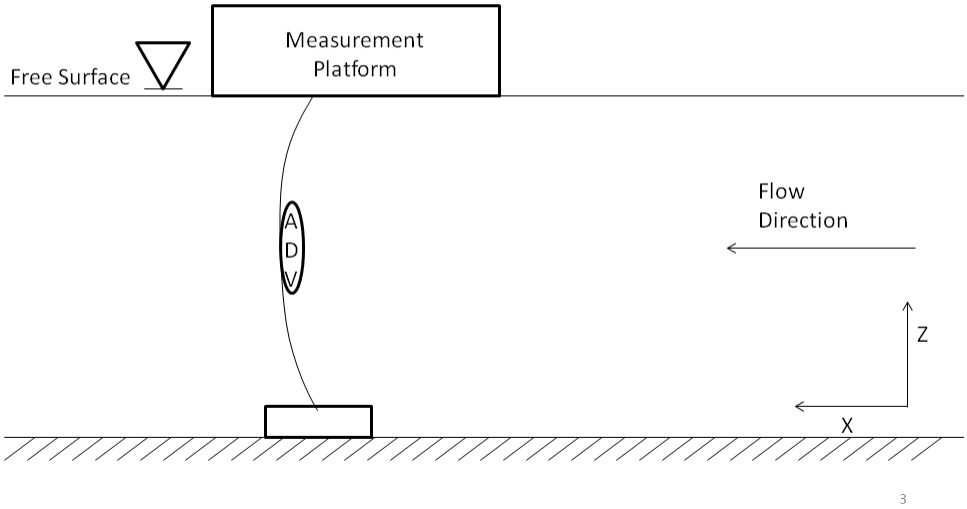

Figure 3.8: Schematic of ADV measurements with blue pontoon winch setup

3.2.2 ADCP

The ADCP measurement procedure begins with the same setup as the ADV measurement. The advantage of the ADCP over the ADV is that the ADCP can capture a velocity profile from a single surface position, and can be secured directly to the measurement platform. Since the platform is relatively stationary, and the ADCP

Figure 3.9: ADV data cable fastened to wire rope

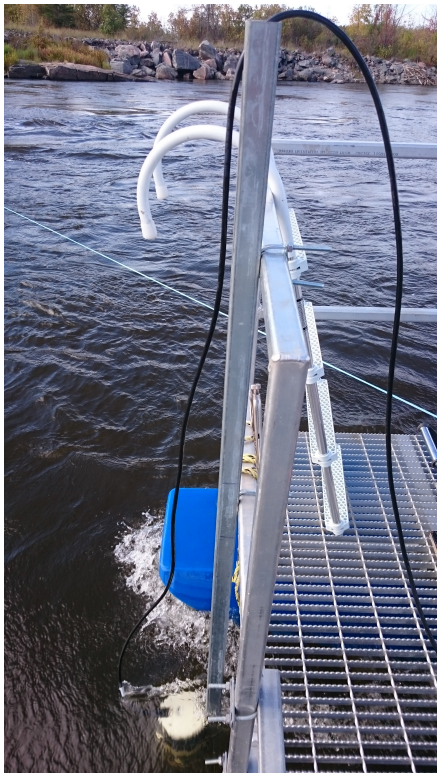

Figure 3.10: ADCP and channel fastened to the front of the measurement boat with U-bolts

is fixed to the platform, this ensures the instrument is stationary, and thus reduces potential error in the readings that would be created from instrument motion.

The setup for the instrument is relatively simple. First, protective rubber is strapped around the instrument to protect it from potential damage from clamping. Next, the device is secured to a steel channel. The data cable is then connected to the device, and the channel is then clamped, using U-bolts, to the front of the fixed platform, such that the ADCP is just below the surface of the water, as shown in Figure 3.10. It is important to note that the orientation of the ADCP should be the same as the ADV, in that the X direction, and subsequently the U velocity, are pointing against the flow direction, which will result in negative U results. This ensures consistency between measurement results.

Once the setup is complete, the ADCP is controlled from a computer and begins

recording. This setup is specifically designed so as to be compatible with the ADV, such that both procedures can be executed at the same time, from the same vessel. Such a set up allows for a detailed comparison of the data, since the two devices are near each other and measuring the same flow. Collecting data at exactly the same point is difficult in the riverine environment, so, for the purposes of the analysis, turbulence and mean flow are assumed to be isotropic, i.e. that they do not vary through the streamwise or spanwise directions. This assumption is reasonable over the distance between the ADV and ADCP.

To interpret the data, the method the ADCP collects data must be understood. The beam of the ADCP spreads as it gets further away from the device. The spread angle of the beam varies with each device model. For the ADCP used in the experiments, the spread angle is 25°. The beam is separated into cells from the device to the riverbed. The velocity is averaged over each cell, which causes a loss in spatial resolution, making it difficult to detect underwater flow structures, especially as if the cell size is relatively large. Additionally, a blind spot exists at the bottom of the beam. The size of this blind spot was 2 m for the measurements performed with the ADCP, meaning that no data 2 m from the riverbed was collected. There is also a "blanking distance" just below the sensor head, where no data is collected. This blanking distance was 0.6 m for the measurtements in this study. A schematic of the ADCP beam is presented in Figure 3.11.

3.2.3 HADCP

Another form of the ADCP that is used for flow characterization is the Horizontal Acoustic Doppler Current Profiler (HADCP). This device is used to obtain a "top down" view of the channel velocities and takes measurements from the side of the channel. It sends acoustic beams horizontally across a flow channel. This

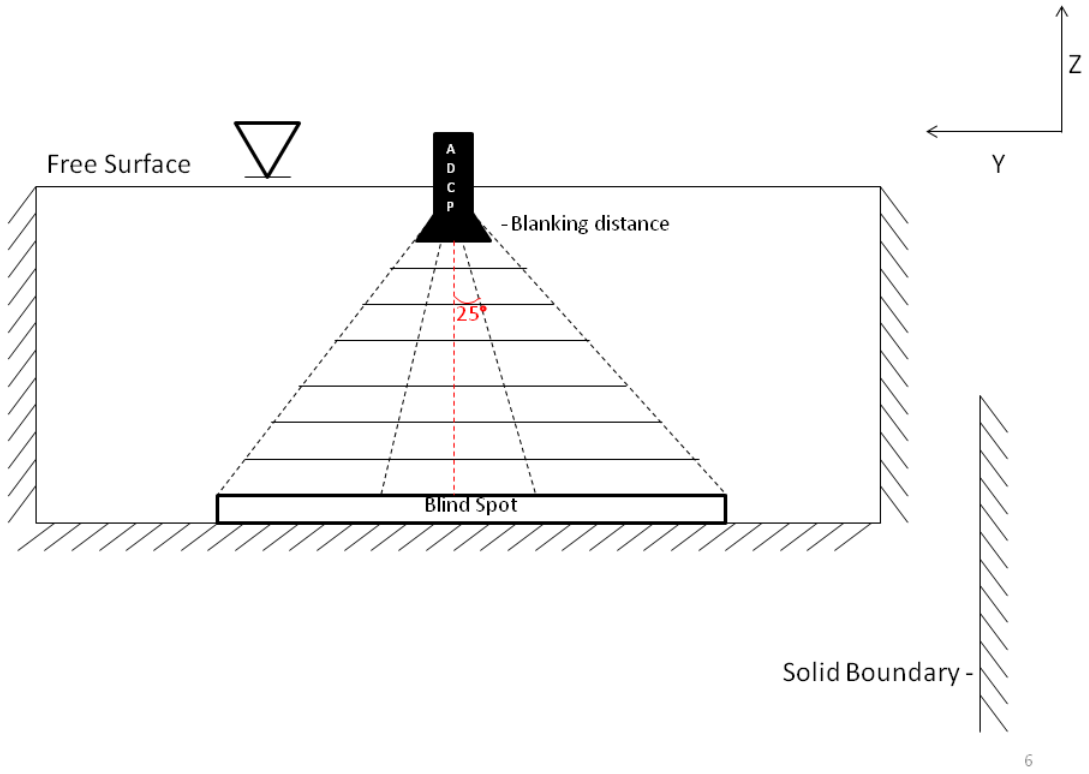

Figure 3.11: Schematic of ADCP beam spread, blanking distance and blind spot. The M9 ADCP has four beams, three of which can be seen in the schematic

device samples a spanwise-streamwise plane of the velocity, which is required for the deployment and location of surface-mounted turbines. It can be a critical tool to address performance standard requirements, such as IEC/TS-62600-200 [85], as it avoids having to place a vessel on top of mooring lines and in front of a turbine. Its orientation provides safety advantages to navigate with both a fixed and moving platform. A custom attachment is developed to fix the HADCP to the motorized boat and fixed platform, as shown in Figure 3.12. Since this type of ADCP does not gather vertical profile information, it cannot be compared with the ADCP, ADV or shear probe data, however, the device contributes to hydrokinetic site characterization. The HADCP can capture the wake of small objects near the surface of the water [86]. The HADCP discussed here is manufactured by Teledyne RD Instruments.

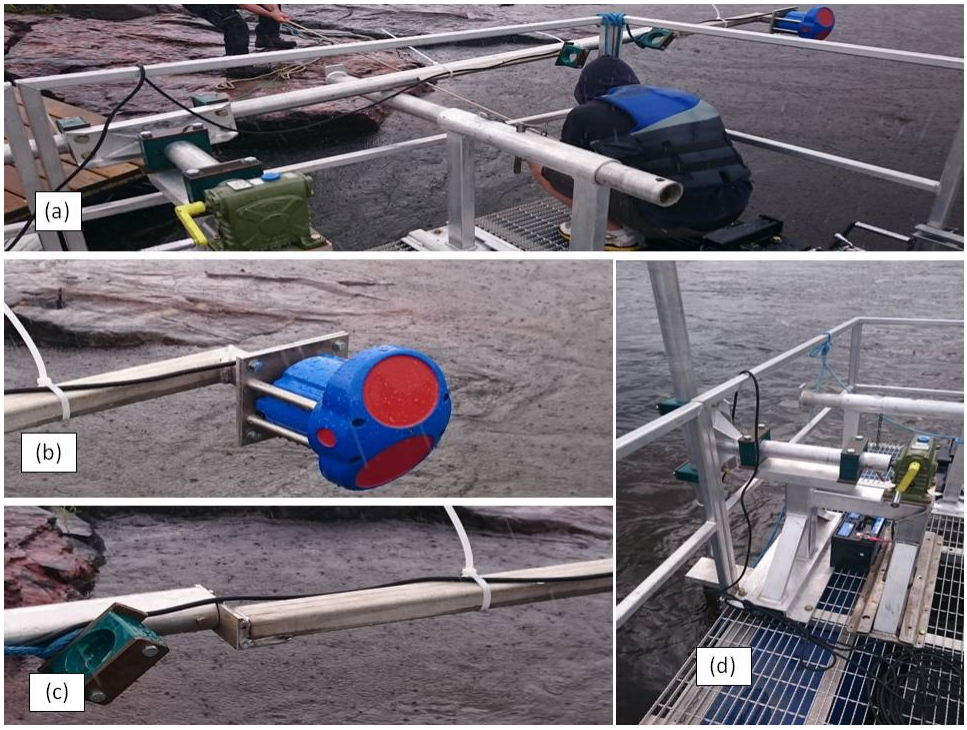

Figure 3.12: (a) Point measurement system on the fixed measurement platform, (b) adapter and H-ADCP attached to the depth arm, (c) method of securing the instrument cable to prevent cable vibration, and (d) measurement system in operation with hand crank to rotate the depth arm in and out of the water

The first step to using the HADCP is to identify a reach of river to be characterized. Then, as the device collects data in horizontal bands across the river, multiple cross-sections can be selected. For the measurement to be set up properly, the GPS coordinates of each measurement location of the fixed or mobile platform must be recorded. Interpolation between the cross-sections can be performed to obtain a full contour of the desired river reach.

The procedure when using the mobile platform is similar to the surface and free stream measurements, in that the driver of the measurement boat must keep the boat as stationary as possible during measurement. Contour plotting can be done in plotting software, such as Tecplot or GIS software, as presented by Birjandi *et al.* [86]. Flow data shows the high velocity areas of the river, and give an indication of the best locations to perform detailed depth measurements and to place a turbine. The

results of the contour plotting can be seen a technical report written by Birjandi *et al.* [86], for the CHTTC channel.

The designed measurement system for both the mobile platform and fixed platform allow the measurement depth of the HADCP to be adjusted, which allows for the characterization of HKT sites within 2 m of the water surface. The HADCP is a useful device, not only for characterizing a river section, but also for visualizing the inflow and wakes of turbines, to compare with power measurements obtained from the turbine. Finally, the software of the HADCP allows for the amount and size of bins across the column to be adjusted by the user, and not pre-set by the software, as with some other ADCPs. All these advantages make the H-ADCP an ideal instrument for the characterization of potential hydrokinetic turbine sites.

3.2.4 Shear probe

The shear probe works on the principle of piezo-electricity, and the one used in the characterization experiments in this study is designed by Rockland Scientific Instruments. The instrument is designed to be dropped into a flow, allow gravity to carry it down to the bottom and subsequently retrieved. During this time, the piezo sensors located on the bottom face of the shear probe collect data on the fluctuations of the velocity in two directions, streamwise and spanwise, or X and Y, respectively. The collected data results in a profile, using the pressure sensor in the shear probe as a depth gauge. The instrument is designed to be launched from a boat that is drifting with the flow [31]. An image of the shear probe is shown in Figure 3.13. The instrument is an inclined profile instrument due to the drag of the flow forcing it downstream. Additionally, the instrument can be fastened to the platform. The shear probe does not collect data on the mean flow, instead, it captures velocity fluctuations. The shear probe adds to turbulence in hydrokinetic characterization. The turbulence

Figure 3.13: (a) Shear probe designed by RSI to be used in turbulence characterization (b) shear sensors which collect data as the instrument descends through the water column

data is compared with the ADV and the ADCP turbulence readings.

The procedure to launch this in characterization measurements is to assemble the shear probe on shore, because the sensors on the shear probe are very sensitive and are prone to damage, and attach a rope to it, so as to retrieve the device. A knot is tied in the rope at a length corresponding to the maximum measurement depth. This depth is usually 0.5 m above the river bottom, so as to avoid damage to the sensors. Then, a mobile platform is moved up to the measurement point and the shear probe is placed in the water. Then, the engine is quickly put in reverse and then to neutral, so as to immediately get the boat moving with the flow. Then, the shear probe is dropped and the rope is given a large amount of slack, so that shear probe is not dropping at an angle caused by a taught rope. Finally, once the knot on the rope reaches the fingers of the operator, the device is pulled back onto the boat.

This procedure can be repeated multiple times to obtain multiple profiles of velocity fluctuations. The data is stored on the shear probe itself, and is retrieved at a later time.

It is important to note that the sensors on the shear probe must be installed with directionality in mind. For example, the U shear probe is to be pointed against the flow direction, and the V shear probe is to be pointed directly perpendicular to this in the streamwise direction. This is so that the results are clear and understandable. However, when installing the sensors, the operator must take care that the U shear probe is aligned with something on the shear probe, such as the power magnet, so as to have a reference to the X direction.

3.2.5 Sonar

Sonar cameras, while not directly used for characterization, can be useful for the maintenance and upkeep of a hydrokinetic turbine testing facility. Since riverine environments often have no visibility, it is important to have a method of viewing objects under the water. The CHTTC employs a sonar camera to identify issues below the water. At the CHTTC, there are two forms of sonar regularly deployed: an ARIS sonar camera with a robotic mount, as well as a Humminbird sonar system with integrated GPS.

The ARIS camera is used for detailed viewing applications, such as observing sub-surface turbines in operation, as well as identifying items that may have fallen to the bottom of the river but are still retrievable. For example, researchers at the centre are able to capture sub-surface turbines in operation using this camera. An example of this application is shown in Figure 3.14, where a Clean Current turbine is monitored. The camera is also used to perform environmental assessments, such as observing fish behaviour around operating turbines.

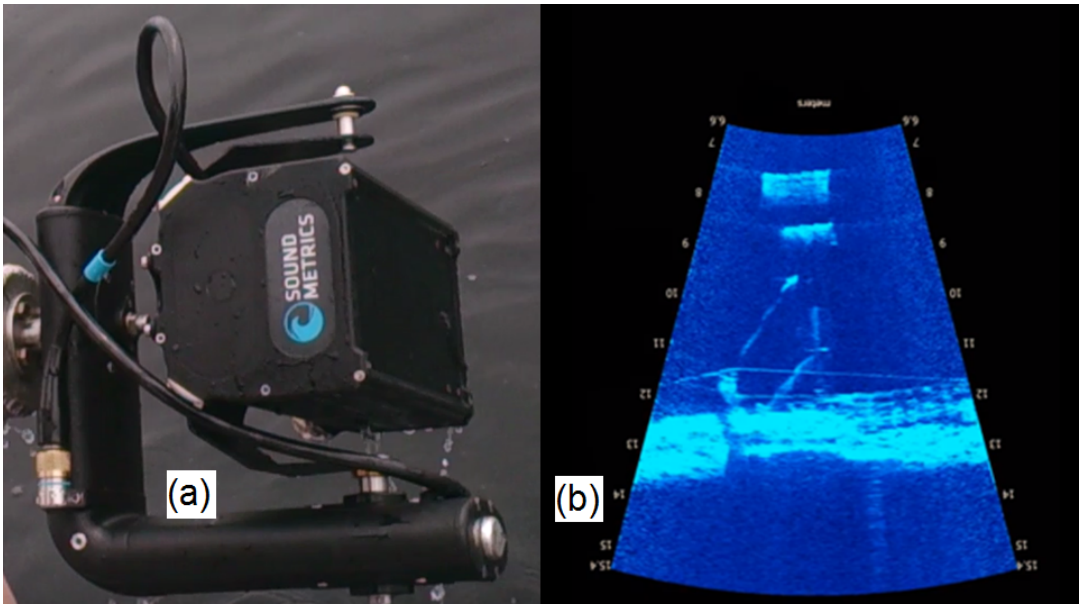

Figure 3.14: (a) Sonar camera employed at CHTTC attached to robotic mount and (b) underwater imagery of a sub-surface turbine captured with ARIS underwater sonar camera at the CHTTC

The sonar system with GPS is used for viewing applications which do not require as high of a resolution. This includes using it for bathymetry and for viewing of underwater objects. This is useful to perform a scan to determine if it is safe to put measurement equipment in the water near the river bottom or banks. The sonar system is also capable of viewing underwater in a variety of angles using side-imaging, so this makes it optimal for large-scale viewing of an underwater environment.

3.3 Boundary layer measurements

Characterization of the boundary layer in a riverine environment provides the location where the mean flow starts to decrease, and subsequently, the power density decreases. This analysis is particularly useful for turbines that are mounted on river bed, it quantifies the power reduction compared to the free-stream section.

The ADCP cannot be accurately used to assess the turbulent parameters of a

Table 3.2: Data recording frequencies for final characterization measurements

Instrument	Data Recording Frequency [Hz]	Sampling Frequency [MHz]
ADV	64	6
ADCP	1	1
Shear Probe	512	0.512

boundary layer. This is due to multiple reasons. The first is that there is a "blind spot" at the bottom of the ADCP column, in that no data is collected in this region. The size of this region varies, however, at the CHTTC, it is approximately 2 m in size, which could potentially cause the ADCP to miss the boundary layer entirely, or miss a large enough portion such that the boundary layer cannot be accurately visualized. The second reason is that, the deeper that the ADCP measures, it must perform more spatial averaging, due to the spread of the beam. This decreases the accuracy of the measurement and raises more uncertainties. Finally, due to the slower frequency output rate, small scales of turbulence could be missed, causing an inaccurate turbulence characterization of the boundary layer. The ADV and the shear probe are thus more suitable for the characterization of a boundary layer in a riverine environment. The frequencies of the instruments are summarized in Table 3.2

3.4 Bathymetry

The bathymetry of a channel is critical for the characterization of a hydrokinetic site. The bathymetry provides an indication of the safety of the site, i.e. where shallow and potentially hazardous regions are, as well as indicating the depths for the ideal placements of each of the different types of turbines. For example, a bottom-mounted turbine should be placed in an area with a relatively flat riverbed.

The procedure to measure the bathymetry is to take a mobile platform equipped with a GPS and a single-beam sonar system, as shown in Figure 3.15. Because the sonar

Figure 3.15: Humminbird 898c HD GPS and sonar system.

system has a single beam, it is much preferable to a multi-beam system, as single beam minimizes the reflection from steep river banks. One of the capabilities of this system is that it connects with the sonar system on the platform and scans the bottom, displaying the results on screen, to the boat driver. This display can be recorded for later observation. These recordings can later be brought onto a computer with the HumminbirdPC software, and further viewed with the HumViewer software. The HumViewer software can also export .kml files which contain the GPS coordinates and depth measurement, in meters, of each "ping" of the sonar. This data can be copied into a data file or excel file for further processing.

Multiple passes are recorded along the desired channel area using the boat. A recording is performed with the sonar for the duration of each pass. Measurements are performed in a time frame where changing water level is assumed to be insignificant. However, in the cases where the measurements exceed an hour or when they are taken across multiple days, they can be corrected based on the water level data supplied by Manitoba Hydro.

3.5 Characterization of the CHTTC channel

One of the objectives of the research was to calibrate the CHTTC for hydrokinetic turbine testing. To do this, the stationary profile measurement procedure for the ADV

and ADCP, as well as the procedure for the shear probe are performed simultaneously, so as to provide data that can be used for characterization, as well as for a comparison of measurement devices.

First, a preliminary survey of the Seven Sisters channel is performed using the free stream and surface measurement technique with the mobile platform. Ten points are measured along the channel, so as to get an understanding of the range of velocities to be expected in the free stream flow at the CHTTC. The points are selected arbitrarily, but spaced so as to ensure a good, preliminary survey of the channel. These measurements were performed on August 7th, 2014, and their relevance to hydrokinetic characterization is shown in the test matrix in Table 3.3. The ten points selected are shown in Figure 3.16.

Table 3.3: Test matrix of characterization measurements performed at the CHTTC. All test requirements are from Table 1.1. o - major test meets corresponding test requirement. x - sub-test meets corresponding test requirement.

Test	Sub-test	Mean velocity	Turbulence	Time scale	Length scale	Dissipation rate	Velocity profile	Boundary layer	Bathymetry
Surface measurements		o	o						
Bathymetry measurements									o
HADCP surface measurements		o	o						
Point A measurements		o	o				o	o	
	1	x	x	x	x	x			
	2	x	x	x	x	x			
	3	x	x	x	x	x			
	4	x	x	x	x	x			
	5	x	x	x	x	x			
	6	x	x	x	x	x			
	7	x	x	x	x	x			
	8	x	x	x	x	x			
Point B measurements		o	o				o	o	
	1	x	x	x	x	x			
	2	x	x	x	x	x			
	3	x	x	x	x	x			
	4	x	x	x	x	x			
	5	x	x	x	x	x			
	6	x	x	x	x	x			
	7	x	x	x	x	x			
	8	x	x	x	x	x			
Point C measurements		o	o				o	o	
	1	x	x	x	x	x			
	2	x	x	x	x	x			
	3	x	x	x	x	x			
	4	x	x	x	x	x			
	5	x	x	x	x	x			
	6	x	x	x	x	x			
	7	x	x	x	x	x			
	8	x	x	x	x	x			

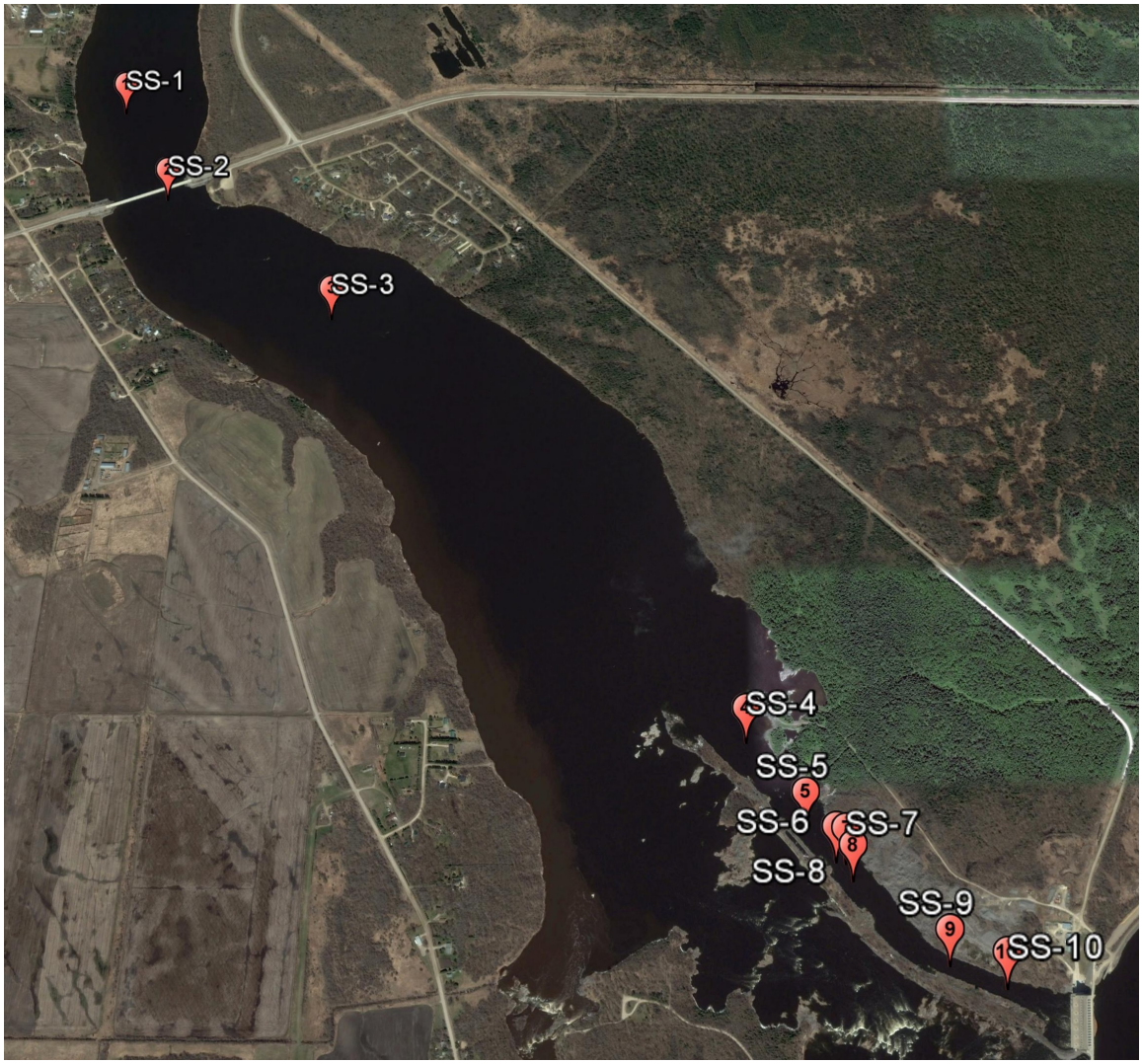

Figure 3.16: Google Earth view of the ten locations selected for a preliminary characterization survey of the CHTTC

A bathymetric survey is then performed using the method explained in Section 3.4. The bathymetric survey yielded interesting results far upstream and downstream of the CHTTC, however, in the portion of the river closest to the CHTTC, the channel is man-made, and thus is a uniform depth for a large reach of river.

Next, a survey is done using the HADCP, which provides a more comprehensive understanding of the free stream flow. A sample of these results are available in Reference [86]. The details of this survey are further given in the technical report written by Birjandi *et al.* [86]. The measurements were performed between July 14th

and July 16th of the year 2015.

Finally, between September 28th and October 1st 2015, characterization measurements are performed at the CHTTC, using the profile measurement technique for the ADV, ADCP and shear probe simultaneously. Measurement points are selected based on the availability of anchor points for the pontoon boat. There are three anchor points that are easily accessible and that are available to be used for characterization measurements. A Google Earth view of the channel, with the measurement points, labeled Point A, Point B and Point C, along with many of the obstacles in the channel, is shown in Figure 3.17

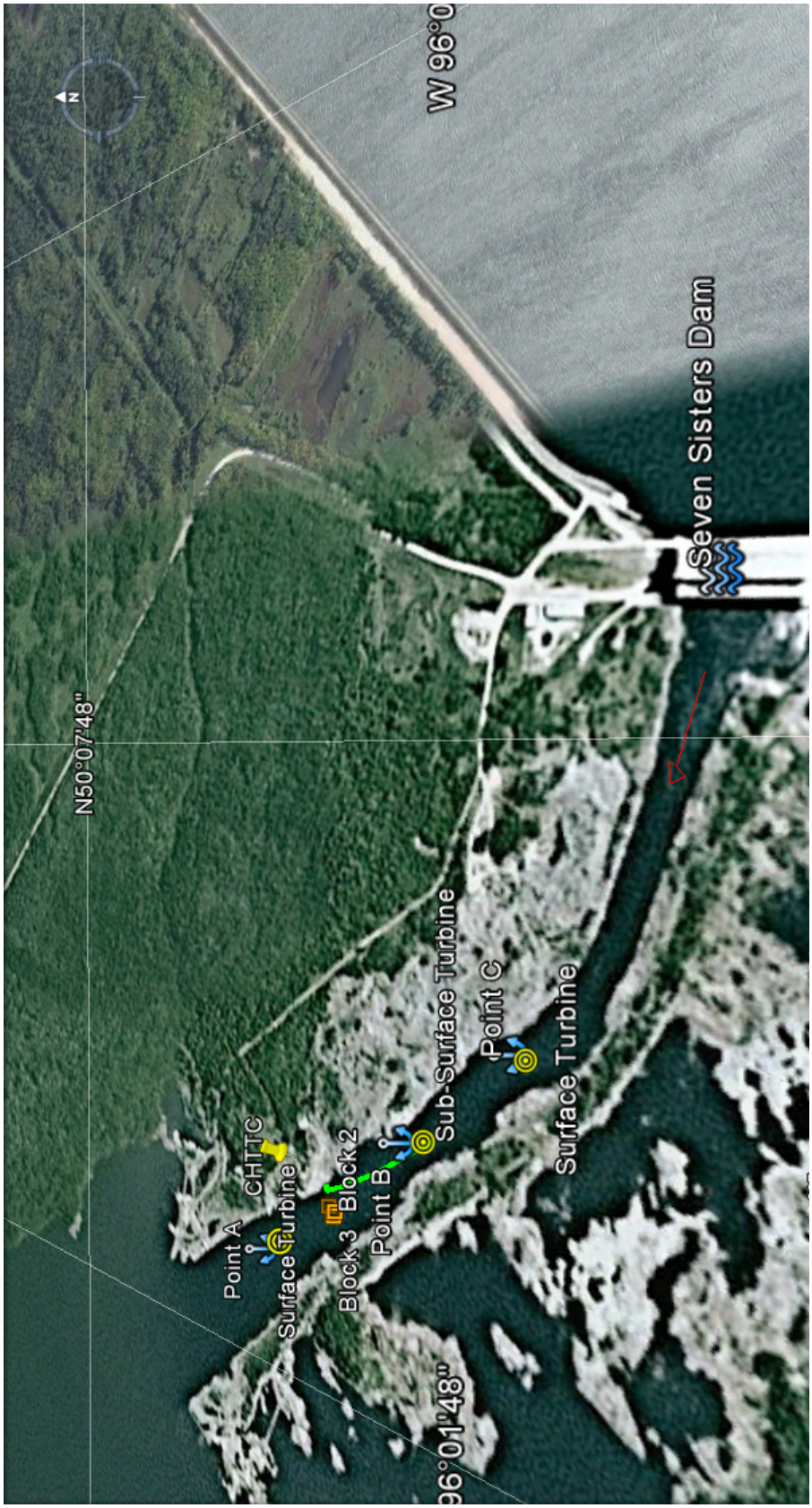

Figure 3.17: Google Earth view of the three points selected for final characterization measurements of the CHTTC

3.6 Challenges with measuring flow velocities in energetic river sites

Collecting data in a riverine environment is much different than that of a lab. In a laboratory, the flow conditions are carefully generated, monitored and maintained. In a riverine environment, the flow conditions are generated by nature and cannot be maintained. In a laboratory environment, since the layout and geography of the environment is designed, it is much more accessible to measurement equipment and has convenient locations for measurements. In a riverine environment, there is no control over the geography or the environment, and all measurements and equipment designs must be made to work with the environment, since the environment cannot be altered to a large extent. Additionally, there are natural obstacles to performing measurements, as well as man-made obstacles which can pose a threat to researchers and equipment. In this section, challenges associated with measurements in riverine environments are discussed.

3.6.1 Mobile platform motion

For the mobile platform procedure, the platform must be kept as stationary as possible during measurements. In high energy flows, keeping the mobile platform stationary can be challenging. Since the navigator reacts to water currents, this means that the platform must move for the driver to feel a need to react. Even if the driver's reaction time is relatively fast, there still requires motion for the driver to correct. This means that the boat is always moving in the flow, however small the movements are. Additionally, the boat is moved vertically if a wave passes by. These motions affect the flow measurements, as the relative motion of the platform and, by extension, the measurement instrument, changes the flow speed perceived by the measurement

instrument.

It is assumed that, if the boat driver is trained, the position of the boat will fluctuate about one point, but the movements are sufficiently small, relative to the rest of the river, such that the measurement point can still be considered a point. It is also assumed that the region through which the boat is moving, however small, does not experience any changes in mean flow or mean turbulence. Therefore, given a long enough recording, the mean flow and turbulence levels can be extracted from the data, so long as the assumptions do not differ from the reality of the measurement.

Note that the fixed measurement platform anchored to the shore line experiences movement, but to a much lesser degree than a motorized boat.

3.6.2 ADV motion

In the profile, surface and free stream type measurements, the ADV is susceptible to motion. In the surface and free stream measurements, this comes in the form of the movement of the measurement platform. In the case of the velocity profile measurements, this comes in the form of the vibration of the cable.

The ADV has an IMU which records the orientation, angular velocity and translational acceleration of the ADV in three dimensions. Thus, it is possible to extract motion from the ADV data using a post-processing code. This code involves obtaining the orientation of the probe, either with the IMU itself or by assuming the first recorded data point is in line with the flow. Next, once the initial orientation is known, the orientation at the next data point, or time step, can be calculated by knowing the angular velocity of the first point and multiplying it by the length of the time step, which is the measurement period, or the inverse of the frequency of the device. The change in angle is then known, and the new orientation of the ADV is

known. The tangential component of the angular acceleration is seen by the device as a translational acceleration. This can be removed from the IMU acceleration data by knowing the radius of rotation. The angular acceleration is calculated by assuming that the time difference is sufficiently small such that the acceleration function can be approximated as linear, expressed as:

$$\alpha = \frac{\partial \omega}{\partial t} \approx \frac{\Delta \omega}{\Delta t} \tag{3.1}$$

where α is the rotational acceleration of the device, $\Delta\omega$ is the change rotational velocity read by the device between two time steps and Δt is the change in time between two data points. Once the rotational acceleration is calculated, the translational acceleration perceived by the device due to the rotation can be calculated by multiplying by the radius of curvature. This radius of curvature depends on the experimental set up, as well as which axis the ADV is rotating about. This gives us an acceleration offset.

Once the offset acceleration is known, this can be removed from the acceleration data which is output by the IMU. Then, the translational acceleration can be applied to the velocity readings by using the assumption that translational acceleration is constant over the measurement period, which is a reasonable assumption, as long as the frequency of the instrument is kept relatively high. In this case, the acceleration value is multiplied by the time step and subsequently subtracted from the velocity reading at that data point. It should be noted, in the results presented in Chapter 4, this motion compensation is not applied as the procedure is not yet robust. Further analysis of this motion compensation and associated error is being studied within the research group. A future study will quantify the error in the procedure due to instrument motion. This section is supplied as a suggestion for those considering these procedures.

3.6.3 Measurements near operating hydrokinetic turbines and safety considerations

One of the challenges working with hydrokinetic turbines is that they pose obstacles to equipment and personnel, and impact safety. At the CHTTC, anchor blocks, mooring cables, operating turbines, shallow and narrow channel sections are a few examples that need to be addressed. For reference, refer to Figure 3.17. To ensure that equipment is not damaged and that the risk to research personnel is mitigated, the researchers at the CHTTC have developed several guidelines and best practices.

Firstly, the GPS locations of every item that gets placed into the water is recorded. From this, a map of the potential hazards is created. This map can be uploaded into the GPS and sonar system, to aid the navigator. This is particularly useful for objects that are below the water surface, such as cables and shallow areas. The navigator is then required to have this map visible at all times when operating the boat and to use it to avoid all hazards.

Secondly, if any measurement equipment is in the water, it is imperative that the measurement platform does not make any significant movements. For example, for surface and free stream measurements, the navigator is keeping the boat as steady as possible, and is ensuring that any small movements do not cause the motor or instrument to contact rocks or mooring lines. However, when the measurement location is being changed by a significant distance, all measurement devices must be brought out of the water and back into the boat, until the next measurement location has been reached.

Finally, it is important that when operating in an unfamiliar environment or river system, a preliminary scan of the environment is performed, to identify any potential hazards. This is done using the GPS and sonar system to scan the depth of the

water in the region. Once sufficient surveying has been done and hazards have been identified, operations may begin after developing a plan.

3.6.4 Water quality

In highly energetic sites, the quality of the water and visibility can be poor. Unlike in a laboratory, the water in a riverine environment cannot be filtered or cleaned. Additionally, seeding particles like milk are difficult to add to the water to increase the quality of acoustic velocity measurements because of environmental sensitivity and complexity. This leaves few options to develop measurement procedures to get high quality data by having enough seeding particles. It is important, for this reason, to use measurement devices which are robust, and do not require excessive seeding particles. Additionally, they must be able to handle various water temperatures, given that the water temperature changes with season and geographic location.

There is also the issue of debris in rivers. In the case of the CHTTC, debris is not an issue, as the centre is located downstream of a dam. Any debris that is encountered at the CHTTC would have to be generated between the dam and the centre. In other locations, care to ensure the safety of the measurement platforms and equipment while operating is critical.

Finally, the issue exists of the cleanliness of the water. Such water will corrode instruments and hydrokinetic devices, as seen in a study done by Oakridge National Laboratory [19]. This means that it is desirable to have instruments that are corrosion resistant, especially for long term measurements.

3.6.5 Drag forces on underwater components

As previously discussed, in riverine environments, the flow conditions are not controlled by the researcher. For this reason, measurement equipment should be designed to handle a variety of flow environments. The major effect this has on the design of the equipment is the drag caused by high speed flows. In the case of the measurement designs created for the CHTTC, each measurement system is robust enough to handle either low or high speed flows, or the system can be easily modified for either case. For example, for the mobile platform, the pole system is designed to be strong enough to withstand very high flow speeds, however, the exact limits of the system have not been tested beyond 4.5 m/s. The strength of the system can easily be increased by changing the diameter of the poles, or by changing the clamp design. In the case of the profile measurement system for the ADV, more weight can be added to the bottom of the cable, so as to increase the weight-to-drag ratio.

To those unfamiliar with riverine environments, the speed of a river can be deceiving to the naked eye. Obviously, turbulent water looks fast from the surface, however, from experience at the CHTTC and at other locations along the Winnipeg River, it is apparent that some locations can have high speed flows, above 2.5 m/s, with no indication of the speed from the surface. This makes measurement potentially unsafe for those who are unfamiliar with riverine environments. The amount of drag on even a cable can be deceiving, as is found during the design of the ADV cable system. When the pulley system was tested, the amount of drag force on the cable and weight makes it nearly impossible to pull up by hand, while in still water, the system could be easily retrieved by one person. This means that the design process for a riverine environment must be iterative, especially since flow speeds and water levels can change.

Finally, turbulence can add another degree of complexity to the design of measure-

ment systems. Since eddies can vary in size and velocity, when they hit measurement equipment, they cause varying degrees of drag and vibration. Additionally, since turbulence can be time and space sensitive, the amount and size of the eddies will vary with time and measurement location. This means that the design of the measurement system must incorporate this, by minimizing vibration to prevent any resonance from the changing frequency of the eddies.

3.6.6 Vibration of measurement equipment

Vibration of measurement equipment is a serious problem, since it can damage the measurement device, it can cause fatigue and crack propagation on the equipment structure, and it can influence the device readings. For this reason, extra care should go into the design of measurement systems to prevent vibration. In some cases, it is difficult to eliminate vibration entirely. For example, in the case of the ADV profile system, the cable goes to the bottom of the river and is subject to a large amount of eddies along its length. A possible way to reduce this would be to increase the diameter of the cable, effectively making it a pole. However, this adds other difficulties of the system, such as excessive drag forces being added to the whole system, making it harder to keep the boat stationary and making retrieval of the device difficult.

Another method of addressing the vibration, in the case of the ADV profile measurement system, is to retroactively develop a method of removing the vibration of the ADV from the data, by using the built-in accelerometer. This requires an intimate knowledge of the device, as well as mathematics and physics. For example, the accelerometer generates noise, so the noise must be somehow filtered out, before finding out the true forcing frequencies.

A final example of equipment vibration is in the case of the fixed measurement platform. The arm system that it is equipped with vibrates more violently than

the system on the mobile platform. This is for a few reasons, some of which are that the gear box adds degrees of freedom and components, allowing for more vibration, as well as the fact that the poles are smaller in diameter than those on the mobile platform, making them react more to the same amount of forcing. This was corrected by adding a mechanical stopper on the side of the fixed platform, just below the water surface. There are slots for the depth arm to fit into, which restrict the motion of the pole, and therefore the vibration of the device.

3.6.7 Acoustic beam reflection

For instruments that use acoustic beams to collect data, it is possible to encounter some beam reflection off the walls of a channel, if it is narrow enough [28]. This can cause inaccurate data to be output by the ADCP. The United States Geological Survey, suggests that to avoid this phenomenon, the ADCP should be kept as far away from the side walls as the channel is deep [28]. For example, if the channel is 10 m deep, it is suggested to keep the ADCP at least 10 m from the side of any channel.

In addition to beam reflection off the sides of walls, beams can also be reflected off surface waves, which can cause an issue if the beam comes near the water surface. For the vertical ADCP, so long as it is at the water surface looking down, this is not an issue, because the device is usually completely submerged, so the beam is at least a device length away from the water surface. For the HADCP, this can be an issue. Data taken near the water surface can be contaminated by reflection off of the water surface, making the echo that returns to the device stronger than the actual data [87]. To address this, one must find the angle of spread of the ADCP in the direction approaching the water surface. The idea then, is to place the HADCP at a depth such that the beam does not spread to the water surface. This can be

done by measuring the width of the channel with a range finder or GPS, then using trigonometry, the required depth of the HADCP can be found.

3.6.8 Other challenges

Due to the nature and market of HKTs, HKT sites are typically located in remote areas. These areas are not well equipped with supplies and access roads are inconsistent. This can make accessing and measuring these areas difficult. Additionally, having enough crew members may be a challenge, depending on the location and hiring crew members can also be difficult, especially if the area is remote or there is a lack of technical personnel in the area.

The cost of accurate acoustic flow measurement instruments is high. Support structures can be designed at a lower cost relative to the instruments, but the cost of the measurement instruments, as well as the cost of accessing the site creates a challenge when performing characterization measurements. Bolts and fasteners must be lubricated to avoid seizing due to corrosion. Additionally, if a boat driver or crew member must be hired, this will further increase the cost of the procedures.

Finally, inclement weather can adversely affect measurement operations. Rain can create hazardous conditions, such as slippery shorelines and mud, which makes it difficult to launch boats and carry equipment to and from the water. If there is lightning, the operations must be canceled until it is safe to be on the water again. Additionally, hot and cold weather also add complications. In hot weather, frequent breaks must be taken and water must be available to ensure the safety of the crew and to prevent heat stroke. In cold weather, survival suits must be worn in place of life jackets and warm-up breaks must also be taken.

3.7 HKT resource characterization

There exist a few methods, to characterize the hydrokinetic resource on a large scale. These include some numerical approaches that involve using the geometry of a river and predict the flow with hydrologic modeling [10]. Our research group is proposing to use satellite and aerial winter imagery of rivers to identify open locations in an otherwise frozen environment [11]. The satellite imagery and the simple surface measurements methods will be discussed in this thesis.

3.7.1 Ice openings and satellite imagery

It is known that high velocity flow impedes ice formation at the water surface. The exact flow speed at which surface ice cover is prevented is not well characterized, however some estimate it to be above 0.6 m/s [88] [89]. Carstens [89] postulates that it is due to the increased turbulence of the water.

It is possible to gain high resolution satellite images of frozen landscapes during winter time and search for openings in otherwise frozen rivers. This method can cover a large area cost-effectively. These open locations can then be further tested for suitability for hydrokinetic turbines by physically going to the site in question and measuring the flow velocity and turbulence levels. This narrows down the search to a discreet number of areas, instead of having to manually search the whole river reach. Ice openings was used for finding the location of test sites for HKTs by Dr. Eric Bibeau starting in 2005. More details are available in Reference [11].

3.7.2 Application of mobile platform measurements

After potential hydrokinetic turbine sites have been identified, local measurements can be performed by using the zodiac boat to travel through a river reach and measure the flow velocity at a number of locations using ADV or ADCP. These locations can be identified with the ice openings technique, or from flow simulations supplied by NRCan [10]. Even without specific locations in mind, the river reach can be navigated and characterized at multiple locations where visual observation of the flow indicates high velocity.

If specific locations are identified, they can be uploaded into a GPS system. Multiple points around the GPS location can be measured. When using this method, it is recommended to have some form of water navigation chart for the region. This is because high flow velocities and increased turbulence can be due to rapids or very shallow regions. These types of environments can damage equipment.

Chapter 4

Channel measurement results and comparison

The flow measurement data collected at the CHTTC is compiled into a database for analysis purposes. In this section, the data from the different forms of measurement are presented and the results of the analysis are discussed. Calculations are performed in Matlab, with a code developed within our research group. Some results are then imported into excel for additional calculations. Plots are created using Matlab.

4.1 Surface measurements

In the survey of Seven Sisters, ten locations were selected, based on either the apparent velocity at that location, or based on the distance from the previous point. This section outlines the results from these measurements, which were performed just below the surface using the ADV.

Table 4.1: Results from a survey of the Seven Sisters channel. Location ID can be seen in Figure 3.16.

Location ID	Umean [m/s]	Vmean [m/s]	Wmean [m/s]	ADV correlation [%]	ADV SNR	Number of spikes removed
SS-1	1.786	0.364	0.023	95.589	28.37	56
SS-2	2.413	0.348	0.112	95.725	28.25	46
SS-3	0.866	0.178	0.029	97.108	28.55	8
SS-4	1.813	0.311	0.078	96.858	27.95	8
SS-5	2.034	0.413	0.097	96.591	28.00	13
SS-6	2.150	0.465	0.115	96.720	28.06	64
SS-7	1.604	0.285	0.104	96.600	28.13	43
SS-8	2.285	0.450	0.115	96.348	28.17	28
SS-9	2.698	0.546	0.138	94.366	29.67	56
SS-10	2.301	0.554	0.116	92.323	31.67	31

4.1.1 Raw data

The data that was collected was of good quality, with a high correlation average of 95.8% and a high SNR average of 28.7. Each data point was taken over a two minute duration, as these measurements were done as a survey, to measure how the flow velocity changes throughout the channel.

4.1.2 Results

Referring to Figure 3.16, the characterization survey yielded results of time-mean streamwise velocities found in the range of 0.86 to 2.68 m/s, with point SS-3 having the lowest velocity and SS-9 having the highest velocity. A summary of the results is presented in Table 4.1.

With these results it is possible to locate the areas of the channel with the fastest flow velocities. For site characterization purposes, this data can be used to select portions of the channel for more detailed analysis. Typically, the regions chosen will be the locations of highest velocity. This is due to the fact that hydrokinetic turbines would typically be placed in high velocity areas to capture the most power. Since

high velocity areas are of most interest, it follows that more information about the velocity profile and turbulence at these areas are desirable, so as to be able to predict the performance of a turbine operating in these locations. Additionally, testing of the profile measurement procedure should be verified in the most energetic locations to ensure that the system can be deployed in these conditions.

Once the final points have been selected, detailed velocity profile measurements are performed at the selected locations.

4.2 Velocity profile

The data collected at the CHTTC for the purposes of characterizing the velocity profile reveals interesting flow phenomena that impact turbines. Additionally, since multiple instruments, namely the ADV, ADCP and shear probe, were used to record flow data at the same time, a comparison of these devices can be performed to identify what each device is best for and when to use which device for the flow requirements defined in Figure 1.1 and Table 1.1

4.2.1 Raw data

In terms of the data collected, there are three points down the river, points A, B and C, as well as multiple depth measurements at each point. The ADV is the time limiting factor, with the ADCP attached to the boat and collects data passively. The shear probe is dropped three times to collect turbulence profiles at the beginning and end of each measurement point. The ADV readings are approximately eight minutes in length at each depth so as to be able to capture multiple cycles of the large scale turbulence. Between each reading, time is needed to move the ADV to the new measurement depth. All factors included, it takes approximately 10 to 15 minutes

to perform one ADV reading. This can be used as an estimate for the time required once all of the devices have been set up.

4.2.2 Results

When the ADV is recording, its axis is no longer parallel to the flow axis, as shown in Figure 4.1. This means that the data obtained by the ADV will not be in the same coordinate system as the river. To correct this, the angle can be found using the IMU of the ADV. Since it gathers acceleration data, it is able to sense the acceleration due to gravity. If it is assumed that there are no forces in either of the X or Z directions, the accelerations read by the IMU in those two directions can be attributed to gravity. By comparing this to the acceleration when it is measured in an upright position, the inclination angle ϕ can be found. The velocity data in the X and Z directions are then compensated using this angle and the data can then be read in the same coordinate system as the river.

The mean velocity results of the profile measurement procedure are shown in Figures 4.2 to 4.6 for measurement points A to C. Seven to eight data points are taken for each profile; a spline is used to interpolate the data. This allows for closer comparison of the devices. Each spline is interpolated within the data set of the ADV and the ADCP, using the least shallow measurement between the two devices as the start point, and the least deep as the end point. Figure 4.3 shows an example of a time series recorded by the ADCP at a single point. Additionally, a contour plot of the time series is shown in Figure 4.4

From these figures, we can see that the location of highest streamwise velocity is point C, with point B being a close second. Interestingly, there is a visible velocity defect in the ADV results at point B. This is due to a 15 kW Clean Current underwater turbine located just upstream of point B. What is even more interesting is that the

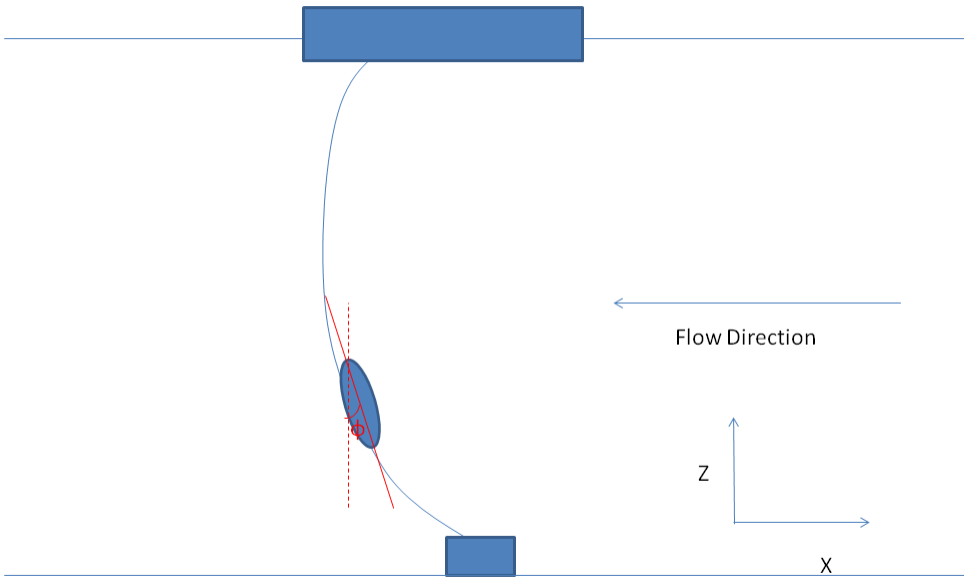

Figure 4.1: Schematic of the angle of the ADV when being used in profile measurements

ADCP does not capture this velocity defect. This is most likely due to the fact that the ADCP performs spatial averaging, and therefore, the portions of the water column that are within the wake of the turbine are averaged by the portions outside of the wake. From this, it can be concluded that the ADCP does not have high enough resolution to reliably and accurately profile hydrokinetic sites with complex flow structures.

In general, the ADCP under-predicts the mean flow, as seen in Figures 4.2 to 4.6. This could again be due to spatial averaging, where some of the slower regions, such as the boundary layer, are averaged into portions of the rest of the profile. However, at point A, it is observable that the profiles captured by the ADV and the ADCP compare well with each other. This is due to the fact that the river is shallower at this point than at points B and C. Due to the shallower depth, the ADCP sets the cells to a smaller size, 0.5 m instead of 1.0 m, for example. The conclusion to draw from this,

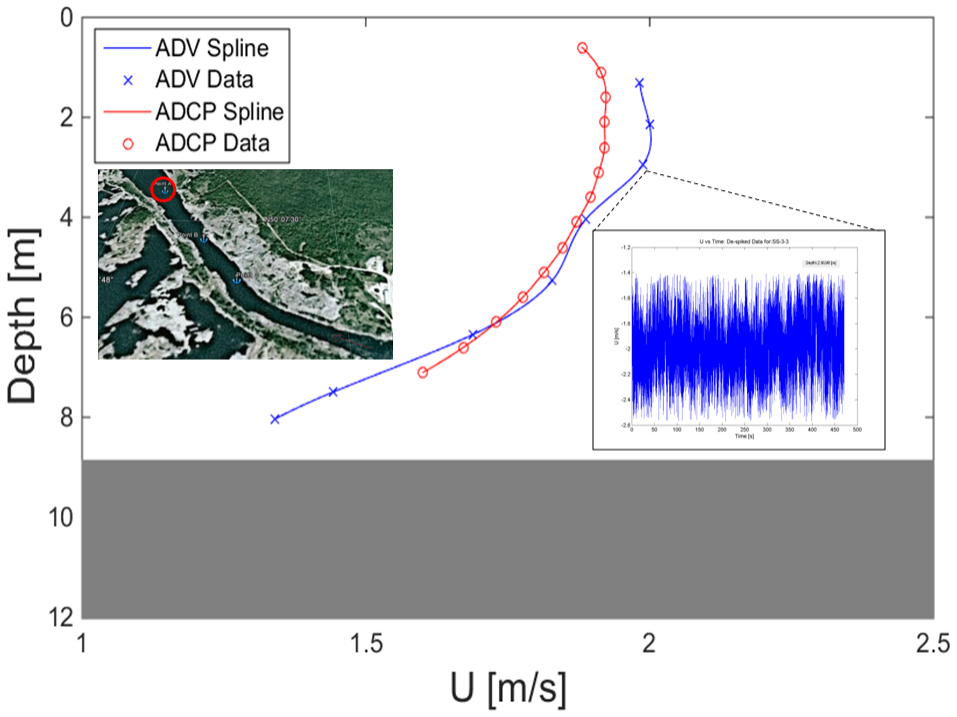

Figure 4.2: Flow profile obtained from the ADV and ADCP for point A. The gray area indicates the river bed. Each data point is a mean value obtained from a time series at the corresponding depth. A sample time series of one of the points is also shown.

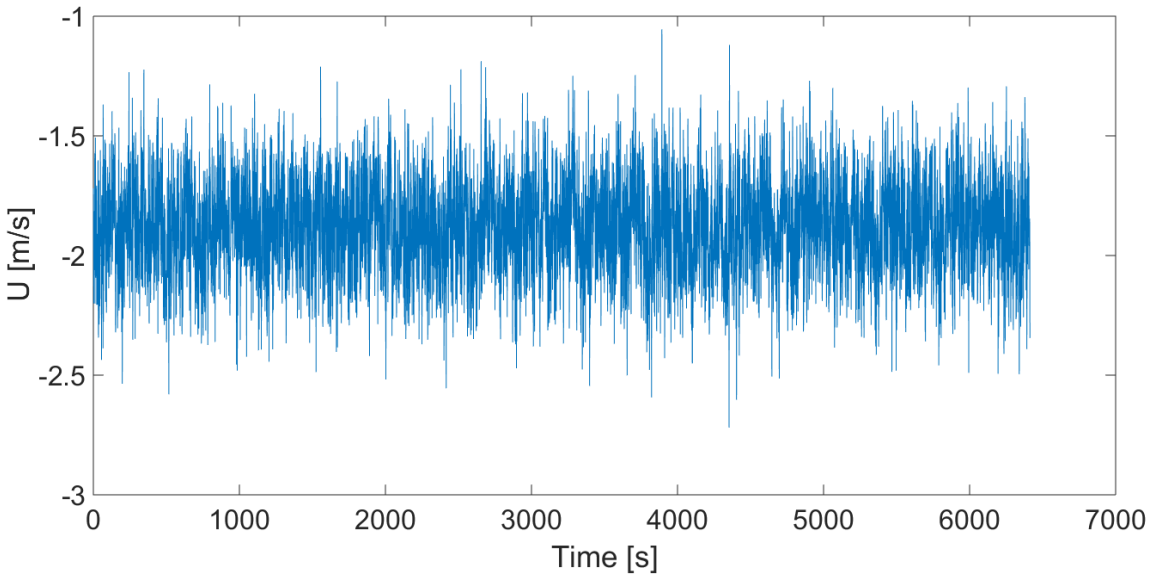

Figure 4.3: Time series of the ADCP recording at point A at 0.6 m depth

is that the ADCP can be used to characterize mean flow if the cell size is sufficiently small. Currently, it is unknown if the decreased cell size would be able to resolve flow

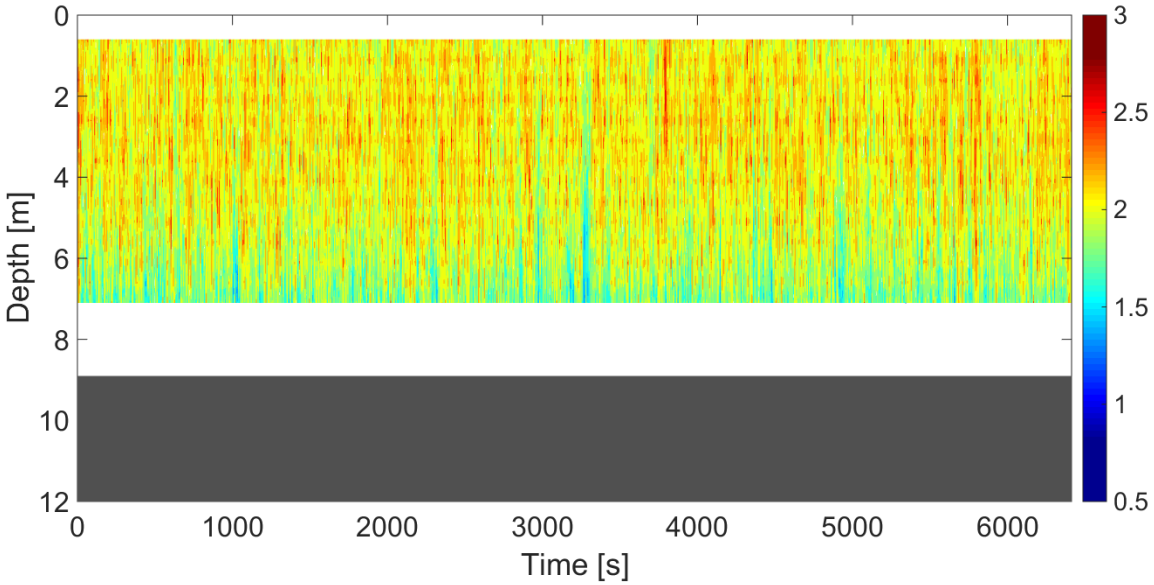

Figure 4.4: Time series contour of velocity measured by ADCP at Point A.

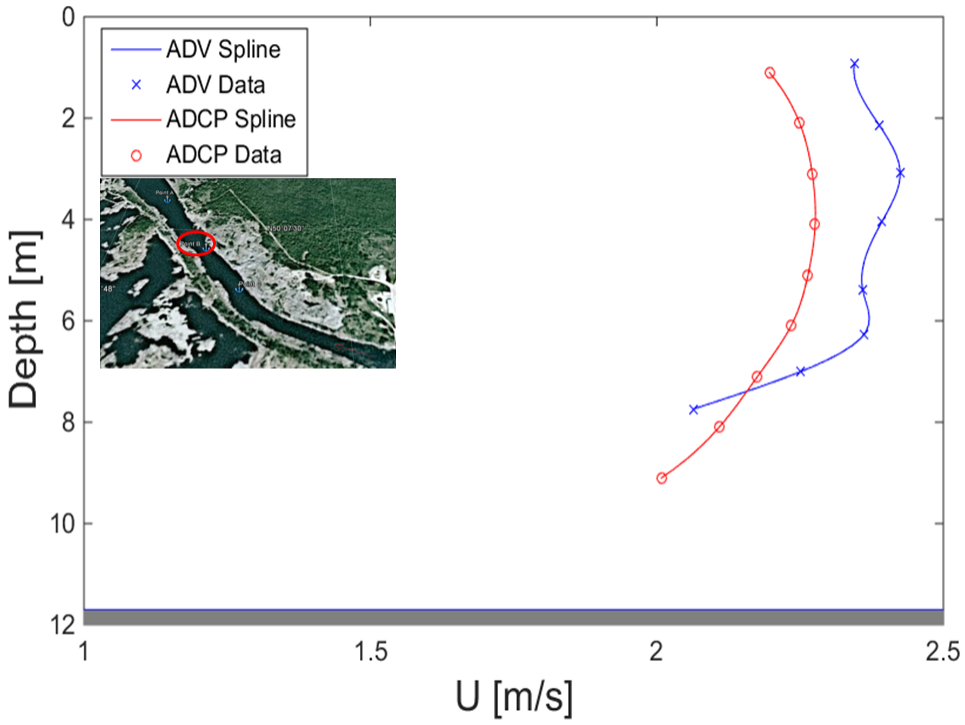

Figure 4.5: Flow profile obtained from the ADV and ADCP for point B

structures that are not resolved with a larger cell size, such as a wake.

Finally, each point was taken on a different day, so the flow is varies with time between each measurement point. Point B and point C have fairly similar maximum

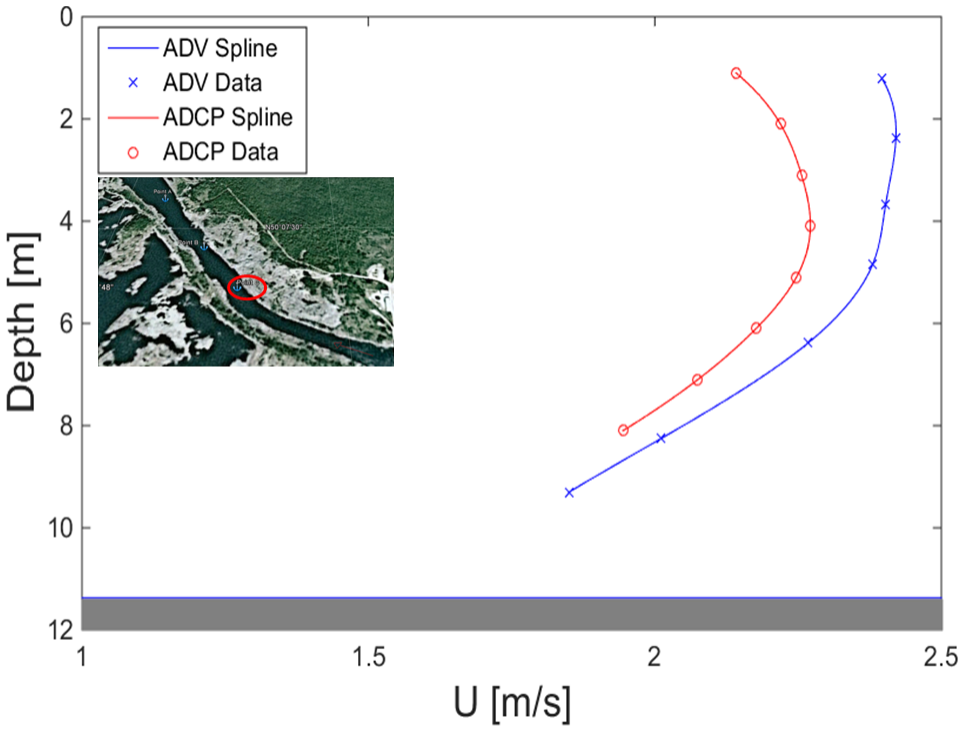

Figure 4.6: Flow profile obtained from the ADV and ADCP for point C

velocities, however, point A has a relatively slow velocity, in comparison to the other two points. This could be due to flow variation with time. Additionally, point A has a wider cross-section, and a larger cross-sectional area. Due to this, this area will have a slower flow velocity, as the volumetric flow rate must be constant at a given time between two locations in the channel.

Concerning the difference in data between the ADV and ADCP, the average percent difference for the mean streamwise velocity is 4.38%. The minimum and maximum differences between the ADV and ADCP are summarized in Table 4.2.

It is observable that the percent differences at point A are the smallest in magnitude, due to the fact that that the cell size at point A is smaller than the other two points, giving higher resolution of the flow.

Since the shear probe measures only turbulence characteristics, the turbulence results of the instrument will not be discussed in this section, but in section 4.5.1. However,

Table 4.2: Maximum and minimum absolute percent differences between ADV and ADCP calculations of mean streamwise velocity at equivalent spline-interpolated depths

	Point	Percent difference [%]
Max	A	4.71
Min		0.10
Max	B	6.36
Min		0.51
Max	C	10.17
Min		4.43

it is important to note how the shear probe descends through the water column, and only a portion of the data can be used. According to the manufacturer of the device, the sensors must be at the leading edge of the instrument. This means that there must be flow in the direction of the probes. This is solved by descending the probe vertically downwards, in which the velocity against the probes is the descent velocity of the device itself. This also means that only the descent contains viable data. Two shear probe data files are created at each measurement point, one during the first ADV measurement and one during the final ADV measurement. This is so that the turbulence data can be better compared. Each data file contains at least three profiles, or descents. The shear probe profiles for the first measurement at point A are shown in Figure 4.7.

For reference, each drop and retrieval of the shear probe will be referred to as a run. Due to the fact that only the descent portion of each run is useable for data analysis, a method is devised to isolate these portions of the data. A code is written in Matlab to address this. Firstly, it starts the profile at 2 m depth because of the method of dropping the shear probe in the water, as the long shear probe starts in the water, transient effects near the beginning of the profile are avoided. Next, the code searches for the inflection point of the pressure,to identify the end of the profile. Therefore, each profile will span a water column 2 m from the surface and will continue until the pressure begins to decrease. The code then repeats this for all profiles. A sample

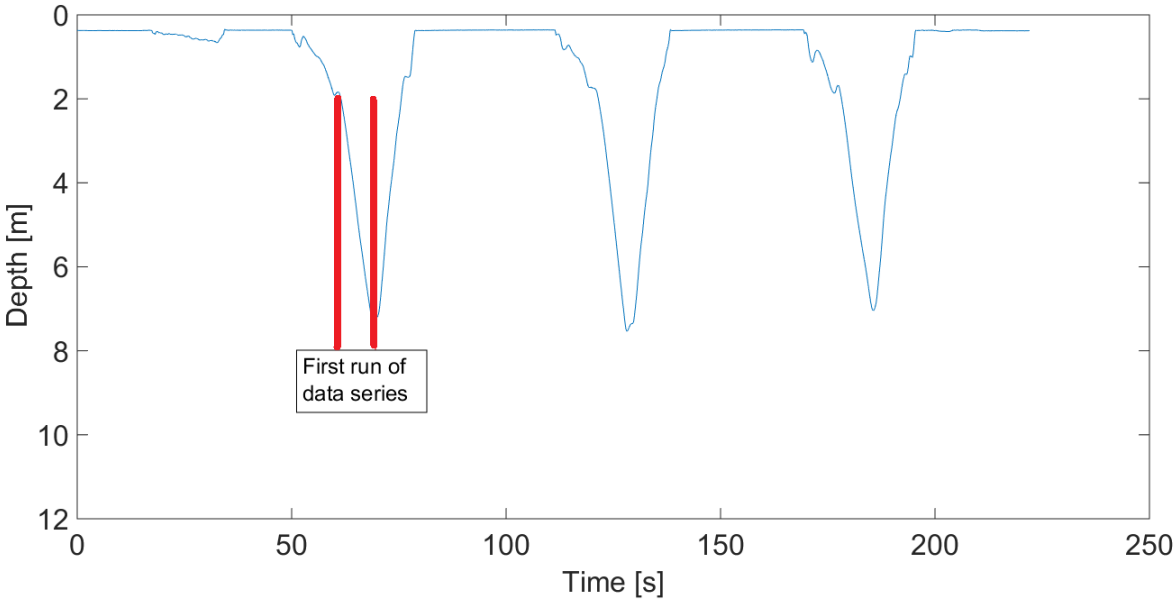

Figure 4.7: Pressure profiles of the shear probe runs, at point A, as a time series

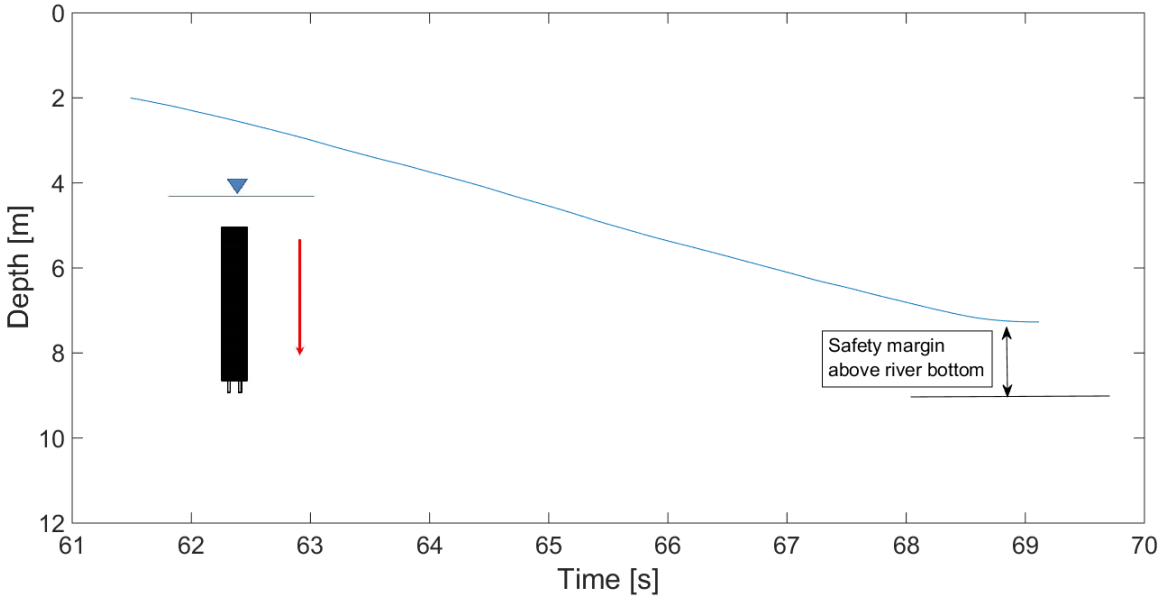

Figure 4.8: One run of the shear probe at point A (refer to Figure 4.7), shown as a time series, isolated using Matlab programming

profile is shown in Figure 4.8.

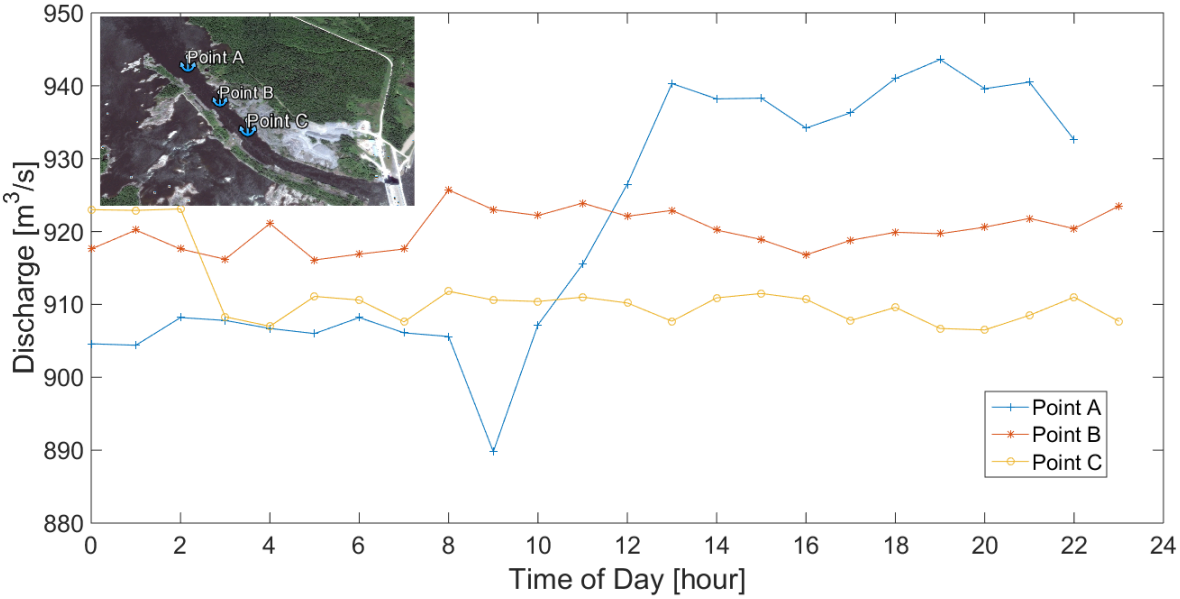

Figure 4.9: Hourly discharge rate for Seven Sisters dam during the days of measurement campaigns at the CHTTC

4.3 Comparison of velocity profile and discharge rate

The maximum velocity varies between all three measurement points. There are many possible sources of this variation. One could be that the changing of the flow rate from the dam is affecting the flow speeds in the channel. In order to determine if the dam is affecting the flow rate, the flow rate data from the Seven Sisters dam is obtained [90]. A plot of hourly discharge rates for the days corresponding to different measurement points can be seen in Figure 4.9.

To compare the velocity read in from the characterization measurements, the start and end time of the measurements is required. This is possible to obtain from the internal clock of each device. Additionally, the vertically averaged velocity for each point is calculated from the ADV data and included for reference. These results are summed up in Table 4.3.

Table 4.3: Start and end times, with corresponding vertically averaged velocity from ADV data for characterization measurements at CHTTC

	Start of measurement	End of measurement	Vertically averaged velocity [m/s]
Point A	10/01/2015 11:22	10/01/2015 13:09	1.770
Point B	9/28/2015 13:06	9/28/2015 15:08	2.323
Point C	9/29/2015 11:27	9/29/2015 13:15	2.247

According to the flow data, the flow rates for points B and C were relatively steady throughout the day, with the flow rate during the measurements at point B being higher than the flow rate during the measurements at point C. This corresponds to the profile averaged velocity data, as point B has a faster profile averaged velocity than point C, however, the difference is only marginal. Point A has the lowest profile averaged velocity, yet, during the measurement times, the flow rate from the dam was always higher than the flow rates during measurements at point C. Additionally, the flow rates during measurement at point A are higher near the end of the recording than they were during measurement at point B. This, and the marginal decrease in flow between point B and C is indicative that the flow rate from the dam does not affect the vertically averaged velocity at the CHTTC. The difference in flow speed between point A and the other two measurement points could be due to the fact that the cross-section is much larger because the river is wider at this point than it is for the other two points, which have similar cross-sections. The increase in discharge during measurements at point A can be attributed to VAR control on the part of the dam.

Finally, all three profiles measured with the ADV are compared in Figure 4.10. The velocities are normalized by dividing velocities by the maximum velocity of the profile specific to that measurement point. The Z position, or the depth of the measurement is normalized by the total depth of the river at the measurement point. At the surface, Z/D is zero and at the river bed, Z/D is one. The resulting plot is shown in

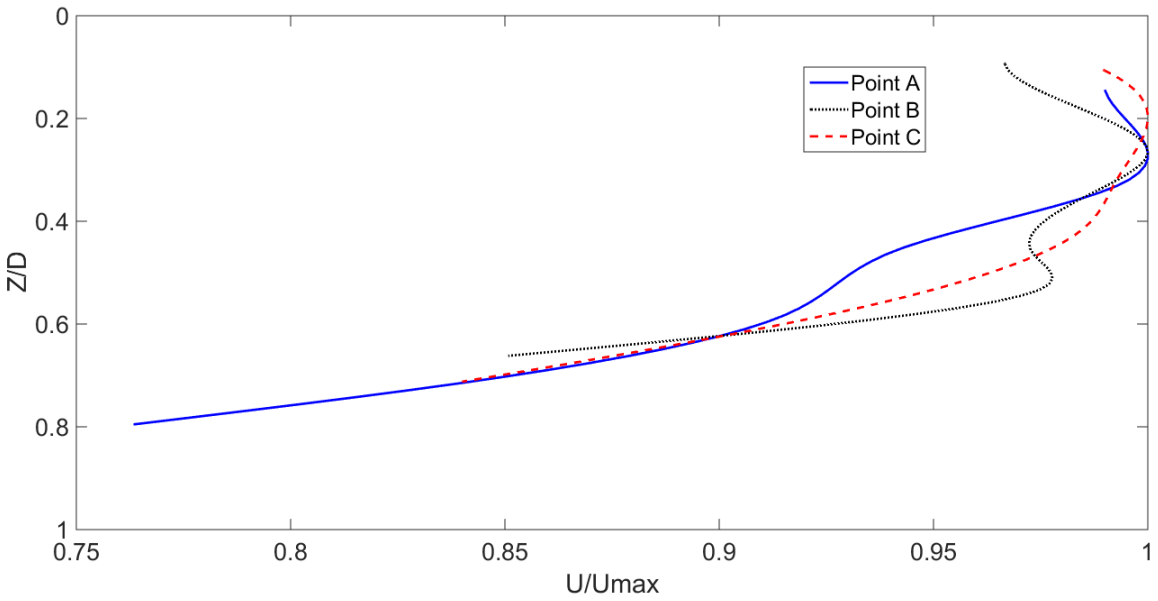

Figure 4.10: ADV depth and velocity normalized flow profiles for measurement points A, B and C

Figure 4.10. It can be seen that for all three measurement profiles, the boundary layer edge is near the same point relative to the river bed. Additionally, all three velocity profiles exhibit a velocity defect near the water surface, which is characteristic of open channel flows. It should be noted that the profiles shown are based on spline-interpolated points from the actual measured data.

The velocities are then converted to power density in W/m^2 and plotted against the normalized depth. The results are shown in Figure 4.11

Boils are visible from the water surface and can disturb the profile. The localized curvature in Figure 4.10 may be caused, in part, by boils. To investigate this, the mean vertical velocity profile is plotted in Figure 4.12.

The spanwise velocities vary between the ADV and the ADCP with an average of 102% difference and the vertical velocities vary with an average of 142% difference. This is contrary to the results found in the streamwise velocity data, where the two devices agreed well. The spanwise velocity ADCP data for point C is approximately

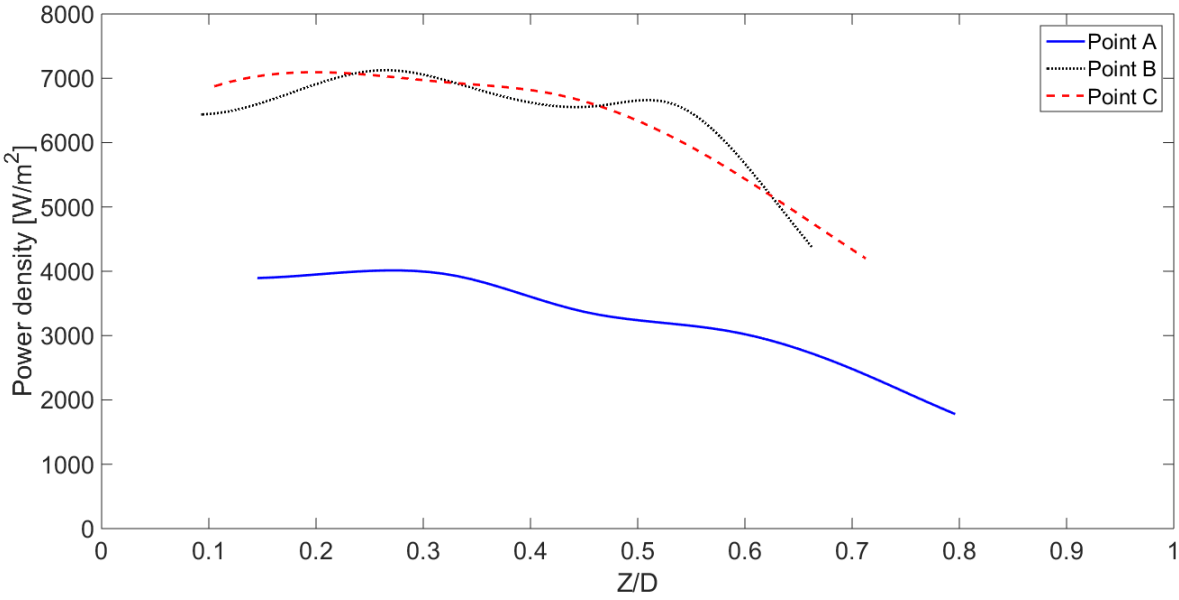

Figure 4.11: Power density profile for each measurement location calculated from ADV results

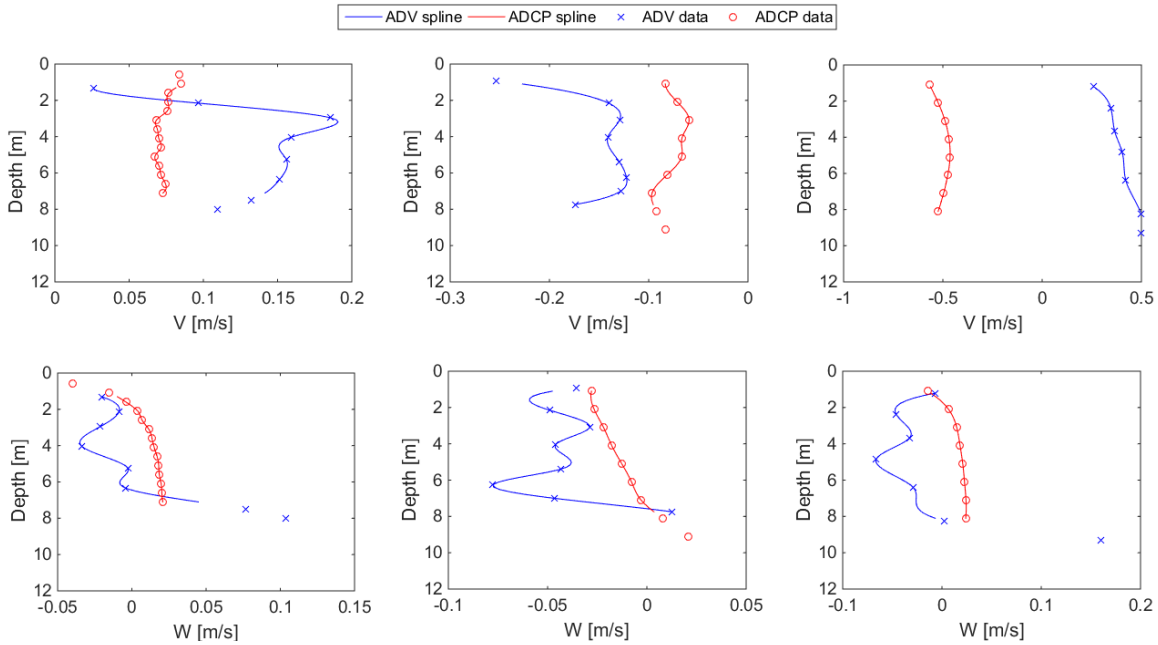

Figure 4.12: Spanwise and vertical velocity profiles at the CHTTC. From left to right: point A, point B and point C

the negative of the ADV data. This is attributed to a poor recording from one of the devices in that component, as the streamwise and vertical components agree relatively well. This point is omitted from the discussion on spanwise velocity. Omitting

point C, the average percent difference between the ADV and the ADCP in spanwise velocity is 39%. A possible explanation is that the spanwise and vertical velocities have relatively small magnitudes compared to the streamwise velocity, so the error in each device, which are displayed in Table 3.1 as ±1 mm/s for the ADV and ±2 mm/s for the ADCP, can have more of an effect on the data. Some, such as Snyder [91], have found that the error of the ADV can be up to 2.5 mm/s, when the device is inclined and pitching of the device can cause an over-prediction of the vertical velocity of 5% to 15% and 5% to 10% of the horizontal velocities.

4.4 Boundary layer

The boundary layer height is difficult to obtain, due to the low spatial resolution and blind spot of the ADCP. For the ADV, the cable method did not allow to measure close to the river bottom. This aspect was later resolved by modifying the design of the system. Instead of using measurement points, a spline is interpolated between the measurement points using Matlab. Matlab can produce as many points on a spline as requested by the user. Therefore, using this spline, it is possible to obtain an estimation of the boundary layer height. The summary of the calculated boundary layer heights can be seen in Table 4.4.

As a fraction of depth, these boundary layer heights are quite high, at times as high as 67% of the water column is the boundary layer region, depending on whether the 99% or 95% boundary layer convention is taken as reference. This compares well with

Table 4.4: Boundary layer heights calculated from ADV and ADCP data

Point	$\delta_{99,ADV}$ [m]	$\delta_{99,ADCP}$ [m]	$\delta_{95,ADV}$ [m]	$\delta_{95,ADCP}$ [m]
A	5.96	5.61	5.14	3.90
B	7.89	6.26	5.04	6.23
C	7.36	6.37	5.39	6.05

Table 4.5: Reynolds number, Froude number and correlating boundary layer thicknesses

Point	$\delta_{99,ADV}/R_h$	$\delta_{99,ADCP}/R_h$	Re	Fr
A	0.78	0.73	1.34×10^7	0.23
B	0.89	0.71	1.86×10^7	0.26
C	0.88	0.76	1.77×10^7	0.27

work done by Tachie *et al.* [44] in an open channel, who found the boundary layer to be in this range as well. However, their work was performed at lower Reynolds numbers (Reynolds numbers based on displacement thickness), with a maximum velocity between 0.33 and 0.74 m/s. For a comparison to other experimental results, the Reynolds and Froude number in the free stream is calculated for each measurement point. The results are shown in Table 4.5.

From Table 4.5, the boundary layer thickness does not vary with Reynolds number. However, Kaji [92] found that, for an open channel flow in a laboratory with a favourable pressure gradient, as the Reynolds number increases, the boundary layer height also increases. The Reynolds number in that experiment, however, was calculated based on channel depth. If the Reynolds number for these experiments is calculated based on depth, the Reynolds numbers for point A, B and C are 1.55×10^7, 2.47×10^7 and 2.40×10^7, respectively. Even in this case, however, there still does not seem to be a relationship between Reynolds number and boundary layer height. If, we remove point B from the trend, it is observable that point A has a lower Reynolds number and lower boundary layer height than point C. This would agree with the work performed by Kaji [92]. It is possible that the boundary layer height for point B is being skewed by the presence of the turbine wake. If that is the case, the data agrees with other experiments.

In terms of relevance of predictive correlations, such as those of Bonakdari *et al.* [54] and Wang *et al.* [55], correlations are applied to the boundary layer thicknesses found in the current study and are summarized in Table 4.6.

Table 4.6: Boundary layer thicknesses relative to depth,

Point	$\frac{Y_\infty}{D}_{99,ADV}$	$\frac{Y_\infty}{D}_{99,ADCP}$	$\frac{Y_\infty}{D}_{95,ADV}$	$\frac{Y_\infty}{D}_{95,ADCP}$	Ar	$\frac{Y_\infty}{D}$ [54]	$\frac{Y_\infty}{D}$ [55]
A	0.668	0.628	0.575	0.437	12.411	0.999	13.623
B	0.674	0.535	0.431	0.533	6.120	0.975	6.961
C	0.647	0.560	0.474	0.532	5.616	0.965	6.360

It is observed that the correlations fail to predict the location of maximum velocity, Y_∞. This could be due to various reasons. The first is that these correlations are developed based on laboratory experiments. Laboratory experiments, in general have relatively low Reynolds numbers when compared to those of the present study. This could significantly affect the efficacy of the correlations. Secondly, the aspect ratio of a river is typically larger than those found in a laboratory, as seen in the current study. This could also significantly affect the ability of the correlation to predict Y_∞. Finally, the correlation from Wang *et al.* [55] is meant for Ar less than 5.2, which puts the results of the current study outside of the scope of this correlation.

It is also seen in Table 4.6 that the range of $\frac{Y_\infty}{D}$ is between 0.43 to 0.67D, which is similar to the ranges found in the literature. This shows that even at a relatively high Reynolds numbers found in rivers, the fraction of the water column occupied by the boundary layer is similar to lower Reynolds, which are found in laboratory channels. For the numbers found in the literature, refer to Table 2.5

In terms of power density, it is possible to determine, from the results, the region of the water column which contains the most amount of energy. To do this, the streamwise velocity profile is taken, since power is proportional to streamwise velocity, and added cumulatively to determine the region of highest power. From the results, it is observed that 75% of the power available in the water column is located in the first 53.6% of the water column from the surface down. The results from this analysis are shown in Table 4.7.

Table 4.7: Percent of water column containing 75% of the power through the column

Point	75% Power
A	58.34
B	49.94
C	52.64
Average	53.64

Table 4.8: Turbulence results from preliminary surface measurements done at the CHTTC in the Seven Sisters channel

Point	TKE $[\frac{m^2}{s^3}]$	TI [%]
SS-1	0.064	11.23
SS-2	0.028	5.59
SS-3	0.014	10.77
SS-4	0.022	6.56
SS-5	0.044	8.25
SS-6	0.022	5.14
SS-7	0.032	6.61
SS-8	0.024	7.80
SS-9	0.042	6.05
SS-10	0.088	10.14

4.5 Turbulence statistics

In terms of power generation, the mean flow statistics are important for hydrokinetic turbines. However, for turbines which use turbulence to create energy, or for predictions of wear and damage to turbines, information on the turbulence of a hydrokinetic site is necessary. For this reason, the turbulence statistics are calculated from the ADV, ADCP and shear probe. The results of these calculations are presented in this section.

4.5.1 Turbulence results for the CHTTC

To further reduce the amount of potential locations, the turbulence characteristics of each surface measurement can be calculated and tabulated. The results are shown in Table 4.8.

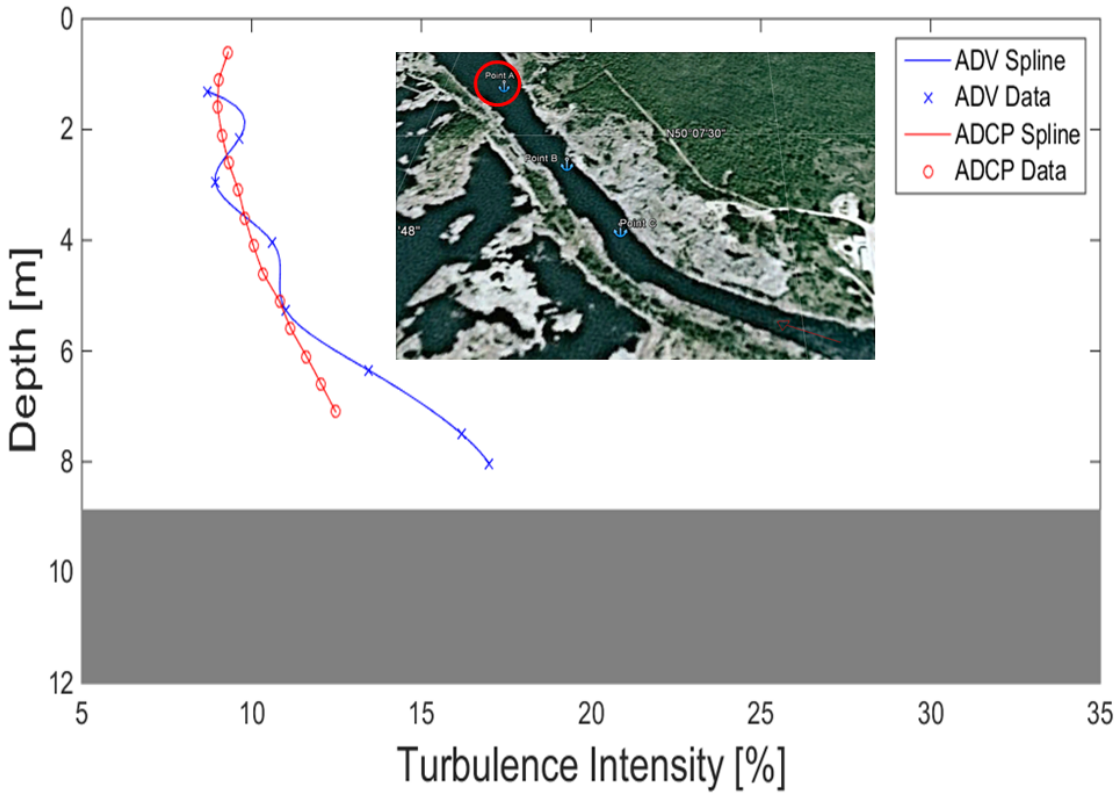

Figure 4.13: Turbulence profile obtained from the ADV and ADCP for point A

It is important to note that the turbulence results achieved with the surface measurement technique may be influenced by factors that are not part of the turbulence of the flow. For instance, boat motion and instrument vibration can have adverse effects on the results. This means that the results achieved using this method should be only used to provide a general idea of the turbulence existing at a given location. From Table 4.8, it can be observed that surface turbulence varies throughout the channel from approximately 5.6% at minimum to approximately 11.2% at a maximum. When observing both Tables 4.1 and 4.8, it is possible to see that there is little correlation between velocity and surface turbulence in the Seven Sisters channel, with an R^2 value of approximately 37%.

For the turbulence profile results, a comparison plot is performed between the ADV and the ADCP. The results are shown in Figures 4.13 to 4.15

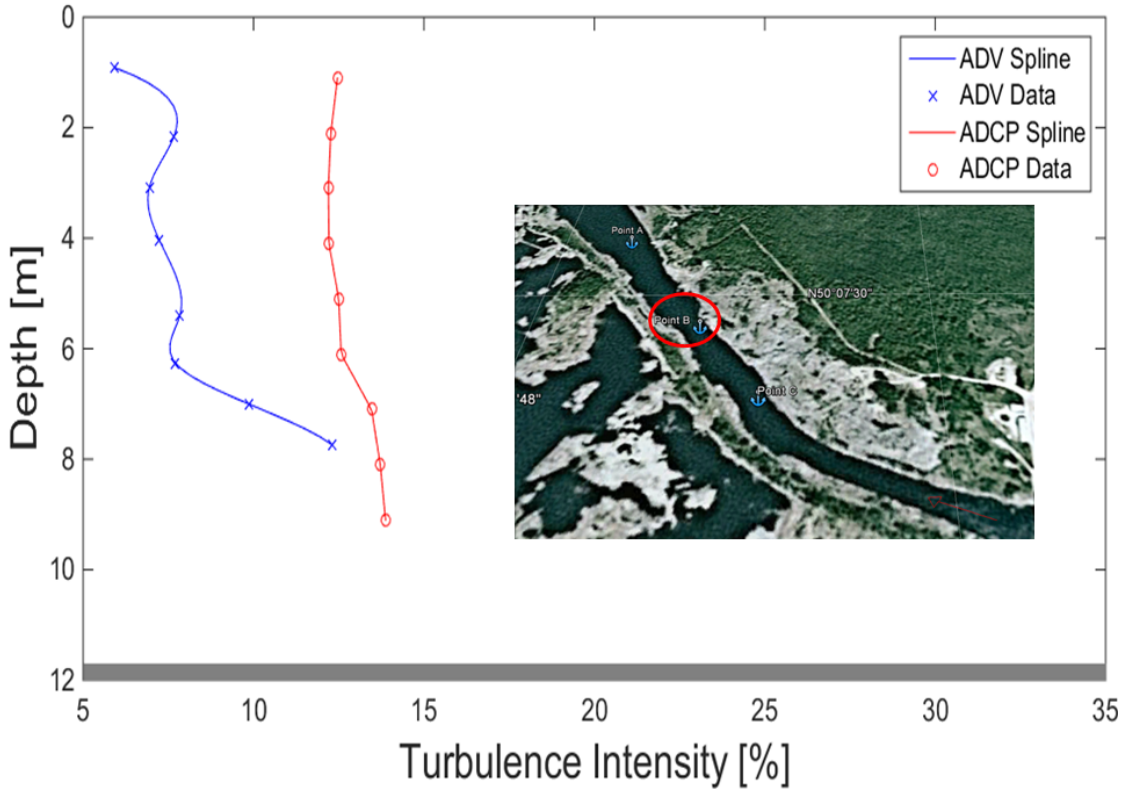

Figure 4.14: Turbulence profile obtained from the ADV and ADCP for point B

All profiles exhibit the same behaviour, that turbulence increases with depth, or as distance from the wall decreases. This is consistent with literature on the topic of turbulence in open channels, such as the work done by Kaji [92].

It should be noted is that in the plot for point C, a data point must be omitted from the profile due to a misreading of turbulence. This is thought to be the combined result of low correlation and high levels of turbulence. This is further addressed in Section 4.5.3. Additionally, at point B, the ADV seems to under-predict turbulence, in comparison to the ADCP, which is not expected because it was assumed that the ADV would measure higher turbulence due to vibration of the cable. At point C, the ADCP is the device which under-predicts turbulence. Finally, at point A, the turbulence intensity observed by the ADV and ADCP agree well with each other. This could be due to the fact that during measurement at point A, the cell size

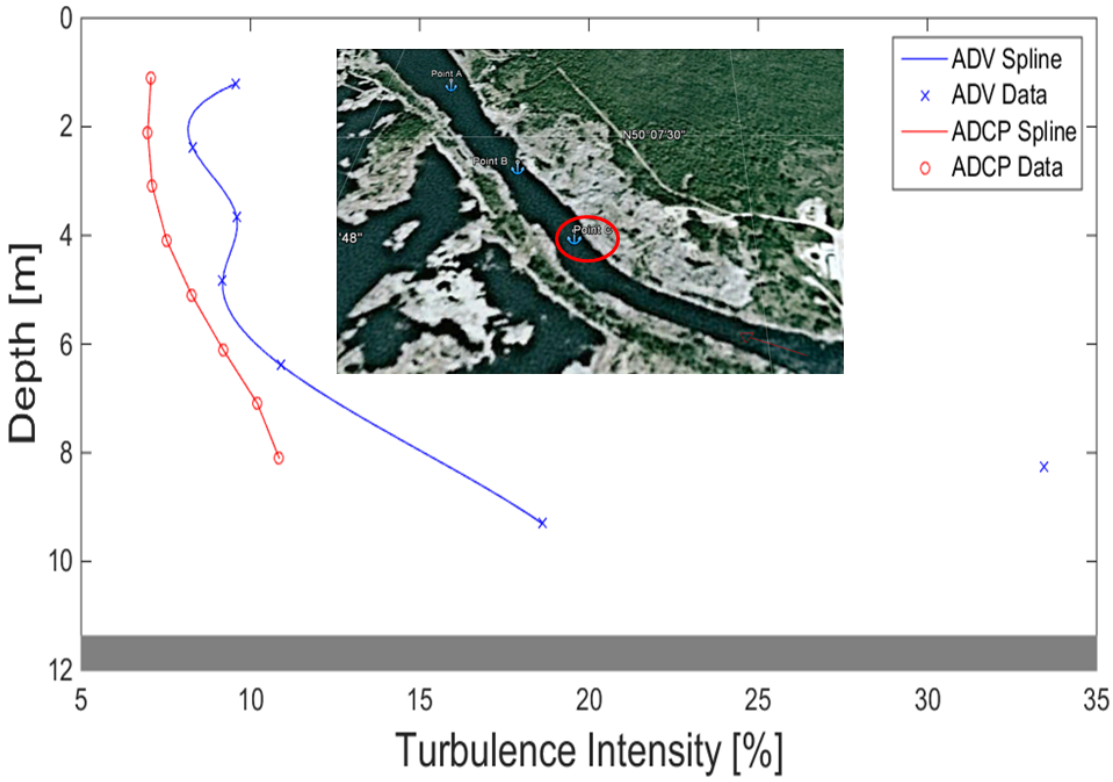

Figure 4.15: Turbulence profile obtained from the ADV and ADCP for point C with erroneous data point omitted

for the ADCP was smaller than the other two points, allowing it to better resolve turbulence data. This result, combined with the fact that the ADV under-predicted turbulence at point B in comparison with the ADCP, points towards the fact that the vibration of the ADV cable does not heavily affect the mean flow or turbulence data.

The average percent difference between the ADV and ADCP data for the turbulence intensity is 30%. A difference is expected due to the low data recording frequency of the ADCP, as well as the low spatial resolution of the ADCP. It is evident that the calculated turbulence intensity varies with the device chosen. The results for the percent differences between the ADV and ADCP on turbulence intensity are summarized in Table 4.9.

Table 4.9: Maximum and minimum absolute percent differences between ADV and ADCP calculations of turbulence intensity at equivalent spline-interpolated depths

	Point	Percent difference [%]
Max	A	18.77
Min		0.26
Max	B	87.74
Min		11.35
Max	C	66.95
Min		1.47

It is shown that the lowest maximum percent difference is observed at point A, which is to be expected due to the reduced bin size of the ADCP, and therefore reduced spatial averaging. The maximum percent difference is observed at point B, which could be a combination of spatial averaging and the wake feature observed due to the underwater turbine. Due to the spatial and temporal averaging of the ADCP, the ADV is the recommended device for measuring turbulence values in rivers.

The turbulence statistics of the ADV and ADCP are compared. All Reynolds normal and shear stresses are calculated and graphed. Note that for the streamwise velocity figures, the U velocities are positive. Due to the orientation and coordinate system of the ADV and ADCP, the results are actually measured as negative but are made positive in post processing. In the profiles of the Reynolds stresses, this correction is not made. The results are shown in Figures 4.16 to 4.18.

In terms of the Reynolds normal stresses, the streamwise components agree in trend and magnitude. The spanwise components agree in trend, however, there is some difference in magnitude, as the ADCP tends to over-predict turbulence, which is consistent with the turbulence intensity comparison. However, the vertical component differs between the ADCP and the ADV. This could potentially be due to the presence of vertical turbulent eddies, also referred to as boils. Since the spatial resolution of the ADCP is lower than the ADV, it is possible that these boils are not captured in the ADCP data. In terms of the Reynolds shear stresses, there is disagreement

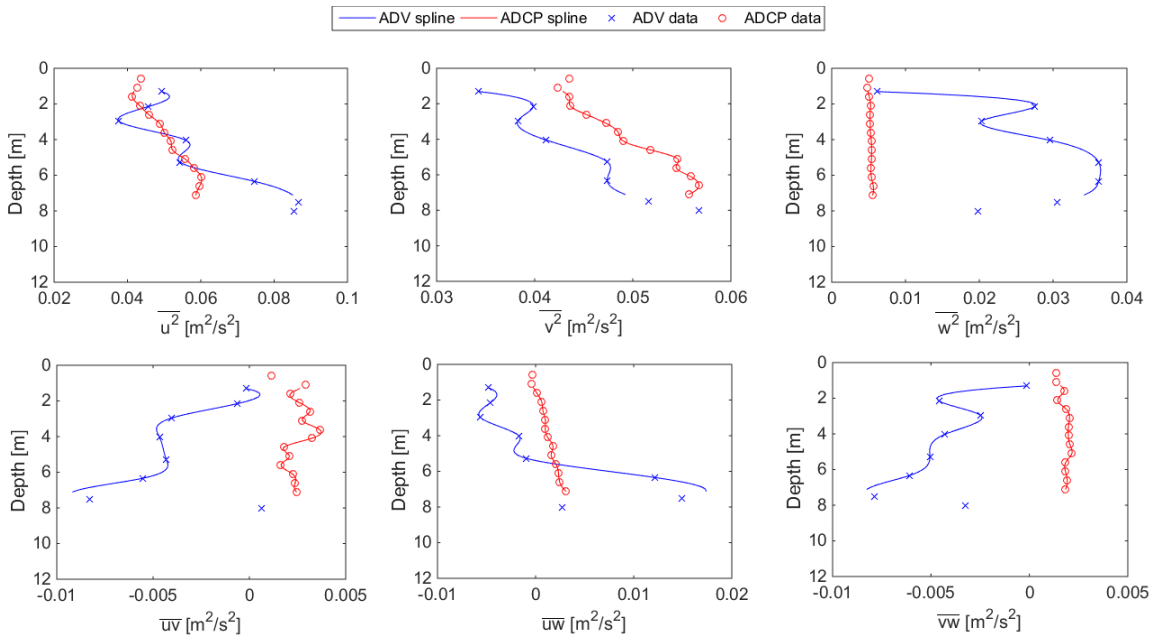

Figure 4.16: Reynolds stress profiles for point A

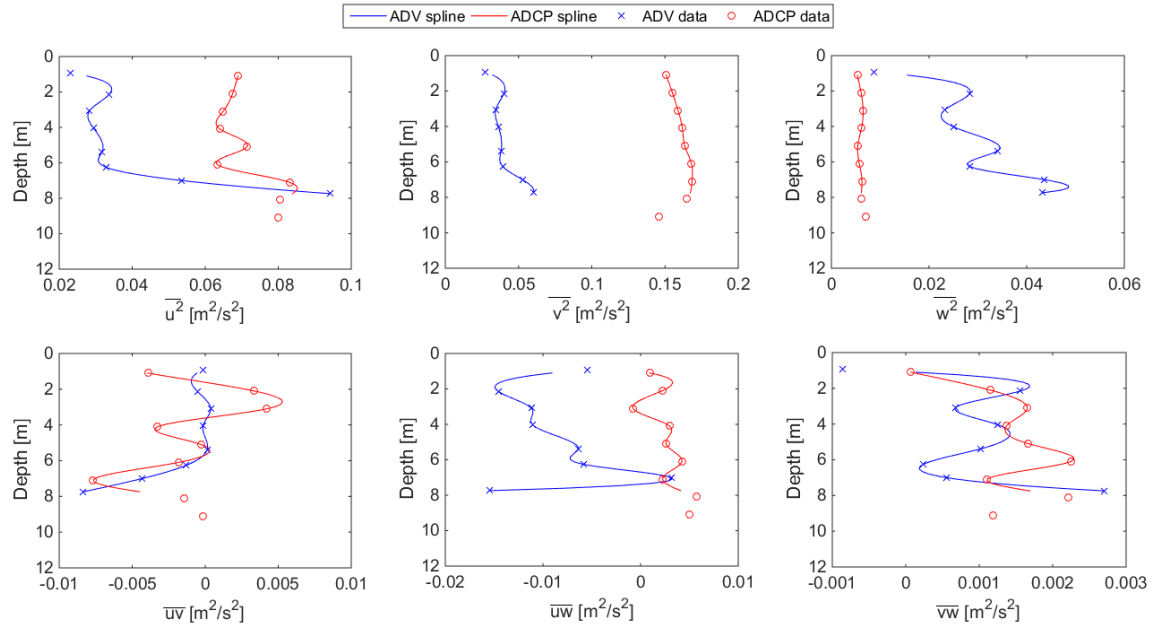

Figure 4.17: Reynolds stress profiles for point B

between all components. This is likely a result of the difference between the spanwise and vertical components seen in the normal stresses. Additionally, from these plots it is evident that turbulence varies with direction and location. This means that the turbulence at the CHTTC is non-isotropic and non-homogeneous.

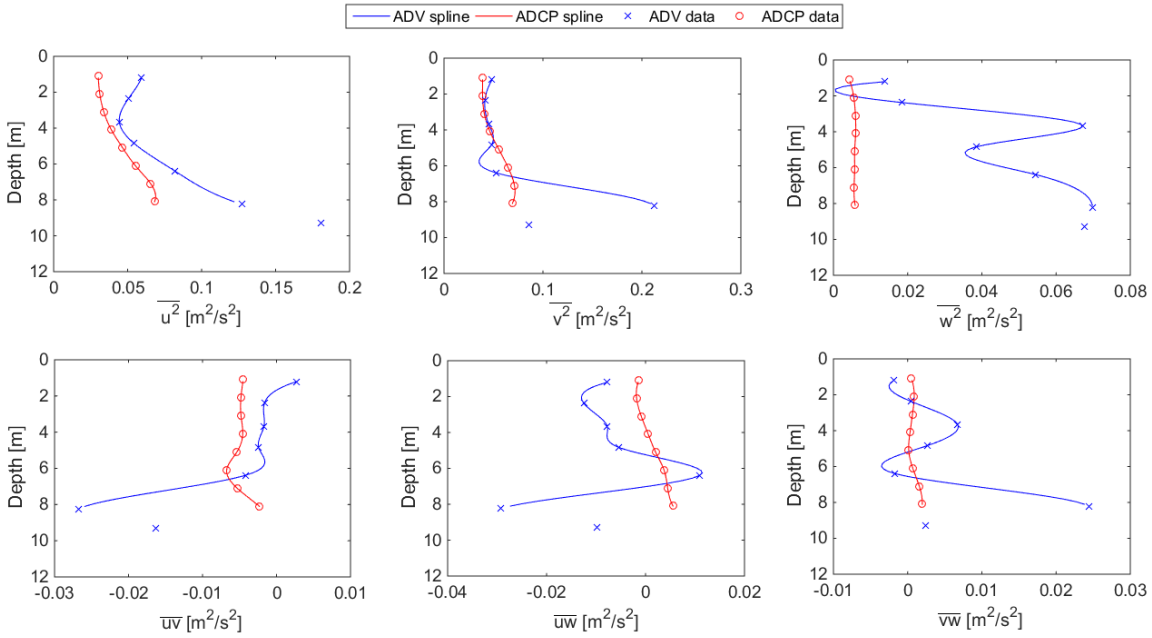

Figure 4.18: Reynolds stress profiles for point C. Note that a despiking method based on correlation is selected for this data set as the data had a large number of spikes

For comparison of the shear probe data to the ADV and ADCP, data analysis and interpretation must be performed. Due to the amount of literature detailing the inability of the ADCP to accurately measure turbulence, only the ADV data will be compared to the shear probe. Though it may not be directly applicable to most types of turbines, to allow for comparison to the shear probe, the dissipation rate must be calculated from the ADV. Using the equation supplied by Nezu and Nakagawa [93], the Kolmogorov length scale can be calculated with Equation 4.1:

$$\eta = 1.1 * \frac{L_x}{Re_L^{\frac{3}{4}}} \tag{4.1}$$

where L_x is the integral length scale, Re_L is the Reynolds number based off of the integral length scale and the root mean square of the velocity fluctuations in the streamwise direction, or u'. The integral length scale is calculated by performing an auto-correlation analysis on the ADV data in a code developed by the research group. The dissipation rate is then calculated for each ADV reading and can be plotted as

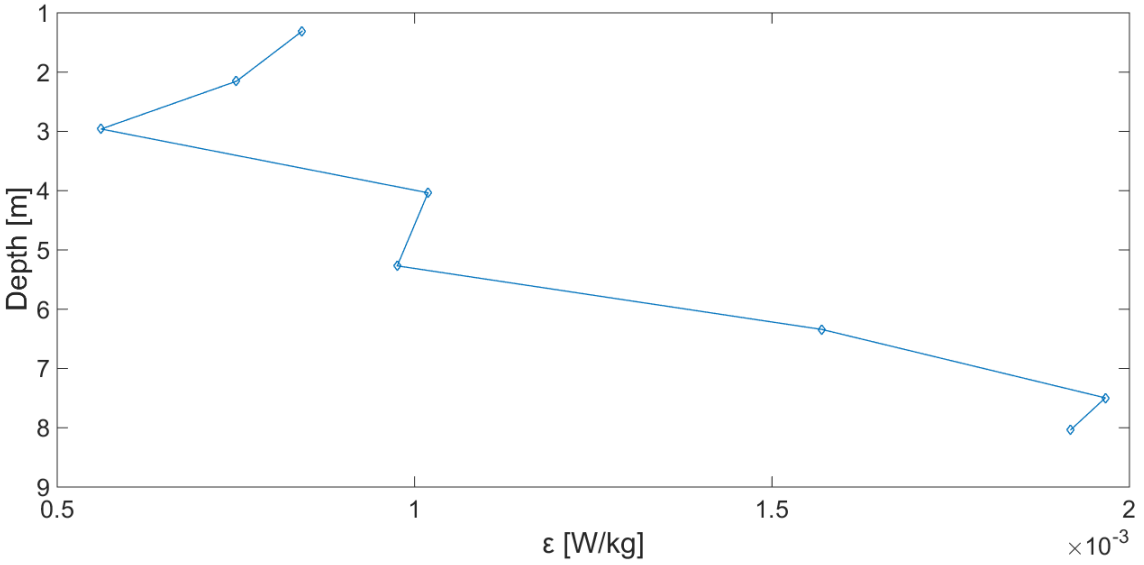

Figure 4.19: Dissipation rate profile obtained from the ADV for point A

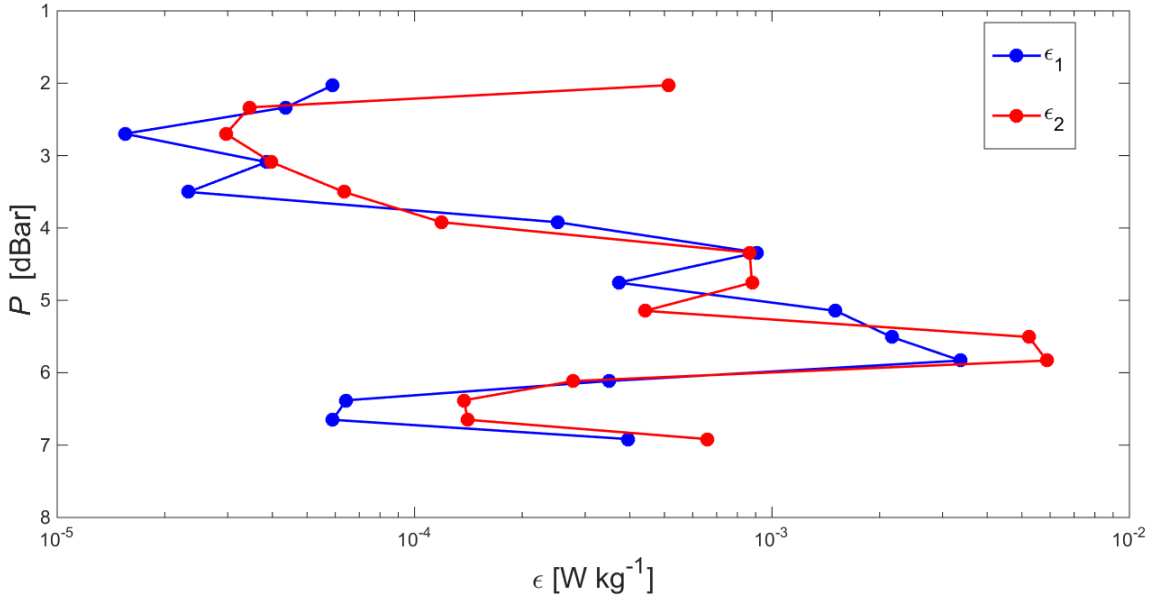

Figure 4.20: Dissipation rate profile obtained from the shear probe for point A for two runs

a profile. The dissipation rate profile for point A is shown in Figure 4.19.

Next, a plot of the dissipation rate profile is shown in Figure 4.20, as calculated by RSI [94]

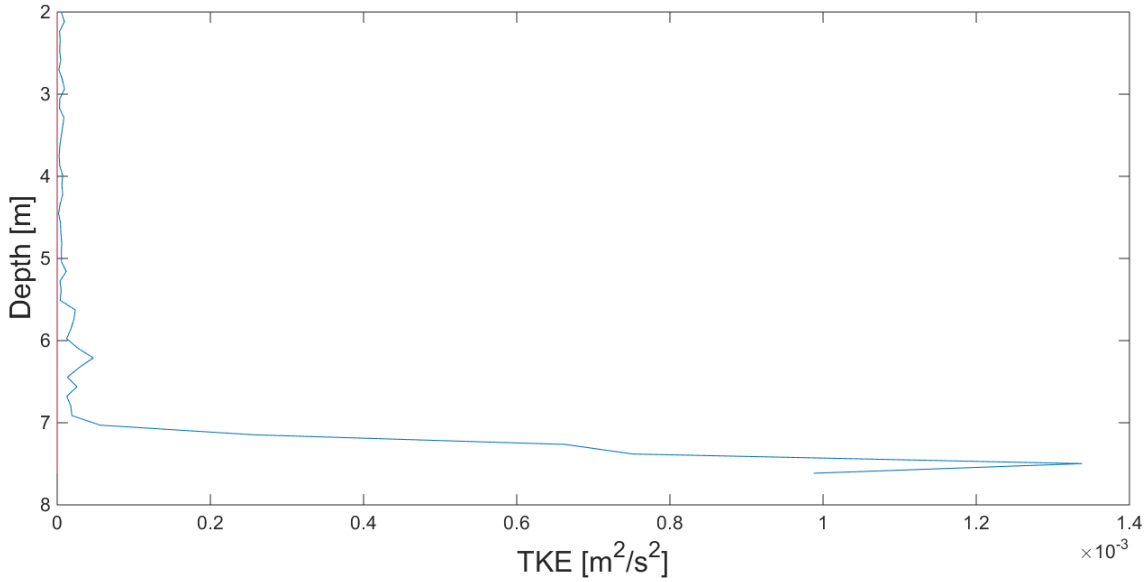

Figure 4.21: Turbulent kinetic energy profile obtained from the shear probe for point A

Additionally, from the shear probe data, it is possible to obtain the velocity fluctuations, and therefore, the turbulent kinetic energy, which is comparable to the ADV. An example plot of the turbulent kinetic energy obtained from the shear probe is shown in Figure 4.21.

The turbulent kinetic energy profile from the data obtained by the ADV is also plotted. This is shown in Figure 4.23

In terms of the dissipation rate, the ADV and shear probe disagree. At point A, the results differ by approximately 91% on average, between the two devices. At point B and C, the results can differ by more. At the surface, the disagreements are larger, sometimes over several orders of magnitude, at points B and C. Figure 4.23 shows a comparison of the dissipation rate measured by the shear probe and the ADV at point A.

There are several possible reasons for the disagreement between the two devices. The shear probe collects data in differential terms. Namely, it collects a variable that is

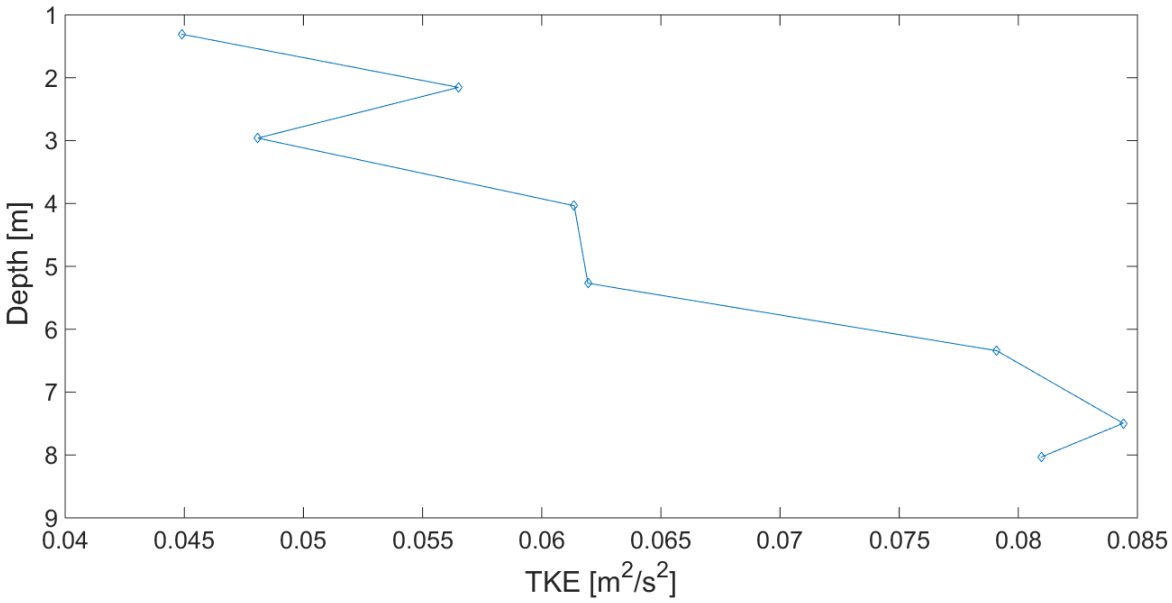

Figure 4.22: Turbulent kinetic energy profile obtained from the ADV for point A

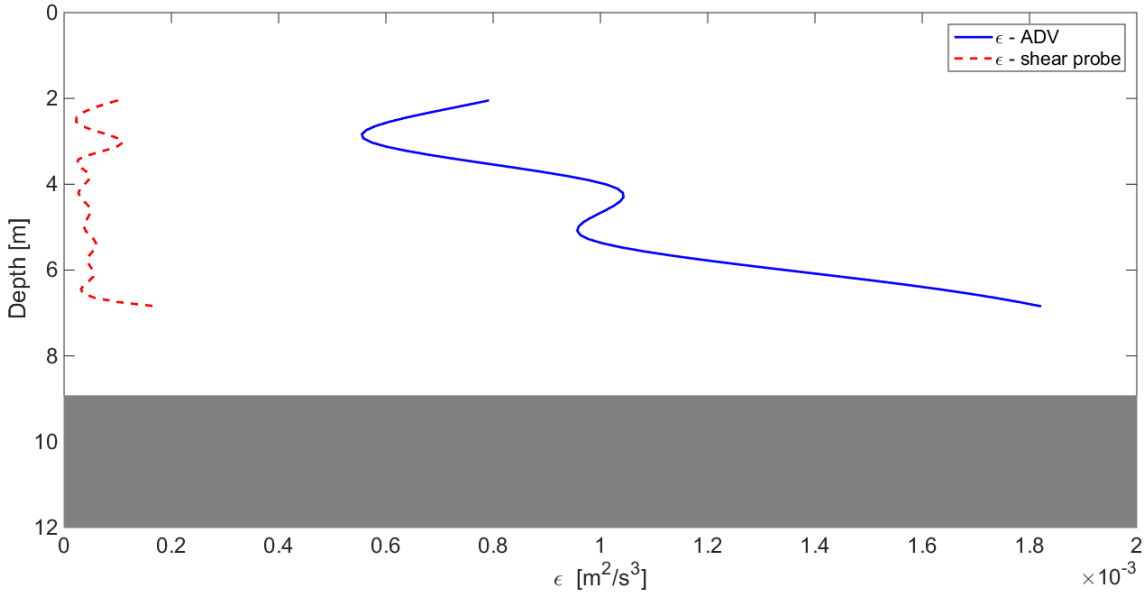

Figure 4.23: Turbulent dissipation rate profile obtained from the shear probe and ADV at point A

directly related to $\frac{\partial u}{\partial z}$ and $\frac{\partial u}{\partial t}$. Using these, an estimation of the dissipation rate is made using Equation 4.2 [31].

$$\epsilon = \frac{15}{2}\nu\overline{\frac{\partial u}{\partial z}^2} \tag{4.2}$$

This is an approximation, and not an exact value of the dissipation rate. Additionally, the correlation by Nezu and Nakagawa [93] is itself a correlation. This is one possible reason why the shear probe and ADV do not agree on the dissipation rate.

In terms of the disagreement with kinetic energy, this is most likely due to the scales captured by the shear probe and ADV. The shear probe is able to capture turbulence scales in the range of 0.01 to 1 m. In rivers, the literature states that the integral scales can be as large as the depth [46]. This means that the shear probe cannot resolve large scale turbulence. These large scales contain more kinetic energy than the smaller scales, and as such, if the ADV is capturing them and the shear probe isn't, this alone can explain the difference between the ADV and the shear probe data.

In terms of utility of the shear probe, it is most suitable for micro-turbulence, as well as the collection of the dissipation rate. On the other hand, the shear probe does not capture macro-turbulence and cannot predict large-scale turbulent kinetic energy. The advantage of this device, however, is the ease with which it is deployed. The reliability of the instrument and the validity of the dissipation rate it presents should be examined further in future studies.

4.5.2 Device-induced turbulence

When a solid body is placed in a fluid flow, vortices are created behind the object. This phenomenon is commonly known as vortex shedding. The vortices are shed at a certain frequency. This frequency is related to the Strouhal number, which is calculated using this equation found in Fox and Mcdonald [12]:

$$St = \frac{fd}{U} \tag{4.3}$$

where, f is the vortex shedding frequency and d is the length scale of the obstruction causing vortices. Additionally, the Strouhal number can be related to the Reynolds number by a correlation given by Williamson and Brown [95]:

$$St = 0.2698 - \frac{1.0271}{Re^{0.5}} \tag{4.4}$$

This is equation is applied to determine the vortex shedding frequencies of the wire cable, as well as the ADV itself. The goal of calculating the vortex shedding frequencies is to determine whether or not the calculated frequencies of these two cylindrical bodies, the ADV and the wire cable, match with frequencies observed by the IMU on the ADV. The results are shown in Table 4.11.

For a comparison to the frequencies experienced by the ADV, the IMU signals are analyzed in the frequency spectrum. An energy spectrum analysis is performed on the spanwise acceleration data obtained from the IMU. The results are shown in Figure 4.24.

From the figure, we can see that forcings affecting the ADV in the spanwise direction occur at just above 1 Hz and as well at roughly 19 to 20 Hz. It is apparent that the frequencies calculated for vortex shedding do not match the frequencies observed

Table 4.10: Vortex shedding frequencies calculated with Equation 4.4 using the mean flow velocity and ADV diameter

Depth [m]	St	f [Hz]
1.30	0.267	7.1
2.15	0.267	7.1
2.96	0.267	7.1
4.04	0.267	6.8
5.27	0.267	6.5
6.34	0.267	6.0
7.50	0.267	5.1
8.03	0.266	4.8

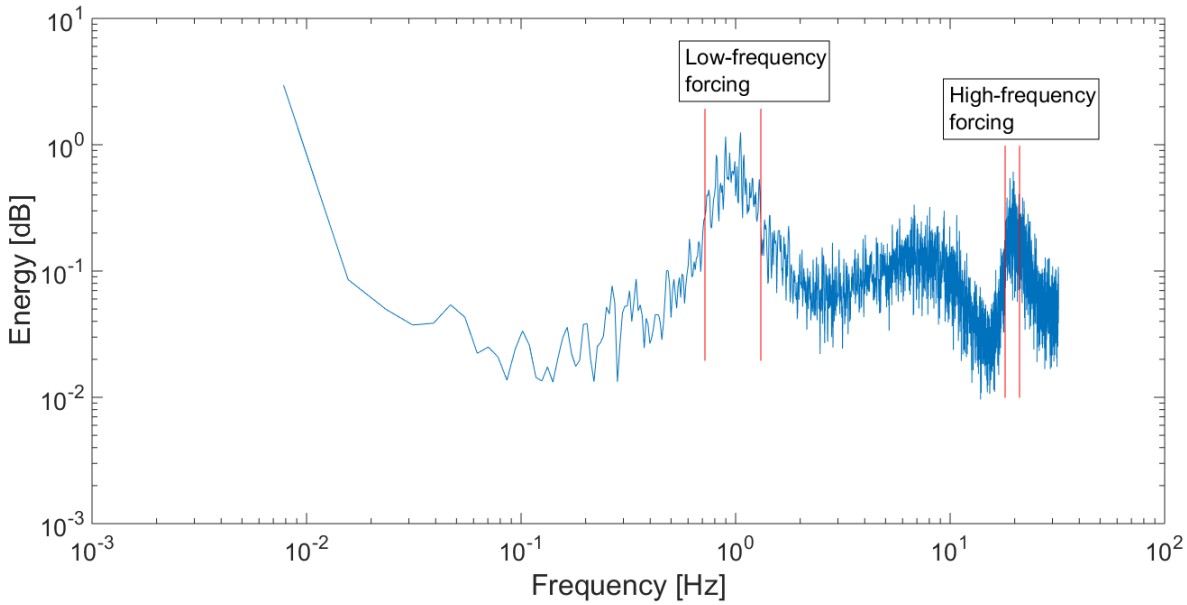

Figure 4.24: Energy spectrum of spanwise acceleration of the ADV for the measurement at 1.3 m depth at point A. At approximately 1 Hz, a peak is observed, indicating that there is a significant low frequency forcing. Another peak is observed at approximately 20 Hz, which indicates a high frequency forcing as well.

Table 4.11: Vortex shedding frequencies calculated with Equation 4.4 using the mean flow velocity and width of ADV measurement unit

Depth [m]	St	f [Hz]
1.3	0.27	1.58
2.2	0.27	1.60
3.0	0.27	1.59
4.0	0.27	1.51
5.3	0.27	1.46
6.3	0.27	1.35
7.5	0.27	1.15
8.0	0.27	1.07

with the IMU. However, the ADV was not the only apparatus on the cable. The unit holding the ADV was also present. Even though it is not cylindrical in shape, nor is it consistently wide, this could be influencing the vortices and forces seen by the IMU. Now, instead of the ADV diameter, the maximum width of the ADV measurement unit is used to calculate the vortex shedding frequencies. The results are shown in Table 4.11.

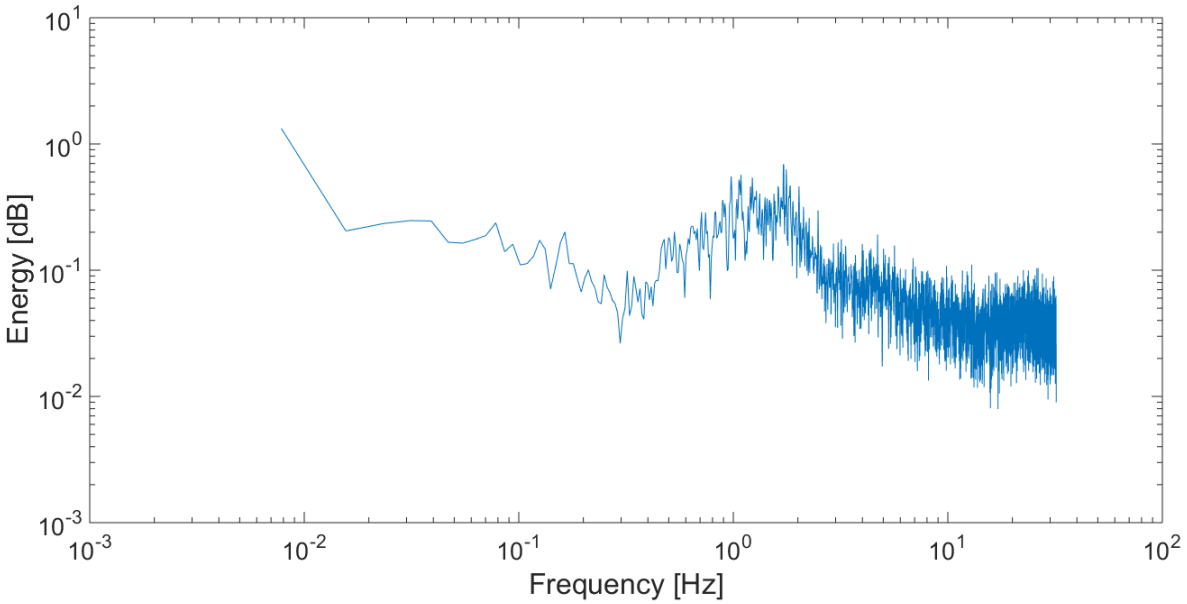

Figure 4.25: Energy spectrum plot for the measurement closest to surface at point B

It is clear that the frequencies calculated using the maximum width of the ADV measurement unit are much closer to the frequencies observed by the IMU. This explains the low frequency forcing observed by the IMU. The high frequency forcing is still uncertain, however.

Additionally, the energy spectrum is calculated and graphed for each measurement point at all depths. The low frequency forcing observed by the IMU is common to all readings, except for some readings at point B. An interesting phenomena is observed in the energy spectrum for these measurements. Referring to Section 4.2.2, a turbine wake is observed in the ADV data for point B. When the ADV is above this wake, the low frequency forcing is observed, as usual. This can be seen in Figure 4.25. However, when the ADV enters the wake of the turbine, this forcing disappears. This can be seen in Figure 4.26.

This disappearance of the low frequency forcing, which is observed in all other ADV readings, persists until the bottom of the channel. What the data indicates is that, if the low frequency forcing is indeed the vortices shed by the ADV measurement unit,

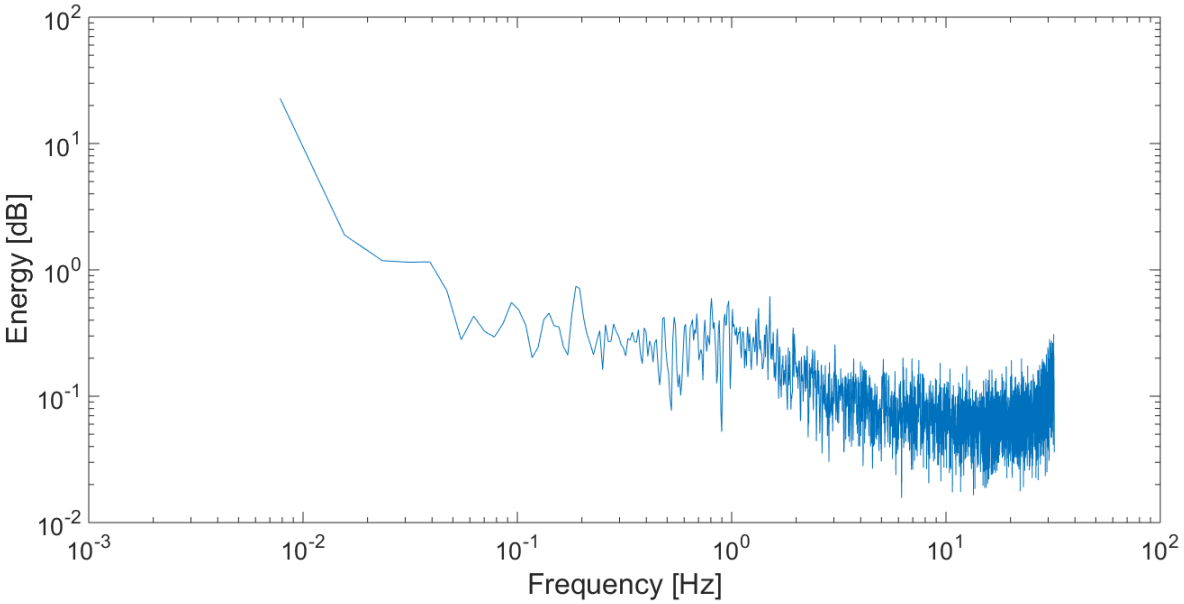

Figure 4.26: Energy spectrum plot for the measurement close to turbine wake at point B

the presence of an external wake seems to suppress this phenomenon. More research on this aspect is required to validate a vortex shedding suppression mechanism.

4.5.3 Uncertainties in turbulence readings

Since acoustic devices have error when they record data, this means that the exact reading of these devices at a certain point in time is not exactly the true velocity of the flow. In addition, the devices can observe spikes, which are data points that are far away from the mean value. There is nothing that can be done to eliminate device error or accuracy issues, however, there are methods to remove spikes from the data set. One method is simply removing spikes that are a certain number of standard deviations away from the mean. This is a simple technique that is easy to employ during post processing. This is the method used in obtaining the velocity and turbulence profiles in Sections 4.2.2 and 4.5.

However, there is an outlier in the turbulence profile at point C. This data point

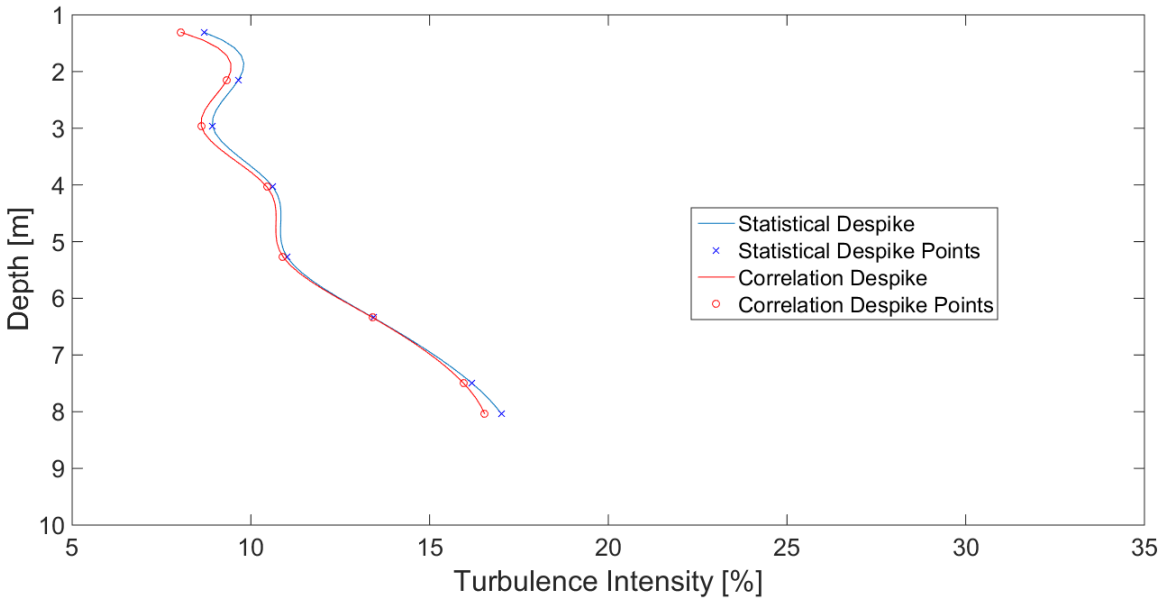

Figure 4.27: Comparison of despiking methods for ADV data for turbulence at point A

is due to the presence of excessive spikes. An alternative method to identify spikes is required to obtain a turbulence profile. One possibility is to use the correlation of the ADV to identify spikes. The correlation values output by the ADV are a measure of how the current measurement point correlates with the previous one and is a measure of the strength of the return pulse [96]. Based on this approach, a program is written to remove spikes from the data if the data point has a correlation value below a threshold which is set by the user. The threshold correlation used is 95%. The results produced are then compared to the data despiked using only the statistical method. Two measurement points are compared in terms of the velocity and turbulence profiles. The results can be seen in Figures 4.27 to 4.30.

From Figures 4.29 to 4.30, the despiking method has little effect on the mean velocity component. However, when observing Figures 4.27 to 4.28, the despiking method can have a significant effect on the turbulence intensity results. This is due to the presence of spikes increasing the perceived turbulence intensity. If all of the low correlation data points are removed, the data becomes more representative of the physical flow.

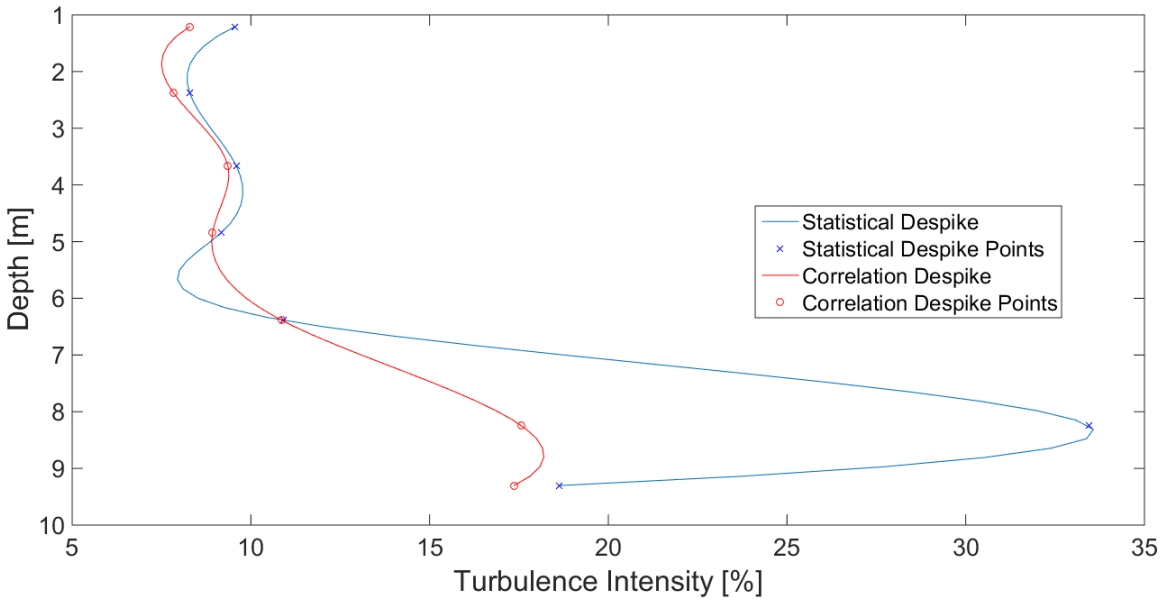

Figure 4.28: Comparison of despiking methods for ADV data for turbulence at point C

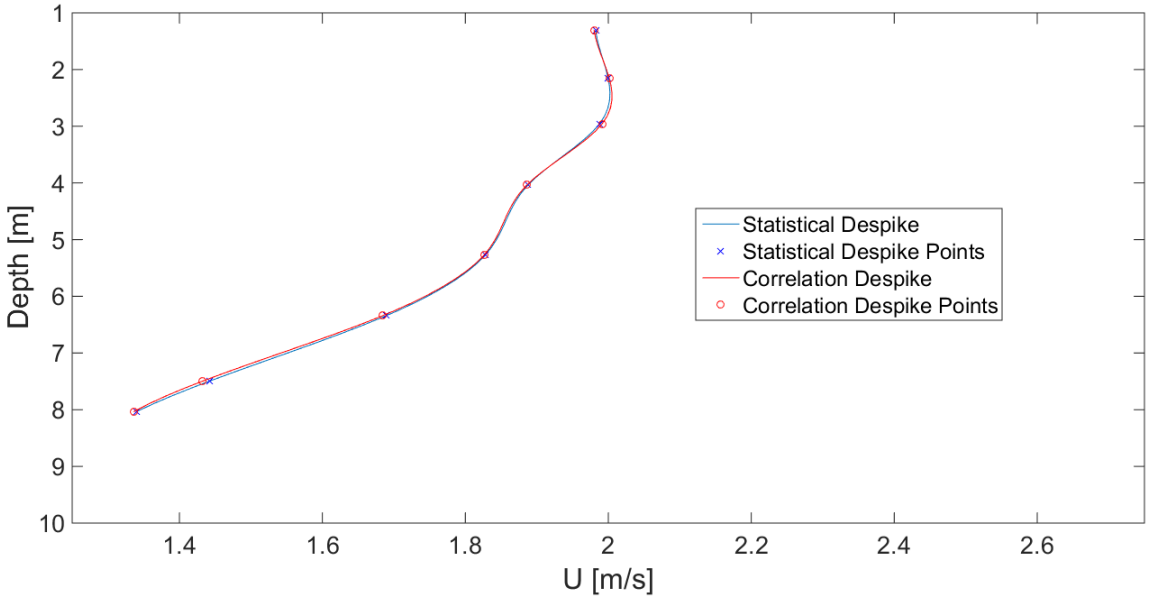

Figure 4.29: Comparison of despiking methods for ADV data for Streamwise velocity at point A

At the same time, this can result in issues for frequency processing. In some cases, the data files can have so much noise that there are few points to interpolate. This creates a problem in the type of despiking algorithm which finds a spike and replaces

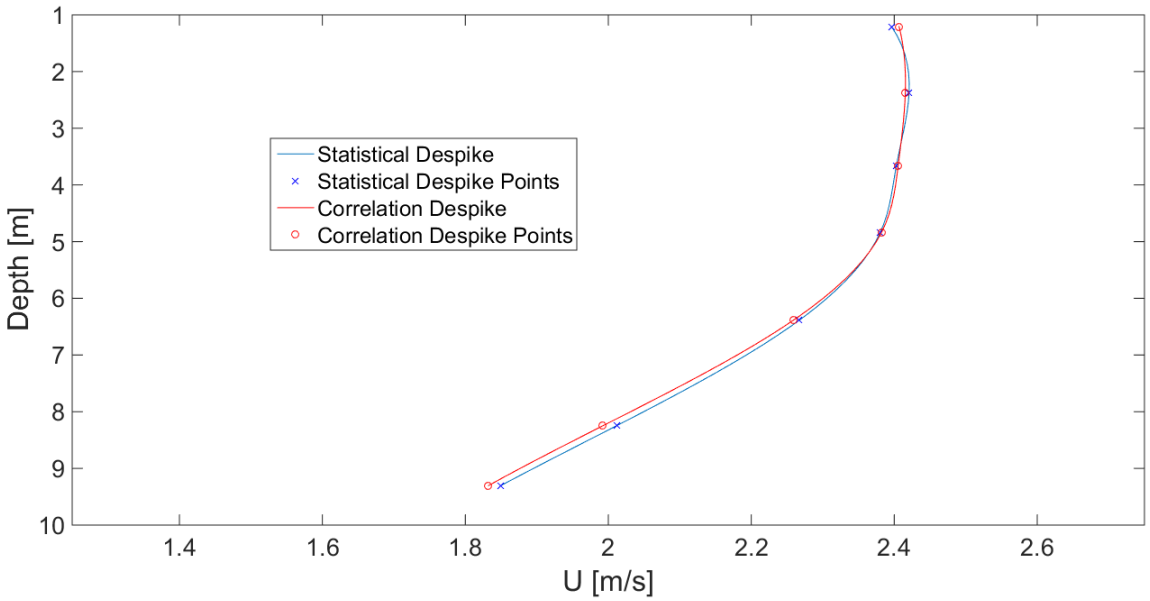

Figure 4.30: Comparison of despiking methods for ADV data for Streamwise velocity at point C

it with a number interpolated from the nearest valid points. This type of despiking is the only type that can be used in conjuction with frequency processing, as there cannot be gaps introduced in the data, i.e. each data point must be the same time step distance from the previous. In cases of highly turbulent data, the correlation despike works well, however, frequency processing cannot be performed on data sets such as these.

In terms of number of spikes removed, Tables 4.12 and 4.13 summarize the number of spikes removed with each despiking method.

It is clear that the number of spikes removed increases when using the correlation despiking method. To clarify this point, the percent differences of spikes removed between the two methods is presented in Table 4.14.

With an averaged combined percent difference of approximately 318%, the correlation despiking method finds and removes more spikes than the statistical method.

The number of spikes in the ADV are greater than in the ADCP and shear probe

Table 4.12: Summary of number of spikes removed from ADV data using the statistical despiking method

Measurement	Point A	Point B	Point C
1	1,372	14,923	2,047
2	913	1,996	1,124
3	827	1,544	1,942
4	848	1,785	1,575
5	647	1,700	907
6	609	2,130	4,286
7	657	1,922	3,667
8	760	4,937	N/A
Max	1,372	14,923	4,286
Min	609	1,544	907
Combined average	2,306		

Table 4.13: Summary of number of spikes removed from ADV data using the correlation despiking method

Data file	Point A	Point B	Point C
1	9,321	16,626	13,483
2	8,452	9,115	9,215
3	7,173	5,934	10,221
4	7,701	7,443	9,947
5	6,361	7,729	7,287
6	6,822	7,959	24,440
7	6,343	10,323	6,664
8	6,912	14,465	N/A
Max	9,321	16,626	2,4440
Min	6,343	5,934	6,664
Combined Average	9,648		

Table 4.14: Percent difference between statistical and correlation despiking methods

Point A	Point B	Point C	Combined
790.77	157.28	422.62	318.41

data. For this reason, despiking methods are compared for the ADV. Additionally, no despiking is performed on the ADCP and shear probe data sets, because there are not enough spikes to sufficiently affect the mean data.

4.6 Bathymetry

Following the collection of bathymetry data (see Section 3.4), post processing is required to visualize the bathymetry of the channel. An assumption made is that the area of interest is sufficiently small such that the GPS coordinates can be flattened reasonably to a 2D cartesian grid.

To begin the analysis, the data is extracted from the sonar system. Then, using the HumminbirdPC and HumViewer software, the data can be converted into ordered columns of Latitude [°], Longitude [°] and Depth [m]. Next, the data table is imported into Tecplot for countouring. A grid is then created using the collection of longitude and latitude points. Once the grid is created, the software interpolates the depth values throughout the grid using the collected ones and finally a contour plot can be created. The results of the bathymetry analysis are shown in Figure 4.31.

The CHTTC channel is relatively flat with some locations where the depth varies. For example, in the north-western portion of the channel, the water level gets shallower. This is where measurement point A is located.

Figure 4.31 shows how the procedure developed to capture the bathymetry of a potential HKT site results in an accurate depiction of the bathymetry of a given river section.

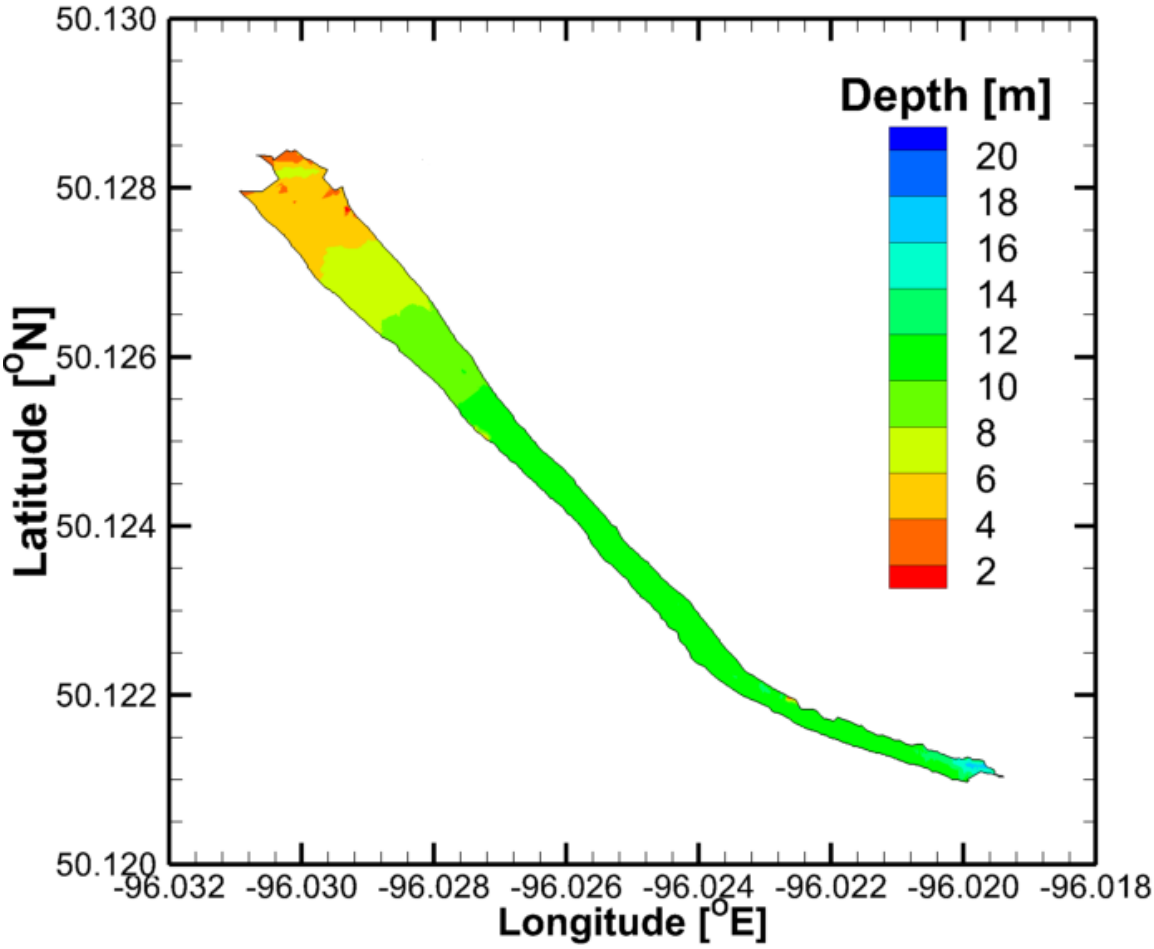

Figure 4.31: Bathymetry of the Winnipeg River at Seven Sisters Manitoba at the CHTTC

Chapter 5

Conclusions and recommendations

5.1 Conclusion

In summary, there are effective approaches to characterize a potential deployment site for a hydrokinetic turbine. In this thesis, a number of approaches are tested. Firstly, a preliminary assessment is performed over a large area. This preliminary assessment involves using the ADV to measure at several selected points in the area to get an idea of the velocities in the region. Once the high velocity locations have been selected, a measurement campaign can be performed.

The measurement campaign is performed using three instruments: the ADV, the ADCP and the shear probe. Anchors are installed on both shores of the river at these locations. A fixed measurement platform is equipped with a winch system to be able to lower the ADV down to any desired depth. The fixed platform is then anchored to both sides of the shore and measurement can begin. First, the ADV is attached to the winch system. Then, the ADCP is secured to the front of the platform as rigidly

as possible. Finally, the shear probe is prepared and secured in a mobile platform to perform repeated deployments. The ADCP is set to record for the duration of the time spent at the measurement point. The ADV performs short measurements at multiple depths, the length of which is determined based on the expected large scale turbulence and depth of river. The shear probe is then deployed at the beginning of the ADV measurements and then at the end of them. The larger number of shear probe deployments, the better, so as to collect a wealth of data.

The data are imported into Matlab and calculations are performed to find the components of the flow. Mean flow and turbulence results are obtained from the ADCP and the ADV. Turbulence results are also obtained from the shear probe. The mean flow compares well between the ADV and the ADCP, with an average percent difference of 4.38%. However, the ADV captures detailed flow features, such as turbine wakes, while the ADCP does not. This is due to the spatial averaging present in the ADCP data. There are, however, disagreements between the ADV and ADCP in the turbulence results at an average of 30%. Due to the characteristics of the ADCP, the turbulence values are mis-predicted, and the ADV is therefore the recommended device to perform turbulence measurements in rivers. In terms of a comparison to the shear probe, the turbulent kinetic energy differs by orders of magnitude due to the fact that the shear probe is a micro-turbulence instrument, while the ADV captures large and small scales. The small scales that are captured by the shear probe do not contain as much energy as the large and small scales captured by the ADV. Additionally, the approximation of dissipation rate differs between the ADV and the shear probe by a minimum of 60%. This is due to the fact that two different approaches for the approximation of dissipation rate are used for each instrument. This is further supported by the fact that the values obtained differ between readings at a single point, when the results should at least be similar.

In terms of spectral analysis, it is found that two major forces are observed in the spanwise acceleration data obtained from the accelerometer on-board the ADV, one near 1 Hz and one near 20 Hz. The low frequency forcing is canceled when the ADV is in the presence of an underwater turbine wake. Additionally, the 20 Hz frequency is only seen in measurements where there is no turbine wake present in the velocity profile. There is evidence in the vortex shedding frequency data, that this low frequency could be the result of vortex shedding caused by the ADV measurement unit.

Two despiking methods are investigated: one using standard deviations, called the statistical method and the other using the correlation data collected by the ADV, called the correlation method. It is found that the statistical method does sufficiently well in despiking unless there is a large amount of turbulence. In this case, it is necessary to use the correlation despiking method, which increases the number of spikes removed. If the data is not highly turbulent, the correlation despiking method can still be used, as it does not greatly affect the turbulence or mean velocity profiles in the absence of excess turbulence.

In conclusion, the characterization of a potential hydrokinetic turbine site can be performed if the right equipment and supports used. Each instrument in this study has merits for the application, however, the ADV is the most accurate instrument of the three compared in this study and is recommended for accurate data collection. If only mean velocity data is required, the ADCP is a useful instrument as well. When a better understanding of the effect of turbulence micro-structure on hydrokinetic turbine operation is obtained, the shear probe can provide this data with little deployment equipment required. This instrument has the potential to help address whether or not micro-turbulence affects hydrokinetic turbine performence

5.2 Recommendations and future work

The determination of optimal sites for hydrokinetic turbines will benefit from future work. For instance, the disappearance of the low frequency forcing in the spanwise ADV acceleration in the presence of a turbine wake is an interesting phenomenon and could have applications for moving equipment underwater, which would include turbine farms. It is important to find out if this frequency is simply suppressed or removed altogether. Additionally, the source of this forcing, while it could be vortex shedding, is still unclear. It would be ideal to understand this forcing, which involves finding its source.

Another area to expand on is the accuracy and associated error terms of the ADV in collecting turbulence data. The ADV data agrees with literature, but just how well this data physically represents the flow is unclear. An error analysis should be performed on the use of the ADV measurement system to see if it agrees with more stationary measurements using the ADV. Error terms of the ADV measurement procedure must be characterized to assess how well the measurement procedures developed in this study can accurately characterize a hydrokinetic site.

It is recommended that more points in the Seven Sisters channel are characterized, so as to provide input or comparison data for a computational fluid dynamics (CFD) analysis of the channel. This would provide a much needed comparison of real, in-situ flow measurements, with the predictions of computational and numerical methods. To obtain such data, more characterization points would have to be selected throughout the channel in the streamwise direction and multiple profile measurements at each streamwise location should be performed across the span. This would provide a grid-like structure of results and would make for easy incorporation or comparison to CFD results.

Additionally, the assessment time dependency of characterization measurements should be performed. The profile measurements in this thesis are measured over three different days at three different streamwise locations. One location should be performed on multiple days, at multiple water levels and over long periods of time, so as to assess how repeatable characterization measurements are, and how the velocity profile varies over the year. This would be of use in predicting seasonal power fluctuations if a turbine were to be placed in such a location.

Also, a comparison should be made between the data collected from the mobile platform and the data collected from the stationary platform. In this case, an experiment should be set up such that data is collected with the mobile and stationary platforms at the same time. This could be used to compare the two methods and determine how they differ, and how the mobile platform measurements may predict the flow that would be observed in the stationary platform measurements.

Finally, since the channel at the CHTTC is basic in terms of geography, it is desirable to determine how the measurement procedure presented in this study is applicable to other geographic locations. For example, the Seven Sisters channel is relatively narrow. Some rivers can be much larger in the spanwise direction. While the same method for securement of the fixed platform could be used, it may be more ideal to come up with another way of securing the fixed platform in wide channels.

Bibliography

[1] F. Mosallat, "Turbine model."

[2] C. Smith, "Vortex illustration."

[3] R. G. Miller, S. R. Sorrell, H. Lane, S. Kt, and R. G. Miller, "The future of oil supply," 2014.

[4] R. S. J. Tol, "Quantifying the consensus on anthropogenic global warming in the literature: rejoinder," *Energy Policy*, vol. 73, p. 709, 2014.

[5] Enerdata. (2017) Global energy statistical yearbook 2017. [Online]. Available: https://yearbook.enerdata.net/

[6] T. Tyrrell, J. G. Shepherd, and S. Castle, "The long-term legacy of fossil fuels," *Tellus, Series B: Chemical and Physical Meteorology*, vol. 59, no. 4, pp. 664–672, 2007.

[7] M. S. Güney and K. Kaygusuz, "Hydrokinetic energy conversion systems: a technology status review," *Renewable and Sustainable Energy Reviews*, vol. 14, pp. 2996–3004, 2010.

[8] N. Bullard, J. Isola, and E. Zindler. (2013) Renewable energy now cheaper than fossil fuels in australia. [Online]. Available: http://about.bnef.com/press-releases/renewable-energy-now-cheaper-than-new-fossil-fuels-in-australia/

[9] K. Kusakana and H. J. Vermaak, "Hydrokinetic power generation for rural electricity supply: case of South Africa," *Renewable Energy*, vol. 55, pp. 467–473, 2013. [Online]. Available: http://dx.doi.org/10.1016/j.renene.2012.12.051

[10] W. Jenkinson, "Canada s sydrokinetic power potential," 2013.

[11] S. E. d'Auteuil, E. L. Bibeau, A. H. Birjandi, and C. Ridd, "Riverine hydrokinetic resource assessment and site selection using low cost satellite and aerial winter imagery," in *Marine Energy Technology Symposium*, 2015.

[12] P. J. Pritchard, *Fox and McDonald's introduction to fluid mechanics*, 8th ed. John Wiley & Sons, 2011.

[13] CHTTC. (2017) Canadian Hydrokinetic Turbine Test Centre website. [Online]. Available: http://chttc.ca

[14] Nortek AS, "Comprehensive manual," Nortek AS, Tech. Rep., 2013.

[15] N. Nidzieko, D. Fong, and J. Hench, "Comparison of Reynolds stress sstimates derived from standard and fast-ping ADCPs," *American Meteorological Society*, 2006.

[16] E. M. Horstman, T. Balke, T. J. Bouma, C. M. Dohmen-Janssen, and H. S. J. M. H, "Optimizing methods to measure hydrodynamics in coastal wetlands: evaluating the use and positioning of ADV, ADCP and HR-ADCP," *Coastal Engineering*, pp. 1–11, 2010.

[17] H. M. Tritico, M. C. Stone, and R. H. Hotchkiss, "Turbulence characterization in the wake of an obstruction in a gravel bed river," *American Society of Civil Engineering*, no. 509, pp. 780–789, 2002. [Online]. Available: http://www.scopus.com/inward/record.url?eid=2-s2.0-1642568830&partnerID=40&md5=7eee4436d0fc57194b3175506a95cce1

[18] G. Voulgaris and J. H. Trowbridge, "Evaluation of the acoustic Doppler velocimeter (ADV) for turbulence measurements," *Journal of Atmospheric and Oceanic Technology*, vol. 15, no. 1, pp. 272–289, 1998.

[19] B. Gunawan, V. Neary, and J. Colby, "ADV measurements for turbulent inflow characterization in the East River New York City," Tech. Rep., 2011.

[20] T. M. Clunie, V. I. Nikora, S. E. Coleman, H. Friedrich, and B. W. Melville, "Flow measurement using flying ADV probes," *Journal of Hydraulic Engineering*, vol. 133, no. 12, pp. 1345–1355, 2007. [Online]. Available: http://ascelibrary.org/doi/10.1061/(ASCE)0733-9429(2007)133:12(1345)

[21] J. J. H. Vanzwieten, M. N. Egeland, K. D. V. Ellenrieder, W. Lovenbury, D. Beach, and L. Kilcher, "Experimental Evaluation of Motion Compensated ADV Measurements for In-Stream Hydrokinetic Applications," 2015.

[22] J. W. Lovenbury, "Evaluation of motion compensated ADV measurements for quantifying velocity fluctuations," Ph.D. dissertation, 2013.

[23] S. Gooch, J. Thomson, B. Polagye, and D. Meggitt, "Site Characterization for Tidal Power," *OCEANS 2009, MTS/IEEE Biloxi - Marine Technology for Our Future: Global and Local Challenges*, pp. 1–10, 2009.

[24] J. Colby and D. Corren, "Detailed inflow measurements for kinetic hydropower systems in a tidal strait," Tech. Rep., 2008.

[25] M. Muste, K. Yu, T. C. Pratt, and D. Abraham, "ADCP measurements at fixed river locations," *ASCE/EWRI and IAHR International Conference on Hydraulic Measurements and Experimental Methods*, vol. 113, p. 73, 2002.

[26] M. Shives and C. Crawford, "Methods for determining TKE and dissipationn rate from ADCP," Tech. Rep., 2015.

[27] C. M. García, P. R. Jackson, K. A. Oberg, K. K. Johnson, and M. H. García, "Characterizing a December 2005 density current event in the Chicago River, Chicago, Illinois," *World Environmental and Water Resources Congress 2006*, 2006.

[28] D. S. Mueller, C. R. Wagner, M. S. Rehmel, k. A. Oberg, and F. Rainville, *Measuring discharge with acoustic Doppler current profilers from a moving boat*, 2013, no. December. [Online]. Available: http://search.proquest.com/docview/50234694?accountid=25565/nhttp://rl3mq7xr4s.search.serialssolutions.com/?ctx_ver=Z39.88-2004&ctx_enc=info:ofi/enc:UTF-8&rfr_id=info:sid/ProQ:georefmodule&rft_val_fmt=info:ofi/fmt:kev:mtx:journal&rft.genre=article&rft.jti

[29] M. Muste, K. Yu, and M. Spasojevic, "Practical aspects of ADCP data use for quantification of mean river flow characteristics; part I: moving-vessel measurements," *Flow Measurement and Instrumentation*, vol. 15, no. 1, pp. 1–16, 2004.

[30] M. Muste, K. Yu, T. Pratt, and D. Abraham, "Practical aspects of ADCP data use for quantification of mean river flow characteristics; part II: fixed-vessel measurements," *Flow Measurement and Instrumentation*, vol. 15, no. 1, pp. 17–28, 2004.

[31] F. Wolk, J. Hancyk, and R. Lueck, "Turbulence measurements using non-acoustic sensors in a high-flow tidal channel," in *1st Asian Wave and Tidal Conference Series*, 2012, pp. 1–5.

[32] T. Ross, "A video-plankton and microstructure profiler for the exploration of in situ connections between zooplankton and turbulence," *Deep-sea Research Part I: Oceanographic Research Papers*, vol. 89, pp. 1–10, 2014.

[33] O. Kocsis, H. Prandke, A. Stips, A. Simon, and A. Wüest, "Comparison of dissipation of turbulent kinetic energy determined from shear and temperature microstructure," *Journal of Marine Systems*, vol. 21, no. 1-4, pp. 67–84, 1999.

[34] S. Woods, W. Hou, W. Goode, E. Jarosz, and A. Weidemann, "Measurements of turbulence for quantifying the impact of turbulence on underwater imaging," *2011 IEEE/OES/CWTM 10th Working Conference on Current, Waves and Turbulence Measurement, CWTM 2011*, pp. 179–183, 2011.

[35] Y. Tanaka, I. Yasuda, S. Osafune, T. Tanaka, J. Nishioka, and Y. N. Volkov, "Internal tides and turbulent mixing observed in the Bussol Strait," *Progress in Oceanography*, vol. 126, pp. 98–108, 2014. [Online]. Available: http://dx.doi.org/10.1016/j.pocean.2014.04.009

[36] J. M. Mcmillan, A. E. Hay, R. G. Lueck, and F. Wolk, "Vertical profiles of turbulence metrics in Grand Passage , Nova Scotia," *International Conference on Ocean Energy*, no. November, 2014.

[37] I. Fer and M. Bakhoday Paskyabi, "Autonomous ocean turbulence measurements using shear probes on a moored instrument," *Journal of Atmospheric and Oceanic Technology*, vol. 31, no. 2, pp. 474–490, 2014.

[38] V. Neary, B. Gunawan, M. Richmond, V. Durgesh, B. Polayge, J. Thompson, M. Muste, and A. Fontaine, "Field measurements at river and tidal current sites for hydrokinetic energy development: best practices manual," Oakridge National Laboratory, Tech. Rep. September, 2011. [Online]. Available: http://info.ornl.gov/sites/publications/Files/Pub32922.pdf

[39] A. Birjandi, E. Bibeau, and J. Woods, "Investigation of macro-turbulent flow structures interaction with a vertical hydrokinetic river turbine," *Renewable Energy*, vol. 48, no. 0, pp. 183 – 192, 2012.

[40] J. Woods, "Hydrokinetic Turbine Systems for Remote River Applications in Cold Climates," Ph.D. dissertation, 2017.

[41] V. I. Nikora and G. M. Srnare, "Turbulence characteristics of New Zealand gravel-bed rivers by," *Journal of Hydraulic Engineering,*, vol. 123, no. 9, pp. 764–773, 1997.

[42] A. N. Sukhodolov, "Structure of turbulent flow in a meander bend of a lowland river," *Water Resources Research*, vol. 48, no. 1, pp. 1–21, 2012.

[43] V. I. Nikora, P. Rowinski, A. Suchodolov, and D. Krasuski, "Structure of river turbulence behind warm-water discharge," *Journal of Hydraulic Engineering*, vol. 120, no. 2, pp. 191–208, 1994.

[44] M. F. Tachie, D. J. Bergstrom, and R. Balachandar, "Rough wall turbulent boundary layers in shallow open channel flow," vol. 122, no. September 2000, pp. 533–541, 2014.

[45] I. Nezu, "Open-channel flow turbulence and its research prospect in the 21st century," *journal of hy*, vol. 41, no. April, pp. 229–246, 2004.

[46] A. G. Roy, T. Buffin-Blanger, H. Lamarre, and A. D. Kirkbride, "Size, shape and dynamics of large-scale turbulent flow structures in a gravel-bed river," *Journal of Fluid Mechanics*, vol. 500, pp. 1–27, 2004.

[47] A. Shvidchenko and G. Pender, "Macroturbulent structure of open-channel flow over gravel beds," *Water Resources Research*, vol. 37, no. 3, pp. 709–719, 2001.

[48] M. Arango, "Resource Assessment and Feasibility Study for Use of Hydrokinetic Turbines in the Tailwaters of the Priest Rapids Project," p. 158, 2011.

[49] A. Abbaspour and H. K. Saeed, "Numerical investigation of turbulent open channel flow with semi-cylindrical rough beds," *KSCE Journal of Civil Engineering*, vol. 18, no. 7, pp. 2252–2260, 2014.

[50] B. Afzal, M. A. Faruque, and R. Balachandar, "Effect of Reynolds number, near-wall perturbation and turbulence on smooth open-channel flows," *Journal of Hydraulic Research*, vol. 47, no. 1, pp. 66–81, 2009.

[51] R. Balachandar and M. F. Tachie, "A study of boundary layer-wake interaction in shallow open channel flows," *Experiments in Fluids*, vol. 30, no. 5, pp. 511–521, 2001.

[52] M. Tachie, R. Balachandar, and D. Bergstrom, "Open channel boundary layer relaxation behind a forward facing step at low reynolds numbers," *Journal of Fluids Engineering, Transactions of the ASME*, vol. 123, no. 3, pp. 539–544, 2001.

[53] M. F. Tachie, D. J. Bergstrom, and R. Balachandar, "Roughness Effects on the Mixing Properties in Open Channel Turbulent Boundary Layers," *Journal of Fluids Engineering*, vol. 126, no. 6, p. 1025, 2004. [Online]. Available: http://fluidsengineering.asmedigitalcollection.asme.org/article.aspx?articleid=1430101

[54] H. Bonakdari, F. Larrarte, L. Lassabatere, and C. Joannis, "Turbulent velocity profile in fully-developed open channel flows," *Environmental Fluid Mechanics*, vol. 8, no. 1, pp. 1–17, 2008. [Online]. Available: http://link.springer.com/10.1007/s10652-007-9051-6

[55] X. Wang, Z.-Y. Wang, M. Yu, and D. Li, "Velocity profile of sediment suspensions and comparison of log-law and wake-law," *Journal of Hydraulic Research*, vol. 39, no. 2, pp. 211–217, 2001.

[56] V. Neary, B. Polagye, B. Gunawan, and K. Colby, "Tidal energy site resource assessment: technical specifications, best practices and case studies," Oak Ridge National Laboratory, Oak Ridge, Tech. Rep., 2013.

[57] M. Muste, H. C. Ho, and D. Kim, "Considerations on direct stream flow measurements using video imagery: outlook and research needs," *Journal of Hydro-Environment Research*, vol. 5, no. 4, pp. 289–300, 2011.

[58] R. Lueck, F. Wolk, J. Hancyck, and K. Black, "Hub-height time series measurements of velocity and dissipation of turbulence kinetic energy in a tidal channel," *2015 IEEE/OES 11th Current, Waves and Turbulence Measurement, CWTM 2015*, 2015.

[59] S. Matt, W. Hou, S. Woods, W. Goode, E. Jarosz, and A. Weidemann, "A novel platform to study the effect of small-scale turbulent density fluctuations on underwater imaging in the ocean," *Methods in Oceanography*, vol. 11, no. 2014, pp. 39–58, 2014.

[60] A. E. Hay, J. M. McMillan, R. Cheel, and D. J. Schillinger, "Turbulence and drag in a high Reynolds number tidal passage targeted for in-stream tidal power," *Oceans 2013 San DIego*, pp. 1–10, 2013. [Online]. Available: ftp://128.171.151.230/bhowe/outgoing/IEEEOES_2013/papers/130503-133.pdf

[61] A. Kalnach, J. Kalnach, A. Mutule, and U. Persis, "Potential of the Lower Daugava for siting hydrokinetic turbines," *Latvian Journal of Physics and Technical Sciences*, vol. 50, no. 2, pp. 3–14, 2013. [Online]. Available: http://www.degruyter.com/view/j/lpts.2013.50.issue-2/lpts-2013-0007/lpts-2013-0007.xml

[62] H. Toniolo, P. Duvoy, S. Vanlesberg, and J. Johnson, "Modelling and field measurements in support of the hydrokinetic resource assessment for the Tanana River at Nenana, Alaska," *Proceedings of the Institution of Mechanical Engineers, Part A: Journal of Power and Energy*, vol. 224, no. 8, pp. 1127–1139, 2010. [Online]. Available: http://pia.sagepub.com/content/224/8/1127$\delimiter"026E30F$nhttp://pia.sagepub.com/content/224/8/1127.short/nhttp://www.uaf.edu/files/acep/Toniolo_et_al_2010_Tanana.pdf

[63] K. M. Thyng and J. J. Riley, "Idealized headland simulation for tidal hydrokinetic turbine siting metrics," *MTS/IEEE Seattle, OCEANS 2010*, 2010.

[64] Canadian Hydraulics Centre, "Assessment of Canadas hydrokinetic power potential," National Research Council of Canada, Tech. Rep. March, 2010.

[65] M. Previsic and R. Bedard, "River In-Stream Energy Conversion (RISEC) characterization of Alaska sites," 2008. [Online]. Available: http://oceanenergy.epri.com/attachments/risec/reports/Alaska_Site_Survey_Report_Final.pdf

[66] Georgia Tech Research Corporation, "Assessment of energy production potential from tidal streams in the United States," Tech. Rep., 2011.

[67] A. E. S. Duerr, "Method for marine hydrokinetic turbine array siting in the Florida Current," in *New England MREC 3rd Annual Technical Conference*, no. November, 2011.

[68] E. Lalander, M. Grabbe, and M. Leijon, "On the velocity distribution for hydrokinetic energy conversion from tidal currents and rivers," *Journal of Renewable and Sustainable Energy*, vol. 5, no. 2, pp. 1–20, 2013.

[69] A. Birjandi, "Effect of flow and fluid structures on the performance of vertical river hydrokinetic turbines," Ph.D. dissertation, The University of Manitoba, 2012.

[70] R. J. Cavagnaro, "Impact of turbulence on the control of a hydrokinetic turbine," in *International conference on ocean energy*, 2014.

[71] P. Bachant and M. Wosnik, "Experimental investigation of helical cross-flow axis hydrokinetic turbines, including effects of waves and turbulence,"

ASME-JSME-KSME 2011 Joint Fluids Engineering Conference: Volume 1, Symposia Parts A, B, C, and D, vol. 1, pp. 1895–1906, 2011. [Online]. Available: http://proceedings.asmedigitalcollection.asme.org/proceeding.aspx?articleid=1626211

[72] M. J. Khan, G. Bhuyan, M. T. Iqbal, and J. E. Quaicoe, "Hydrokinetic energy conversion systems and assessment of horizontal and vertical axis turbines for river and tidal applications: A technology status review," *Applied Energy*, vol. 86, no. 10, pp. 1823–1835, 2009. [Online]. Available: http://dx.doi.org/10.1016/j.apenergy.2009.02.017

[73] M. M. Bernitsas, K. Raghavan, Y. Ben-Simon, and E. M. H. Garcia, "VIVACE (Vortex Induced Vibration Aquatic Clean Energy): a new concept in generation of clean and renewable energy from fluid flow," *Journal of Offshore Mechanics and Arctic Engineering*, vol. 130, no. 4, p. 041101, 2008.

[74] L. Gunawan, B. Neary, V.S. Hill, C. Chamorro, "Effects of large energetic vortices on axial-flow hydrokinetic turbines," Oak Ridge National Laboratory, Oak Ridge, Tech. Rep., 2008.

[75] A. Hauet, M. Muste, J. D. Creutin, P. Belleudy, and W. Krajewski, "Discharge measurement using large-scale PIV under varied flow conditions - recent results , accuracy and perspectives -," vol. 36, no. 1998, p. 2006, 2006.

[76] Electric Power Research Institute, "Assessment and mapping of the riverine hydrokinetic resource in the continental United States," Tech. Rep., 2012.

[77] R. Ferguson, "Time to abandon the Manning equation?" *Earth Surface Processes and Landforms*, vol. 35, no. October, pp. 1873–1876, 2010.

[78] P. T. Jacobson, S. V. Amaral, T. Castro-santos, and D. Giza, "Environmental effects of hydrokinetic turbines on fish: desktop and laboratory flume studies," Electric Power Research Institute, Tech. Rep., 2012. [Online]. Available: http://tethys.pnnl.gov/sites/default/files/publications/Jacobson_et_al_2012.pdf

[79] L. Hammar, S. Andersson, L. Eggertsen, J. Haglund, M. Gullström, J. Ehnberg, and S. Molander, "Hydrokinetic turbine effects on fish swimming behaviour," *PLoS ONE*, vol. 8, no. 12, pp. 1–12, 2013.

[80] Normandeau Associates, "An estimation of survival and injury of fish passed through the Hydro Green Energy Hydrokinetic System, and a characterization of fish entrainment potential at the Mississippi Lock and Dam No. 2 Hydroelectric project (P-4306)," no. 21288, pp. 1–82, 2009.

[81] D. P. Struthers, "The spatial ecology and biological responses of wild fishes relative to hydropower development on the Winnipeg River," Ph.D. dissertation, 2016.

[82] Nortek, "Vector ADV datasheet."

[83] River surveyor s5 and m9. [Online]. Available: http://www.sontek.com/productsdetail.php?RiverSurveyor-S5-M9-14

[84] R. S. Instruments, "VMP 250 product datasheet."

[85] IEC, "Marine energy Wave, tidal and other water current converters Part 200: Electricity producing tidal energy converters Power performance assessment," International Electrotechnical Commission, Tech. Rep., 2015.

[86] A. H. Birjandi, S. d'Auteuil, M. Goharrokhi, and E. Bibeau, "Resource assessment at the CHTTC site using horizontal ADCP," Canadian Hydrokinetic Turbine Testing Centre, Tech. Rep.

[87] RDI, "Acoustic Doppler current profiler: principles of operation, a practical primer." Tech. Rep. January, 2011.

[88] G. Ashton, "River ice," in *Ann. Rev. Fluid mechanics*, 1978, pp. 369–392.

[89] T. Carstens, "Experiments with supercooling and ice formation in flowing water," pp. 1–18, 1966.

[90] Manitoba Hydro, "Seven sisters discharge data," Private Communication.

[91] W. H. Snyder and I. P. Castro, "Acoustic Doppler Velocimeter Evaluation in Stratified Towing Tank," *Journal of Hydraulic Engineering*, pp. 595–603, 1999.

[92] M. H. A. Kaji, "Turbulent structure in open channel flow," Ph.D. dissertation, 2013.

[93] I. Nezu and N. H., *Turbulence in open-channel flows*. A.A. Balkema, 1993.

[94] W. Douglas and R. Lueck, "ODAS Matlab library technical manual," Tech. Rep., 2015.

[95] C. H. K. Williamson and G. L. Brown, "A series in 1/sqrt(Re) to represent the strouhal - Reynolds number relationship of the cylinder wake," *Journal of Fluids and Structures*, vol. 12, pp. 1073–1085, 1998.

[96] Nortek, "Information on correlation output from adv," Private Communication.

[97] H. Schlichting and K. Gersten, *Boundary layer theory*, 8th ed. Springer, 2003.

[98] A. Dewan, "Tackling turbulent flows in engineering," *Tackling Turbulent Flows in Engineering*, pp. 1–124, 2011.

[99] K. Avila, D. Moxey, A. de Lozar, M. Avila, D. Barkley, and B. Hof, "The onset of turbulence in pipe flow." *Science*, vol. 333, no. 6039, pp. 192–196, 2011.

[100] B. Jaffe, *Piezoelectric ceramics*. Elsevier, 2012, vol. 3.

[101] CHTTC, "Canadian Hydrokinetic Turbine Test Centre Safe Work Procedures," Tech. Rep. March, 2017. [Online]. Available: http://chttc.ca/files/CHTTC-Safe_Work_Procedures.pdf

Appendix A

Fluid mechanics

A.1 Components of fluid flow

In this thesis, various components of fluid flow are discussed, due to their applications in hydrokinetic turbine technology. Such components include boundary layer and free-stream velocity, as well as turbulence. The boundary layer of a flow refers to a region close to a solid boundary, where flow is slower due to friction or viscosity. The boundary layer extends to a certain distance from the solid boundary, beyond which the mean velocity reaches a maximum value and maintains this until it nears another solid boundary. The boundary layer is characterized by the boundary layer thickness, δ. This thickness is identified as the location at which the velocity reaches approximately 99% of the free-stream, or maximum value [97]. This height depends on surface roughness, flow velocity, flow regime and flow geometry [97]. In open channel flows, such as rivers, the boundary layer thickness from the river bed is important, especially for HKT applications. In most cases, it is beneficial for a HKT to be placed in a region with high velocity so as to produce the maximum amount of power. Power density varies within the water column with velocity cubed. Therefore, knowing the

boundary layer height is important for the design of a HKT. The boundary layer thickness is also important in determining the spanwise distance the turbine should be spaced from the channel side walls.

In addition to the velocity profile, turbulence is important in the characterization of HKTs. Turbulence is characterized by chaotic fluid motion, velocity that fluctuates due to eddies created in the flow. Flows that belong to the turbulent regime apply to industrial applications [98]. Turbulence can be induced by obstacles in the flow, or it can be a result of high velocity, as well as a number of other contributing factors [99]. In rivers suitable for hydrokinetic turbines, the flow regime is turbulent, due to the large Reynolds numbers and large eddies are visible from the surface, which is difficult to reproduce in the laboratory. This means that quantifying turbulence is important for HKTs, and undestand the effects. Mathematically, turbulence is characterized by the change of velocity in time and space. Temporal velocity fluctuations are characterized as deviations from the mean velocity in the three spatial directions, identified as u, v and w corresponding to mean velocities $\overline{U}, \overline{V}$ and $\overline{W}$ respectively. In a time average, taking the average of these values is meaningful, however, simply taking the average of these will always result in zero, because the mean has been removed. Thus, these components are multiplied together in combinations and then averaged, resulting what are called the Reynolds stresses (shear and normal). The Reynolds normal stresses are identified as $\overline{u^2}, \overline{v^2}$ and $\overline{w^2}$, while the Reynolds shear stresses are identified as $\overline{uv}, \overline{uw}$ and $\overline{vw}$. These values are then combined in various ways to calculate quantities such as the Turbulence Intensity (TI) and Turbulent Kinetic Energy (TKE). The turbulence intensity, in particular is a useful way to characterize the turbulence of a region, as it is a single number, typically displayed as a percent.

A.2 Dimensionless groups

Dimensionless groups are an important method of understanding and comparing fluid flows. Since fluid flows can vary in many different characteristics, it is important to create criteria upon which we can compare them. The procedure to create these groups is simple and begins with a general understanding of the physics of fluid motion. For example, we know that important parameters for characterizing a site for hydrokinetic turbines can depend on many variables, which are summarized in Table A.1.

The hydraulic radius is important as it is used as an estimate of the integral length scale for river turbulence, and is defined by Equation A.1.

$$R_h = \frac{A}{P} \tag{A.1}$$

The next step requires combining these parameters into groups. These groups must be dimensionless so as to be able to compare between different fluid flows successfully. A single example of this procedure will be shown, however, all dimensionless groups used are obtained in the same manner. This procedure is presented in Fox and McDonald's Introduction to Fluid Mechanics [12]. The number of parameters is n, the number of primary dimensions is denoted as r, and the repeating parameters with which the groups will be formed (the number of repeating parameters must be $m = r$). In this case, the number of parameters is $n = 14$, and the primary dimensions are length, l, time t and mass, M, making $r = 3 = m$. Three repeating parameters are then selected, which in this case will be hydraulic radius, free-stream velocity and density. The first dimensionless Pi group, named after the Buckingham-Pi theorem, upon which this method is based. One parameter from the original 14 must be selected and multiplied by the repeating parameters raised to a power, and

Table A.1: Important flow parameters for hydrokinetic turbines

Name	Symbol
Boundary layer thickness	δ
Free-stream velocity	U_∞
Nominal turbine design velocity	U_N
Location of maximum velocity	Y_∞
Water density	ρ
Dynamic viscosity	μ
Depth of water column	D
Spanwise length of river	L_Y
Hydraulic radius	R_h
Wetted perimeter	P
Croess-sectional area	A
Acceleration due to gravity	g
Turbulent kinetic energy	K
Turbulence intensity	TI
Dissipation rate	ϵ

subsequently set them all equal to dimensionless numbers, which for now will be called Π_1, for the first Pi group. To begin with, the dynamic viscosity, μ, is selected, yielding Equation A.2.

$$\Pi_1 = (\mu)(R_h^a)(U_\infty^b)(\rho^c) \tag{A.2}$$

Next, variables are replaced with their appropriate units, giving:

$$M^0 * l^0 * t^0 = (M * l^{-1} * t^{-1}) * (l^a) * (l^b * t^{-b}) * (M^c * l^{-3c}) \tag{A.3}$$

Subsequently, the M exponents are equated, followed by the l and then the t. This results in three equations and three unknowns, allowing us to solve for the exponents a, b and c. The results of this comparison are that $a = -1$, $b = -1$ and $c = -1$. The resulting Pi group is given by Equation A.4.

$$\Pi_1 = \frac{\mu}{\rho R_h U_\infty} \tag{A.4}$$

The resulting Pi group is one commonly found in fluid mechanics, and is referred to as the Reynolds number (the Reynolds number is actually defined as the inverse of this group, or $Re = \frac{\rho * R_h * U_\infty}{\mu}$). This number is a ratio of the viscous force to the inertial force of the fluid and is indicative of the type of flow regime (laminar or turbulent), as well as many other fluid qualities. Reynolds number can be further simplified by combining the density and dynamic viscosity, as the are both fluid properties, related to the temperature of the fluid. Reynolds is then given as:

$$Re = \frac{R_h U_\infty}{\nu} \tag{A.5}$$

where ν is the kinematic viscosity, defined as $\nu = \frac{\mu}{\rho}$.

Another important dimensionless group is the Froude number. This number characterizes how the flow is affected by gravity and surface waves. The Froude number is defined by Equation A.6, and is obtained in a similar fashion as the Reynolds number:

$$Fr = \frac{U_\infty}{\sqrt{gR_h}} \tag{A.6}$$

where g is the acceleration due to gravity, equal to 9.81 m/s^2. The Froude number separates the flow into three flow regimes: sub-critical ($Fr < 1$), critical ($Fr = 1$) and super-critical ($Fr > 1$). Sub-critical flows are not affected by gravity and super-critical flows are affected by gravity. Critical flows are in between sub and super-critical, in that they are affected by gravity, but less than super-critical flows.

A.3 The Doppler effect

In experimental fluid mechanics, devices are required to measure the properties of a fluid, such as an Acoustic Doppler Velocimeter, (ADV), which is a device that is used to measure fluid velocity over a small sample volume. This device, among some other devices used in aquatic environments, works by the principle of the Doppler effect, which is the principle that a moving object changes the frequency of a wave interacting with it. To apply this effect, the ADV emits an acoustic pulse (pressure wave) able to travel through water, which bounces off moving particles in the fluid flow. This pulse is then reflected back to the ADV, where the frequency of these pulses are then measured. The change in frequency of the pulses is then related to the velocity of the particles. This velocity is the velocity of the water along the path of the pulse, which can then be translated into usable coordinates with minimal computation. The relationship developed between frequency and velocity is described by Equation A.7 [14], where $F_{doppler}$ is the doppler shifted frequency, F_{source} is the original frequency of the pulses and c is the speed of sound in water.

$$V = \frac{F_{doppler}\frac{c}{2}}{F_{source}} \tag{A.7}$$

Another device that uses this principle is the Acoustic Doppler Current Profiler (ADCP), which samples a relatively wide area, and allows for obtaining a velocity contour or profile across a cross-section of flow, hence their name. This is in contrast to the ADV, which measures a small measurement volume, and can be considered to be a point measurement.

A.4 The piezo electric effect

The piezo electric effect is another method of indirectly measuring the velocity of fluid particles. The piezo electric effect is essentially the conversion of mechanical deformation into a voltage [100]. This voltage can then be measured and a force can be extracted with knowledge of the piezo electric properties of the material. In experimental fluid mechanics, this effect can be used to measure the velocity fluctuations of a fluid flow.

An example of a device that uses this effect is a shear probe, which profiles the flow vertically as it descends down a water column [31]. This devices measures the voltages induced by the deformation of piezo electric sensors which deflect due to velocity fluctuations present in turbulent vortices. These fluctuations are then recorded as a depth series and saved for further analysis.

Appendix B

Sample safe work procedure

In this appendix, the safe work procedure for vertical profile measurements developed at the CHTTC is shown [101].

Marine Renewable Procedure – Blue pontoon surface measurements

Purpose: To perform measurements using an ADV, ADCP or HADCP from the blue pontoon using the measurement arm or other surface mounts the following safety procedures and regulations must be followed.

People: 1 Blue pontoon operator, 3^{+} crewmembers (4 people minimum)

Hazards:
Physical: Pinch points, sprains, strains, cuts, scrapes, crushing, bruising, slipping, falling, drowning, noise, impacts and collisions
Biological: Insects (mosquitos, horse flies, hornets)
Chemical: Fuel fumes, exhaust and gasoline
Environmental: Sun, wind, rain, snow, ice, extreme temperature, waves, rapids and shallow areas

---

Personal protective equipment or safety equipment:

- Personal flotation device
- All safety equipment listed in Section 6.3 of *The Canadian Hydrokinetic Turbine Test Centre Safety Rules and Regulations*
- Work gloves (recommended)

Additional safety regulations:

- Zodiac operator must comply with *Marine Renewable Procedure – Safe boating.*
- Mount operators are to assist the Zodiac operator in watching for river hazards.
- The Zodiac must remain stationary when the ADV or ADCP is in the water unless the measurements require a moving vessel.
- The maximum depth for the ADCP should not exceed ½ meter (1.5 feet).

Education and training prerequisites:

- Training on how to use the measurement arm.
- Computer operator must be knowledgeable and efficient with the ADV or ADCP measurement software

---

Equipment and tools required:

- Laptop (Toughbook recommended)
- ADV or ADCP and all associated cables, clamps, adapters and/or mounts
- Invertor or generator
- Zip ties

Steps to complete task safely:
Set-up for ADV measurements using the measurement arm

1. Attach the ADV to the mount while the blue pontoon is docked and the measurement arm is in a horizontal position and resting on the support.
2. Check that all bolts are tight and that the ADV is secure.
3. Adjust the length of the arm to the appropriate length for the measurements.
4. Check that all bolts on the measurement arm are tightened so that the measurement pole does not rotate or slip.
5. Connect the data cable to the ADV and zip tie the cable at a minimum of two points along the arm.
6. Connect the power cord to the ADV cable and plug it into a power source (preferably an inverter connected to a battery).

7. Set up the computer (preferably a Toughbook) and connect it to the ADV carefully to ensure that the connector pins are not damaged.

Set-up for vertical ADCP measurements using the measurement arm

1. Attach the ADCP to the mount while the boat is docked and the measurement arm is in a horizontal position and resting on the support.
2. Check that all bolts are tight and that the ADCP is secure.
3. Adjust the length of the arm to the appropriate length for the measurements.
4. Check that all bolts on the measurement arm are tightened so that the measurement pole does not rotate or slip.
5. Connect data cable to the ADCP and zip tie the cable at a minimum of two points along the arm.
6. Connect the power cord to the ADCP cable and to a power source (preferably an inverter connected to a battery).
7. Set up the computer (preferably a Toughbook) and connect it to the ADCP carefully to ensure that the connector pins are not damaged.

Set-up for HADCP measurements using the measurement arm

1. Attach the HADCP to the mount while the boat is docked and the measurement arm is in a horizontal position and resting on the support.
2. Check that all bolts are tight and that the HADCP is secure.
3. Adjust the length of the arm to the appropriate length for the measurements.
4. Check that all bolts on the measurement arm are tightened so that the measurement pole does not rotate or slip.
5. Zip tie the HADCP cable at a minimum of two points along the arm.
6. Connect the HADCP cable and to a power source.
7. Set up the computer (preferably a Toughbook) and connect it to the HADCP carefully to ensure that the connector pins are not damaged.

Measurement arm data collection

1. [Optional] – Anchor the blue pontoon according to *Marine Renewable Procedure – Anchoring the blue pontoon.*
2. Open the device software.
3. Using the Humminbird blue water chart and pre-specified waypoints locate a measurement point and drive to it. Check the depth of the measurement location.
4. Rotate the pole to a vertical position using the hand crank provided.
5. Lock the measurement arm in place using the stopper.
6. Begin taking measurements.
7. If the blue pontoon is not anchored during stationary measurements, the boat driver locates a landmark on shore and attempts to hold the boat steady throughout measurement. For moving measurements, the mount operators must help the boat driver look for hazards.
8. While the measurement is taking place, the computer operator records the file ID, the date of the measurement, the start time, the approximate duration of the measurement, the water depth (taken from the sonar) and anything else that may be of interest when post-processing or examining the data.
9. Once the measurement is complete, stop the measurement on the computer and bring the arm back to the horizontal position.
10. Once the arm is back in the horizontal position, the boat driver can move to the next location.

Set-up and measurement procedure for ADCP, HADCP and ADV bolted to the guardrails

1. Wrap protective rubber around the measurement device.
2. Hose clamp the measurement device to the U channel around the previously placed protective rubber.
3. Plug the data cable into the measurement instrument.
4. Using metal plates and ½ inch bolts, bolt the U channel to the blue pontoon guardrail. Ensure that the measurement instrument is oriented properly in the flow.

5. [Optional] – Anchor the blue pontoon according to *Marine Renewable Procedure – Anchoring the blue pontoon.*
6. Open the device software.
7. Using the Humminbird blue water chart and pre-specified waypoints locate a measurement point and drive to it.
8. Connect the measurement device to a power source.
9. Set up the computer (preferably a Toughbook) and connect it to the measurement device carefully to ensure that the connector pins are not damaged.
10. Begin taking measurements.
11. Once completed return to shore before unbolting the measurement instrument from the blue pontoon.

Responsibility, completion and review:

Workers are to ensure that all duties are performed in accordance to training, established health and safety regulations/guidelines, policies and procedures. Notify a supervisor of any injuries, illness, safety or health concerns which are likely to harm anyone on the premises. This task may be monitored periodically to ensure compliance and effectiveness.

Last Revised by: Jody Soviak – March 2017